Systematic Study of Thiazole Incorporated NLO Gradient Bridge Chromophores

Daniel Michael Casmier

A dissertation submitted in partial fulfillment of the requirements of the requirements for the degree of

Doctor of Philosophy

University of Washington

2004

Program Authorized to Offer Degree:
Department of Chemistry

INFORMATION TO USERS

The quality of this reproduction is dependent upon the quality of the copy submitted. Broken or indistinct print, colored or poor quality illustrations and photographs, print bleed-through, substandard margins, and improper alignment can adversely affect reproduction.

In the unlikely event that the author did not send a complete manuscript and there are missing pages, these will be noted. Also, if unauthorized copyright material had to be removed, a note will indicate the deletion.

ProQuest Information and Learning Company
300 North Zeeb Road
P.O. Box 1346
Ann Arbor, MI 48106-1346

University of Washington
Graduate School

This is to certify that I have examined this copy of a doctoral dissertation by

Daniel Michael Casmier

and have found that it is complete and satisfactory in all respects,
and that any and all revisions required by the final
examining committee have been made.

Chair of Supervisory Committee:

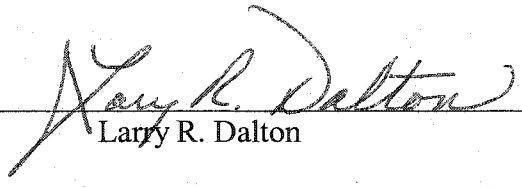

Larry R. Dalton

Reading Committee:

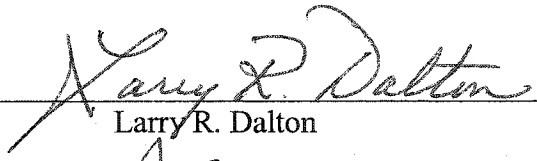

Larry R. Dalton

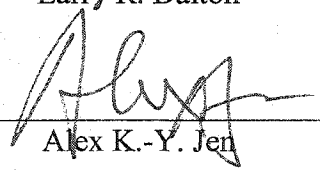

Alex K.-Y. Jen

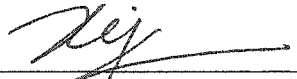

Younan Xia

Daniel Gamelin

Date: 8/9/04

In presenting this thesis in partial fulfillment of the requirements for the doctoral degree at the University of Washington, I agree that the Library shall make its copies freely available for inspection. I further agree that extensive copying of the dissertation is allowable only for scholarly purposes, consistent with "fair use" as prescribed in the U.S. Copyright Law. Requests for copying or reproduction of this dissertation may be referred to Proquest Information and Learning, 300 North Zeeb Road, Ann Harbor, MI 48106-1346, to whom the author has granted "the right to reproduce and sell (a) copies of the manuscript in microform and/or (b) printed copies of the manuscript made from microform."

Signature 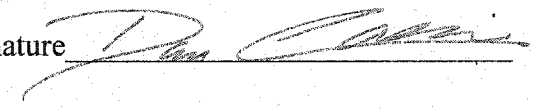

Date 8/1/04

University of Washington

Abstract

Systematic Study of Novel Thiazole Incorporated Gradient Bridge NLO Chromophores

Daniel Michael Casmier

Chair of Supervisory Committee:
Professor Larry R. Dalton
Department of Chemistry

In an exploration of improving the intrinsic first order hyperpolarizability of organic NLO chromophores, sets of novel chromophores were synthesized. These compounds were designed according to a novel gradient bridge concept. Among these novel compounds, the first experimental example of a thiazole "forward" containing chromophore was synthesized. The first order hyperpolarizabilities of these compounds were examined using hyper-Raleigh scattering (HRS) technique. Results obtained at 1.3μm and 880nm revealed that the regiochemical orientation of the thiazole has a marked effect on the hyperpolarizability. Thiazole "forward" showed a 20% improvement in hyperpolarizability relative to chloroform compared to that of thiazole "backward." An additional examination of two of these compounds with respect to their bulk nonlinear optical activity showed that the novel thiazole "forward" containing chromophore possessed an inherit instability in its structure compared to that of its thiophene analogue. The degradation of the thiazole "forward" chromophore occurred through a [4+2] cycloaddition reaction with DMSO. Recommendations to improve the stability of future thiazole "forward" chromophores were discussed. Overall, the first order hyperpolarizability of thiazole containing chromophores can be tailored, but are not stronger than their thiophene analogue.

TABLE OF CONTENTS

LIST OF FIGURES

LIST OF TABLES

ACKNOWLEDGEMENTS

The author wishes to extend his most sincere appreciation to the Department of Chemistry for their support, particularly to Professor Larry Dalton for his encouragement with this challenging project. This dissertation would not have been possible without the indispensable advice of my fellow group members, both past and present. The author also wishes to express gratitude for the love and support of his family and many friends, particularly his father, David Casmier and his fiancé, Angela Slaymaker, throughout the thick and thin of pursuing his doctoral degree.

DEDICATION

To my mother, Patricia Ann Jones Casmier,
whose life, love, and strength will never be forgotten

Chapter 1

A Brief Introduction to Nonlinear Optical Phenomena and Materials for Electro-Optic Light Modulation

1.1 Introduction

The field of photonics, which is the analog of electronics, involves the technology in which information is transmitted, received, stored, and processed through the use of photons. Most of today's modern technology relies on electronic signals for data processing and transmission. However, electronics has reached its theoretical limit and now optical lines have begun to replace where wires used to reside (telephones, cable television, and internet cables, for example). Electronic signals (50GHz) cannot keep pace with the expansion in the telecommunications industry and its demand for broader bandwidth. Since electronic devices cannot meet this demand, superior optical technologies are required.

In this new phase of the information age, there is a need for more efficient and faster relay of communication signals. The types of materials that are needed require a response to changes in electric fields, with either an externally applied potential (electro-optics) or with the electric field component of light (photonics). These materials can be used in a wide variety of everyday applications, ranging from data transmission, data storage, phased array radar, beam steering, and optical

gyroscopes. Nonlinear optical (NLO) materials are the answer as the medium for these various applications.

Since there exists a vast amount of literature concerning the field of nonlinear optics, nonlinear optical phenomena, material characterization, as well as device processing and performance, the following chapter is meant only as a brief review, giving basic terminology and simplified equations. Any further inquiries regarding a more in-depth review and discussion of these topics can be found with the references given herein.

1.2 Nonlinear Optical Phenomena

When a nonlinear optical material is exposed to an electric field (a dc field or the electric field component of a light beam, for example), the material experiences a displacement in charge from its equilibrium position. This response is a nonlinear function of the electric field. To better understand this phenomenon, the nonlinear optical response can best be viewed using the classical picture of the simple harmonic oscillator. Figure 1.1 displays a energy diagram where the charge in a material occupies a stable low energy level. When exposed to an external electric field, an induced polarization occurs in the material, which now occupies an increased energy level. The strength of the electric field dictates whether the polarization (charge separation) in the material responds either in a linear or nonlinear fashion.

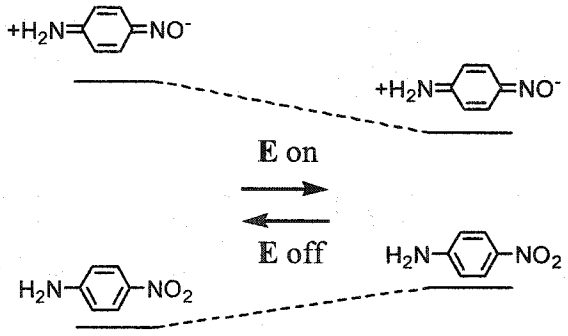

Figure 1.1 Schematic of a nonlinear optical energy levels.

When the electric field component of light is relatively weak, a linear force is exerted on the charge and is displaced from equilibrium, where it can be approximated by a simple harmonic potential. However, if a material is exposed to a strong electric field, the force exerted on the charge can no longer be described as a linear function of the charge displacement. The material responds in a nonlinear fashion, where the approximation of a simple harmonic potential breaks down and a non-harmonic potential is used instead. A schematic representation of these two types of responses is shown in Figure 1.2. In this depiction, the area located between the dotted lines represents the application of a weak electric field, where the induced polarization response in the material is linear in nature. However, the region outside these dotted lines represents an ever increasing and stronger electric field, where a material begins to experience a nonlinear induced polarization response. A mathematical treatment of the basics of this nonlinear optical response at both a microscopic and macroscopic level is described later in this chapter.

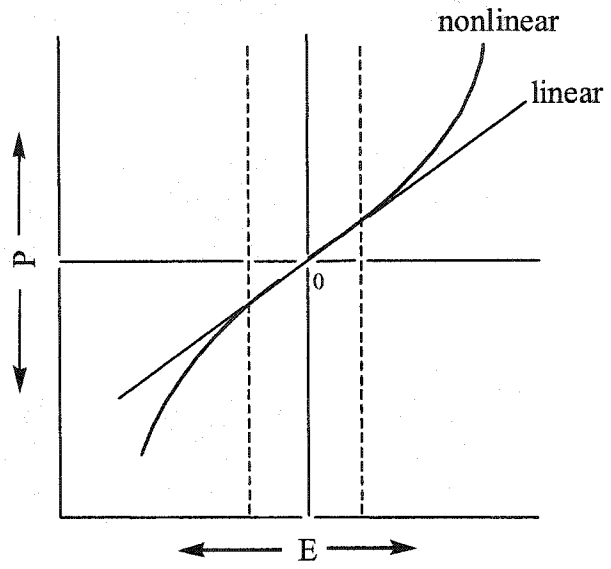

Figure 1.2 Schematic representation of the induced polarization response (P) in a material as a function of exposure to an external electric field (E).

Research based on electro-optic (EO) materials mainly focuses on their use in the modulation of light for fiber optic telecommunications purposes. EO materials act to control the index of refraction of a given material through the application of an ac or dc electric field. This phenomenon is known as electro-optic modulation, which enables one to translate electrical signals from a computer into optical signals on a fiber optic line.

Currently, electro-optic modulation is commercially accomplished through the use of gallium arsenide (GaAs) and lithium niobate ($LiNbO_3$) devices. These inorganic crystalline materials have been used for years but suffer from a number of disadvantages. Lithium niobate possesses a high dielectric constant (ε~28), which

results in perturbation of incoming electromagnetic field in radar applications but also leads to speed mode mismatch between the electric and optical fields in light modulation.[1] Integration into semi-conductor circuitry is also particularly cumbersome with lithium niobate. The maximum electro-optic coefficient of lithium niobate, via electrical engineering manipulations in device design, has reached a plateau of 31 pm/V (for 1.3 microns) some time ago. Additionally, growing and polishing perfect lithium niobate crystals is both tedious and time-consuming.

Due to these limitations for substantial improvement in the electro-optic activity in lithium niobate, there is tremendous interest in the use of organic nonlinear optical materials.[2] These materials hold promise to perform beyond that of lithium niobate.

1.3 The Basis of Nonlinear Optics at the Microscopic and Macroscopic Level

Kerr observed the first nonlinear optic effect in 1875, in which exposure to an electric field resulted in a quadratic response in the refractive index of carbon disulfide.[3] Later, in 1906, F. Pockels observed the linear electric field effect in quartz.[4] Since light and matter ordinarily have a very weak interaction, the field of nonlinear optics did not experience an expansion until the advent of lasers in 1960, which provided a more powerful source of monochromatic light. The laser enabled further understanding of this particular interaction various types of intense light with

materials. Initial research generated the development of applications such as second-harmonic generation and electro-optic modulation.[5-11]

Nonlinear optics concerns itself with the interaction and response of the electromagnetic field of light with the electric field component of a given material. The external electrical field can come from a variety of sources, such as an ac/dc fields, microwaves, or radio frequency waves. At the microscopic molecular level, when a material is exposed to this external electrical field, certain properties in the material change so that the next incoming photon sees it as a different material. The electric field of the photons passing through the material then interacts with electric fields of the nonlinear material. It is this interaction that produces a change in the direction, frequency, or phase of the incoming light. The field of developing novel and improved nonlinear optical materials relies on scientists across many disciplines, including chemists, engineers, materials chemists, and physicists.

Nonlinear optical behavior has been explored in both electromagnetic and quantum mechanical theory, which are quite similar with their treatment of materials interacting with electrical fields. This interaction leads to a degree of polarization in the material, known as the molecular polarization, which is related to how easily an electron can be displaced within a potential well.

1.4 Microscopic and Macroscopic Polarizability

Assuming that the material is both nonconducting and nonmagnetic, the movement of electrons is generally restricted to individual atomic and molecular orbitals. When a material is exposed to an electric field source, the interaction between the two electric fields (material and source) induces a displacement in the electronic distribution within the material. This displacement of charge represents a perturbation of the electronic π-orbitals in a direction that opposes the applied electric field. This electric field exposure results in a molecular polarization, **p**, effectively producing a change in the molecule's ground state dipole moment. When the intensity of the field is weak, the molecular polarization can be expressed in Equation 1.1, where α is the linear polarizability of the molecule and **E** is the applied electrical field.

$$\mathbf{p} = \alpha_{ij}\mathbf{E}_j \qquad (1.1)$$

When this is examined on a macroscopic scale, the bulk polarization **P** of the material (containing many individual polarizations) can be expressed by Equation 1.2.

$$\mathbf{P} = \chi_{IJ}^{(1)}\mathbf{E}_J \qquad (1.2)$$

In this expression, $\chi_{IJ}^{(1)}$ is the linear susceptibility (or the first order polarizability) of the material and $\mathbf{E}_J$ is again the applied electrical field. $\chi_{IJ}^{(1)}$ is a second rank tensor since it relates to all applicable vectors of the polarization **P** with respect to the vectorial quantity **E**, as shown in Equation 1.3.

$$\begin{pmatrix} Px \\ Py \\ Pz \end{pmatrix} = \begin{pmatrix} \chi 11 & \chi 12 & \chi 13 \\ \chi 21 & \chi 22 & \chi 23 \\ \chi 31 & \chi 32 & \chi 33 \end{pmatrix} \begin{pmatrix} Ex \\ Ey \\ Ez \end{pmatrix} \tag{1.3}$$

All the above expressions apply when the field applied to the material is relatively weak. However, when the field is intense but not strong enough to alter the binding forces between nuclei and the surrounding electrons, a nonlinear polarization and susceptibility response is observed. Expressions for these molecular and bulk responses are given in Equations 1.4 and 1.5.

$$\mathbf{p} = \alpha_{ij}\mathbf{E}_j + \beta_{ijk}\mathbf{E}_j\mathbf{E}_k + \gamma_{ijkl}\mathbf{E}_j\mathbf{E}_k\mathbf{E}_l + \ldots \tag{1.4}$$

$$\mathbf{P} = \chi_{IJ}^{(1)}\mathbf{E}_J + \chi_{IJK}^{(2)}\mathbf{E}_J\mathbf{E}_K + \chi_{IJKL}^{(3)}\mathbf{E}_J\mathbf{E}_K\mathbf{E}_L + \ldots \tag{1.5}$$

Assuming that the electric field is not strong enough to break nuclear forces (also known as dielectric breakdown), a molecule can be polarized such that β_{ijk} and γ_{ijkl} are the first and second order molecular hyperpolarizabilities. In Equation 1.5,

$\chi_{IJK}^{(2)}$ and $\chi_{IJKL}^{(3)}$ are the second and third order hyperpolarizability in the bulk material (third and fourth rank tensors, respectively). From Equations 1.4 and 1.5, the indices I, J, K, and i, j, k represent the principal directions of the crystal (bulk) and molecular coordinate systems. Tensor properties dictate that the medium must be noncentrosymmetric in order for the second order hyperpolarizability, $\chi_{IJK}^{(2)}$, to be nonzero. When a poled EO material is subjected to an electric field applied along one spatial direction (z), the material is said to possess $C_{\infty v}$ rotational symmetry along this axis. In this condition, only 3 of the 18 tensor elements can be non-zero in the matrix element expression for $\chi_{IJK}^{(2)}$.[7] In cases where the electric field frequencies involved in the second order process are far lower than the absorbance frequency of the chromophore (at resonance), then Kleinman symmetry is applicable.[12] This condition translates into the retention of two independent non-zero tensor elements, χ_{33} and χ_{13} (or χ_{zzz} and χ_{zxx}) as expressed in Equation 1.6.

$$\chi^2_{ijk} = \begin{bmatrix} 0 & 0 & 0 & 0 & \chi^2_{xxz} \\ 0 & 0 & 0 & \chi^2_{yyz} & 0 \\ \chi^2_{zxx} & \chi^2_{zyy} & \chi^2_{zzz} & 0 & 0 \end{bmatrix} \qquad (1.6)$$

Of these two remaining tensor elements, χ^2_{zzz} is parallel to the polar axis while χ^2_{zxx} is perpendicular to this polar axis. The overall electro-optic coefficient elements for these vectorial elements are r_{33}, which is parallel to the polar axis, and r_{13}, which is

perpendicular to this axis (Figure 1.3). The most meaningful term, r_{33}, is related to the bulk second order hyperpolarizability as expressed in Equation 1.7.

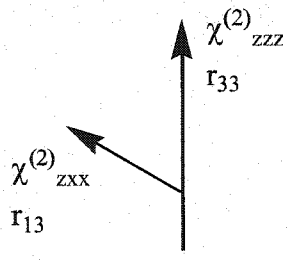

Figure 1.3 The orientation of the nonlinear electro-optical tensors.

$$r_{33} = -2\,\chi^{(2)}_{zzz} / \; n^4 \qquad (1.7)$$

In this expression, r_{33} is directly proportional to the second order hyperpolarizability ($\chi^{(2)}_{zzz}$) and inversely proportional to the refractive index (n) of the material.

A simplified explanation as to why noncentrosymmetric conditions are necessary to facilitate a second-order nonlinear optical response can be seen in the example of benzene under a potential given by Prasad.[7] As shown in Figure 1.4, when a molecule such as benzene (which possesses a center of inversion symmetry) is placed under a potential, the molecule is polarized in such a way that the dipole created has positive and negative components to it that oppose each other in opposite directions with equal magnitude. When examining odd numbered terms only in the series expansion of the polarization, we find mathematically that both polarization vectors are equal in magnitude. If, however, an even numbered term in the series

expansion is included, the total of the polarization vectors that oppose each other no longer have equal magnitude. The result of this treatment is a mathematically forbidden expression. The only way the even terms of the polarization can hold equal magnitude is if the molecule in question was asymmetric in nature.

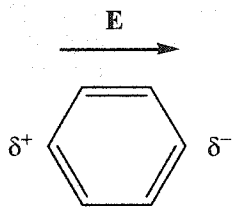

Symmetric - odd only

$$| a(E)^1 + c(E)^3 | = | a(-E)^1 + c(-E)^3 |$$

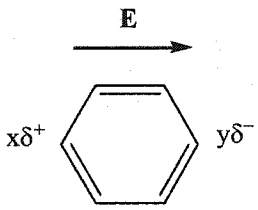

Symmetric - odd + even

$$| a(E)^1 + b(E)^2 + c(E)^3 | \neq | a(-E)^1 + b(-E)^2 + c(-E)^3 |$$

$$\cancel{aE} + bE^2 + \cancel{cE^3} - \cancel{aE} + bE^2 - \cancel{cE^3} \neq 2bE^2$$

Figure 1.4 Schematic representation of linear and nonlinear polarization responses of benzene under a potential.

From this example, it can be seen how odd numbered terms in the polarization expansion (first order polarizability, second order hyperpolarizability, etc.) do not require noncentrosymmetric ordering, while even numbered terms in the expansion (first order hyperpolarizability and higher ordered terms) possess this unique orientation requirement. The asymmetric dipolar chromophores effectively need to be "pointing" in the same direction (Figure 1.5). It should be noted that nonlinear optical effects greater than the second order hyperpolarizability are extremely weak in their susceptibilities and therefore are difficult to use on a practical level. They are not the focus of this work since we are interested in EO effects, which are second

order. NLO effects cover a broad range of topics and applications. Instead, EO effects due to the first order hyperpolarizability are the focus of this chapter.

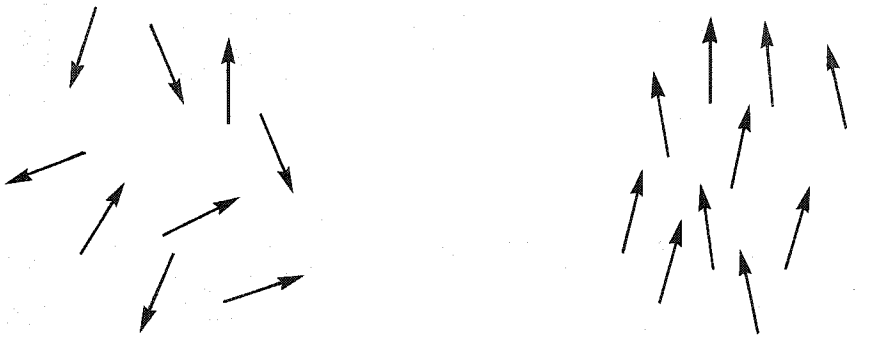

Figure 1.5 Orientational effects on electro-optic activity.

Organic nonlinear materials, as illustrated schematically in Figure 1.6 have an extended conjugated molecular framework consisting of an electron rich donor group, π-conjugated bridge unit, and an electron-poor acceptor group. Delocalized π-electrons in a conjugated system can be easily perturbed compared to that of sigma (σ) bonds. EO chromophores of the common neutral charge-transfer type have a molecular dipole associated with them based on the charge separated over a particular distance.

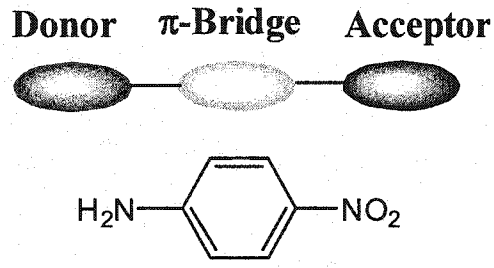

p-nitroaniline

Figure 1.6 Electronic backbone of a neutral charge-transfer EO chromophore.

1.5 The Electro-optic Effect

When a nonlinear optical material is exposed to a external dc (or low frequency) field E(0), the resulting field E is the sum of the optical E(ω) and this external field, given by Equations 1.8 and 1.9.

$$E = E(0) + E(\omega) \text{ or} \tag{1.8}$$

$$E = E(0) + E_0 \cos(\omega t - kz) \tag{1.9}$$

If this expression is substituted into Equation 1.5, and expanded, Equation 1.10 then results, in which the bulk polarization is described and higher ordered terms are ignored.

$$\mathbf{P} = \chi^{(1)}\,\mathbf{E}_0\cos(\omega t - kz) + (\tfrac{1}{2})\,\chi^{(2)}\,\mathbf{E}_0^{\,2}\,[1 + \cos(2\omega t - 2kz)] + \chi^{(3)}\,\mathbf{E}_0^{\,3}$$

$$[(\tfrac{3}{4})\cos(\omega t - kz) + (\tfrac{1}{4})\cos(3\omega t - 3kz)] + \ldots \qquad (1.10)$$

This bulk polarization expansion provides us with an expression for how an incident oscillating electric field can undergo frequency conversion as a result of the nonlinear optical response in a material. The second and third terms in this expression describe the origin of second harmonic and third harmonic (2ω and 3ω) generation, respectively.

1.6 Devices for light modulation with nonlinear optical materials

Perhaps the most common type of device used to exploit the properties of an electro-optic material is the Mach-Zender (MZ) interferometer. The general configuration of the Mach-Zender device is shown in Figure 1.7. The incoming light enters the modulator and is split into two separate beams traveling through two arms. In the telecommunications industry, the two most commonly used wavelengths used are 1.3 and 1.55μm. Both arms of the MZ modulator contain the active NLO electro-optic material, but an electric field is applied to only one of these arms, in the form of an ac or dc field.

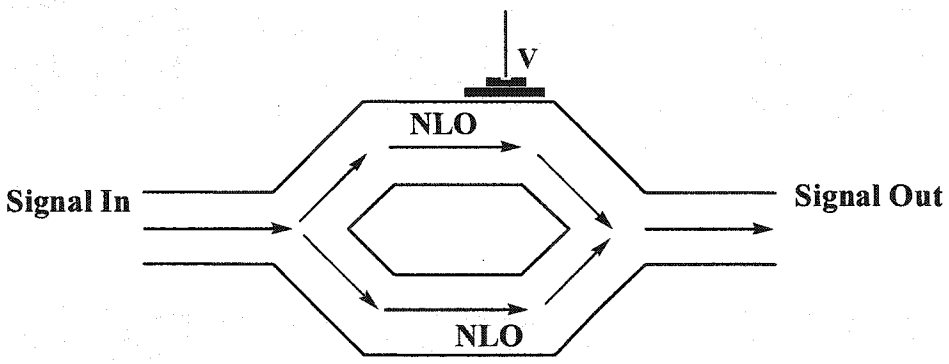

Figure 1.7 Schematic representation of a Mach-Zender (MZ) modulator.

The application of this field results in a voltage-controlled change in the refractive index of the material exposed to the electric field. The voltage is tuned to allow for a phase shift of π in the light wave (a function of arm length). Recombination of the light waves from the two arms generates destructive interference and the results in zero light output. When no field is applied, the light waves recombine to produce the original signal. Therefore, the output is a series of light and "dark" signals. This can be seen as transmission of binary code (1/0) on a fiber optic line. The degree of phase retardation ($\Delta\phi$) when an external electric field is applied can be expressed as Equation 1.11.

$$\Delta\phi = 2\pi\, \Delta n\, L / \lambda = \pi n^3\, r\, E\, L / \lambda \qquad (1.11)$$

In this expression, Δn is the change in the refractive index of the material, L is the modulation length, E is the modulating electric field strength, and λ is the

operational wavelength of light used. A phase shift of π with the propagating light signal (also known as the Pockel effect) through one arm in the MZ modulator can be expressed as Equation 1.12, where V_π is the voltage required for a π phase shift, h is the electrode spacing, r_{33} is the electro-optic coefficient of the material, n is the refractive index, and L is the interaction length between the electrical and optical field over which they co-propagate and interact with each other (this is effectively the length of the material).

$$V_\pi = \lambda h / n^3 r_{33} L \qquad (1.12)$$

Other devices take advantage of this EO phenomenon, such as birefringent and directional coupler modulators. These devices require slightly different applied voltages as well as different active material properties. On account of this, it is important to note that requirements of NLO materials will vary from application to application.

The degree of EO activity (its r_{33} value) required for a material to achieve this type of electro-optic modulation is dictated by several factors. The most important factor required for EO materials, as described earlier, is that of noncentrosymmetric order, in which the chromophores (assuming they are the common charge transfer type) are arranged with their dipoles pointing in the same direction.

1.7 EO Material Processing

There are several methods for inducing noncentrosymmetric order (i.e. creating a dipolar chromophore lattice), which include crystal growth, incorporating chromophores into inclusion compounds, and the sequential synthesis.[13-15] The most common way to achieve this orientation is through the use of an externally applied electric (or poling) field to induce acentric order. This will be the only method discussed within this work.

When an EO material is processed for macroscopic characterization or device fabrication, the chromophore and the desired polymer are dissolved into an organic solvent. This solvent should be carefully chosen so as not to induced phase separation and possess appreciable volatility so that an evenly coated film is produced on the substrate. A poor spin coated film can form regions of aggregates or holes, which lead to unacceptable amounts of light scattering (optical loss). The film is then heated to just below or at the glass transition temperature (T_g) of the polymer, where the active material possesses a greater degree of rotational freedom. A poling field is then applied, which exploits the dipolar nature of the chromophores to break centric ordering and aligns them in the direction of the applied field. The film is then subsequently cooled and may be fabricated further into a device.

As shown in Figure 1.8, an organic EO material can be incorporated into a polymer in a number of ways.

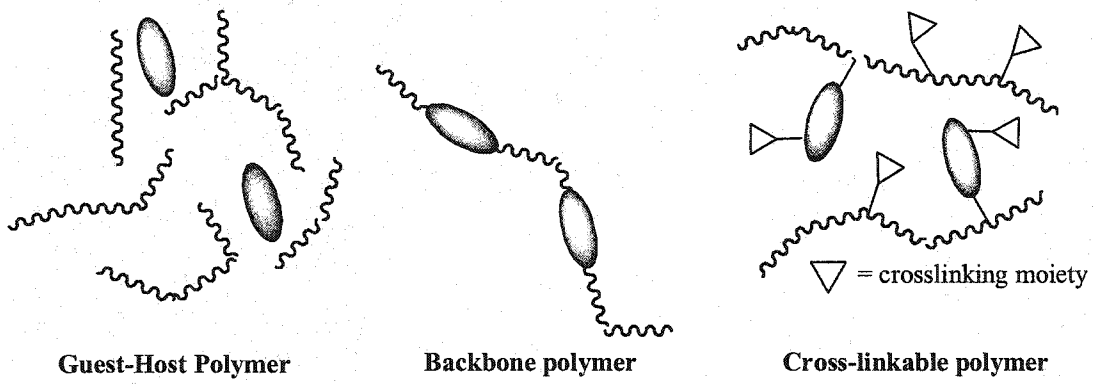

Figure 1.8 Some methods of incorporating EO chromophores into a polymer matrix.

The simplest method is mixing the chromophore with a polymer in an organic solvent and spin-casting to create a guest/host material. This type of chromophore/polymer composite carries with it several disadvantages, which include the following: potential poor polymer/chromophore compatibility which can lead to low chromophore loading density, chromophore phase separation or aggregation, chromophore loss to the cladding layers due to compatibility with the spin casting solvent, sublimation or decomposition of the chromophore at a high poling temperature, and perhaps the greatest disadvantage – the gradual relaxation of the chromophores back into a centric orientation due to chromophore/chromophore interaction dynamics.

1.8 Translation of microscopic to macroscopic nonlinearity

Even though the above description of achieving macroscopic noncentrosymmetric order appears to be straightforward, this strategy is by no means trivial. Perhaps the greatest challenge facing the potential use of polymeric EO materials in various device applications is finding the best way to translate microscopic (molecular) nonlinear optical effects into macroscopic (bulk) effects.

Electric field poling guarantees only partial noncentrosymmetric ordering. Under these circumstances, the overall electro-optic activity of a given material can be expressed in Equation 1.13.[16]

$$r_{33} = |2Nf(\omega)\beta\langle\cos^3\theta\rangle / n^4| \qquad (1.13)$$

In this expression, N is the concentration of chromophores in the material. The ideal concentration that aids in maximizing EO activity for this term will vary from chromophore to chromophore. Increasing the number density of a chromophore will initially increase EO activity, but beyond at a particular value, crystallization and/or phase separation in the films render the material useless. However, if the chromophore is incorporated covalently to the polymer matrix in some fashion, other issues such as poling efficiency and adequate film spin casting come into play. The

term f denotes local field factors at the frequency (ω) used, which describe the attenuation of applied fields (i.e. poling fields by local fields of the chromophores, and term n is the index of refraction of the material. The term $<\cos^3\theta>$ is the order parameter, which describes the average angle of deviation from the ideal orientation of being completely parallel to the direction of the applied poling field, E_{zzz}. A summary of the three major forces acting on the chromophore, are summarized by Equation 1.14.[1,9,17-19]

$$<\cos^3\theta> = L_3\,(\mu F / kT)[1 - L_1\,(W/kT)^2] \qquad (1.14)$$

In this equation, L denotes the Langevin function, F is the electric field encountered by the chromophore, W describes intermolecular electrostatic interaction energy (including chromophore dipole-dipole), k is the Boltzmann constant, and T is the temperature in Kelvin.

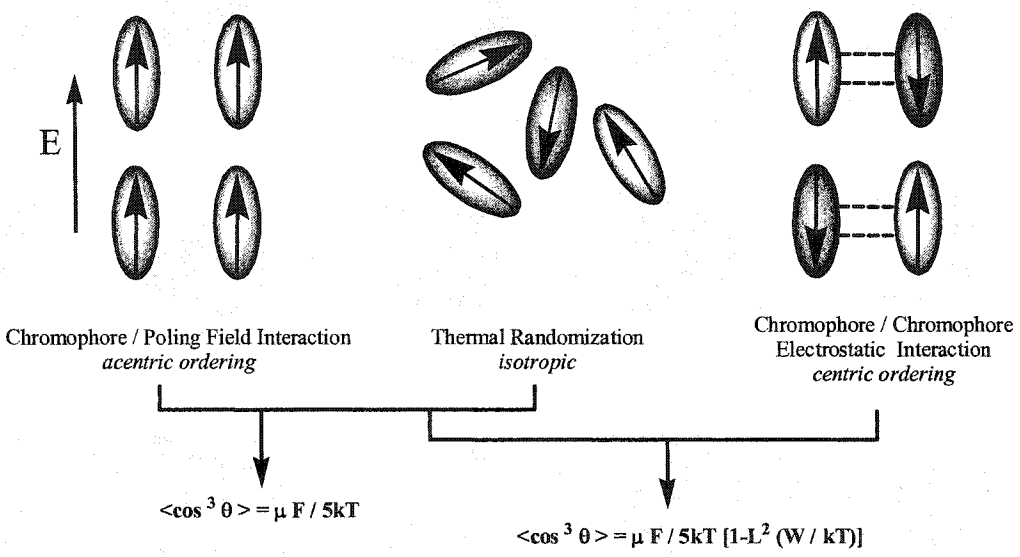

Figure 1.9 Summary of major forces acting on chromophores.

As mentioned, there are three major forces influencing the bulk nonlinear optical response, which to varying degrees drive either centric or acentric ordering. These forces are summarized in Figure 1.9.[20] First, the electric poling field force, E, drives chromophores towards acentric ordering. Second, there is the kinetic energy term, kT, which provides chromophores with energy for mobility to gradually relax back to achieve greater isotropy. Finally, there are electrostatic interactions between chromophores, produced through the interaction of their dipole-dipole forces, which steers the system toward centric ordering as well. This last force acting on EO chromophores was largely ignored in theoretical treatments involving low μβ chromophores such as DANS and Disperse Red 1 (DR1), shown in Figure 1.10, has proven to be quite significant for stronger chromophores.[18]

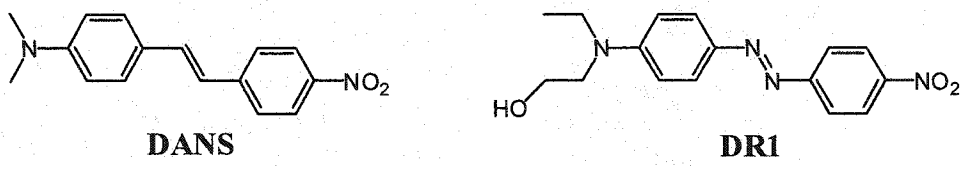

DANS **DR1**

Figure 1.10 Chemical structure of the DANS and Disperse Red I chromophores.

The local environment a chromophore experiences can manipulate its orientation with respect to the applied electric field. The local environment is influenced by not only the degree of rigidity of the surrounding polymer matrix (in other words, the degree of free volume that a chromophore has available to move within given enough kinetic energy) but also includes chromophore-chromophore interactions and chromophore-polymer interactions.

Perhaps the largest factor affecting bulk electro-optical activity is electrostatic interactions between chromophores. Electrostatic interactions between chromophores can become so strong that they become the dominant force acting on chromophores. These interactions increase as the distance between chromophores decrease. This close approach between chromophores drives them to assume centrosymmetric ordering. These dipole-dipole interactions between chromophores represent a low energy configuration due to close approach along their minor axes, which is detrimental to a nonlinear optical response. As mentioned earlier, these interactions were initially largely ignored in research since early charge-transfer chromophores had relatively low dipole moments. Dalton and coworkers

demonstrated through a theoretical study that chromophores with large dipoles (high μβ) possess much stronger electrostatic interactions than that of traditional Disperse-Red type chromophores.[21-23] In systems containing low dipole chromophores, high loading densities over 35 weight % were achieved before this saturation in electro-optic activity occurred. This "roll-over" in electro-optic activity occurred at much lower loading densities in high μβ chromophores than chromophores with lower dipoles.

This decrease in EO response of the bulk material was ascribed to the close proximity of high μβ chromophores at certain loading densities in which electrostatic interactions between chromophores increases dramatically, driving chromophores toward centric ordering. Theoretical calculations and experimental data performed on the FTC chromophore (a high μβ chromophore) showed the influence of chromophore shape on EO activity. It also displayed the potential increase in EO coefficient with the use of a spherically-shaped chromophore, as shown in Figure 1.11.

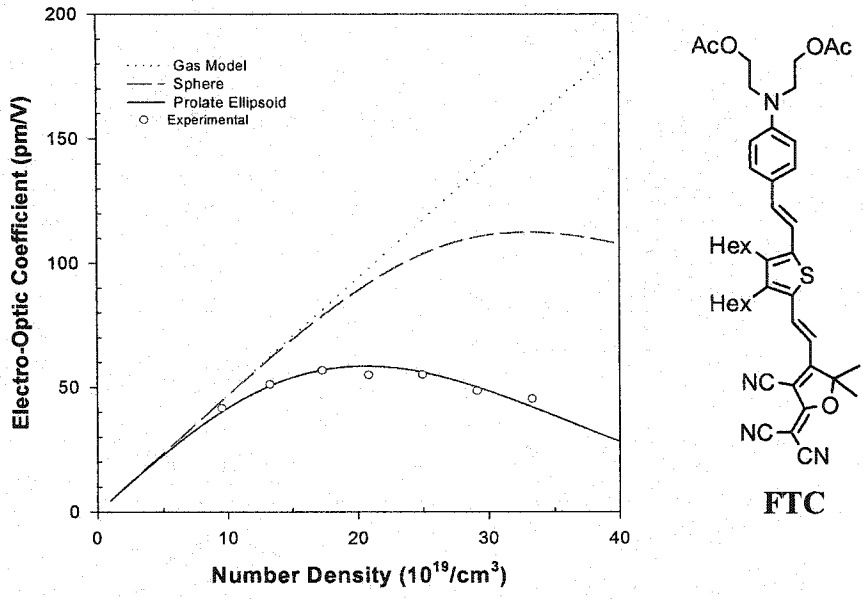

Figure 1.11 A comparison of theoretical calculations on the effects of electrostatics on different FTC chromophore shapes. The circles are experimental values for the FTC molecule located to the right.[18]

This theoretical study illustrated the value of producing nonlinear optical chromophores that possessed a more spherical shape. With this type of shape, the chromophores are effectively encapsulated so that close approach of high $\mu\beta$ chromophores along their minor axes will be minimized, resulting in a higher electro-optic activity at higher loading densities before the "roll-over" occurs.

1.9 Approaches to greater acentric order in EO materials

Since theoretical study by Dalton and coworkers, a number of chromophores with bulky inactive groups surrounding the chromophores at various points of attachment have demonstrated that there is a degree of increased electro-optic activity.[13-15,24-27] In addition to adding steric bulk around chromophores to reduce electrostatics, another approach that has been pursued and modified over recent years has been incorporating the chromophores into a polymer system that chemically crosslinks the chromophore to the polymer matrix following electric field poling. The rationale behind this methodology is to align the chromophores during poling followed by effectively "locking-in" their acentric ordering by inducing a crosslinking reaction between the chromophore and the polymer matrix. This approach reduces the ability of a chromophore to reorient back to a centric configuration (Figure 1.12).

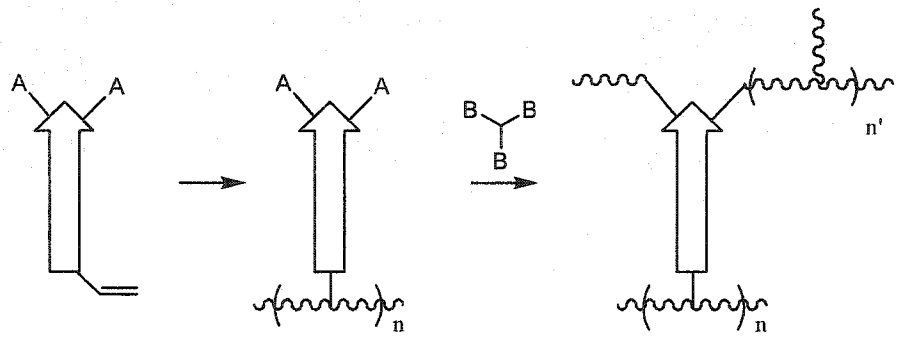

Figure 1.12 Schematic of crosslinking approach. Functional group A reacts with functional group B to produce the rigid crosslinked matrix.

There are several different types of reactions that can be used to produce both the prepolymer as well as generate the crosslinking of the lattice (examples are free radical addition, condensation, or through thermal means). The challenge in this strategy resides in using a polymer system that would enable successful site-isolation of the chromophores, so that close approach of chromophores is minimized and the attenuation of electro-optic activity is diminished.

The type of polymer system for crosslinking must also be chosen carefully. If the polymer integrated with the chromophore is too bulky, this can lead to decreased poling efficiency. Current research thrusts include the use of a reverse Diels-Alder crosslinking functionality where crosslinking the polymer matrix occurs upon cooling the film after poling at or near the glass transition temperature.[28]

More complex chromophore/polymer incorporation methods involve chemically bonding the chromophores to the polymer. These EO polymer systems can include attaching the chromophore at either end as part of the polymer backbone, attachment of one end of the chromophore to the polymer backbone (pendant), or crosslinking the chromophore to the polymer matrix. Hardening of the polymer lattice through crosslinking has emerged as the preferred method, as it has demonstrated not only a more thermally and chemically stable film, but a larger temporal stability (using a comparable loading density to that of a guest-host system).[29] Additionally, the methodology of polymeric crosslinking using dendrimeric chromophore moieties holds the greatest promise for translating microscopic to macroscopic nonlinearity.

Even though there is currently a major research thrust to translate microscopic EO activity to the bulk scale, much remains unknown about how microscopic concepts like molecular hyperpolarizability can be effectively controlled and tailored. Much of the initial research in chromophore design went into how to best exploit the first order molecular hyperpolarizability (β). Quantum mechanical calculations have provided much guidance into how new novel chromophores could be designed and synthesized. The next chapter will examine how theorists and chemists have tried to improve the first order hyperpolarizability of materials.

Notes to Chapter 1

(1) Dalton, L. R.; Harper, A. W.; Wu, B.; Ghosn, R.; Laquindanum, J.; Liang, Z.; Hubbel, A.; Xu, C. *Adv. Mater.* **1995**, *7*, 519-540.

(2) Marder, S. R.; Perry, J. W. *Science* **1994**, *263*, 1706-1707.

(3) Kerr, J. *Philos. Mag.* **1875**, *4*, 337.

(4) Pockels, F. *Lehrbuch der Kristalloptik* Teubner, Leipzig, 1906.

(5) Franken, P. A.; Hill, A. E.; Peters, C. W.; Weinreich, G. *Phys. Rev. Lett.* **1961**, *7*, 118-120.

(6) Shen, Y. R. *The Principles of Nonlinear Optics*; John Wiley and Sons: New York, 1984.

(7) Prasad, P. N.; Williams, D. J. *Introduction to Nonlinear Optical Effects in Molecules and Polymers*; John Wiley and Sons: New York, 1991.

(8) Nie, W. *Adv. Mater.* **1993**, *5*, 520-545.

(9) Dalton, L. R.; Harper, A. W.; Ghosn, R.; Steier, W. H.; Ziari, M.; Fetterman, H.; Shi, Y.; Mustacich, R. V.; Jen, A. K.-Y.; Shea, K. J. *Chem. Mater.* **1995**, *7*, 1060-1081.

(10) Dalton, L. R. *Nature* **1992**, *359*, 269.

(11) Dalton, L. R.; Sapochak, L. S.; Yu, L. *J. Phys. Chem.* **1993**, *97*, 2871-2883.

(12) Kleinman, D. A. *Phys. Rev.* **1962**, *126*, 1977-1979.

(13) Di Bella, S.; Fragala, I.; Ratner, M. A.; Marks, T. J. *Chem. Mater.* **1995**, *7*, 400-404.

(14) van der Boom, M. E.; Zhu, P.; Evmenenko, G.; Malinsky, J. E.; Lin, W. D., P.; Marks, T. J. *Langmuir* **2002**, *18*, 3704-3707.

(15) van der Boom, M. E.; Evmenenko, G.; Dutta, P.; Marks, T. J. *Polym. Mater. Sci. Eng.* **2002**, *87*, 375-376.

(16) Dalton, L. R. In *Advances in Polymer Sciences*; Springer-Verlag: Berlin Heidelberg, 2002; Vol. 158.

(17) Dalton, L. R. In *Electrical and optical polymer systems*; Wise, D. L., Wnek, G., Transtolo, D. J., Cooper, T. M., Gresser, J. D., Eds.; Marcel Dekkar: New York, 1998.

(18) Dalton, L. R.; Steier, W. H.; Robinson, B. H.; Zhang, C.; Ren, A.; Garner, S.; Chen, A.; Londergan, T.; Irwin, L.; Carlson, B.; Fifield, L.; Phelan, G.; Kincaid, C.; Amend, J.; Jen, A. *J. Mater. Chem.* **1999**, *9*, 1905-1920.

(19) Steier, W. H.; Chen, A.; Lee, S. S.; Garner, S.; Zhang, H.; Chuyanov, V.; Dalton, L. R.; Wang, F.; Ren, A. S.; Zhang, C.; Todorova, G.; Harper, A.; Fetterman, H. R.; Chen, D.; Udupa, A.; Bhattacharya, D.; Tsap, B. *Chem. Phys.* **1999**, *245*, 487-506.

(20) Dalton, L. R., personal communication.

(21) Dalton, L. R.; Harper, A. W.; Robinson, B. H. *Proc. Natl. Acad. Sci.* **1997**, *94*, 4842-4847.

(22) Harper, A. W.; Sun, S.; Dalton, L. R.; Garner, S. M.; Chen, A.; Kalluri, S.; Steier, W. H.; Robinson, B. H. *J. Opt. Soc. Am. B: Opt. Phys.* **1998**, *15*, 329-337.

(23) Dalton, L. R.; Harper, A. W. *Polym. News* **1998**, *23*, 114-120.

(24) Londergan, T. M.; Zhang, C.; Ren, A.; Dalton, L. *Polym. Prepr. (Am. Chem. Soc., Div. Polym. Chem.)* **2000**, *41*, 783-784.

(25) Xu, C.; Wu, B.; Todorova, O.; Dalton, L. R.; Shi, Y.; Ranon, P. M.; Steier, W. H. *Macromolecules* **1993**, *26*, 5303-5309.

(26) Luo, J.; Ma, H.; Haller, M.; Jen, A. K.-Y.; Barto, R. R. *Chem. Commun.* **2002**, 888-889.

(27) Song, S.; Lee, S. J.; Cho, B. R. *Chem. Mater.* **1999**, *11*, 1406-1408.

(28) Haller, M.; Luo, J.; Li, H.; Kim, T.-D.; Liao, Y.; Robinson, B. H.; Dalton, L. R.; Jen, A. K.-Y. *Macromolecules* **2004**, *37*, 688-690.

(29) Luo, J.; Liu, S.; Haller, M.; Liu, L.; Ma, H.; Jen, A. K.-Y. *Adv. Mater.* **2002**, *14*, 1763-1768.

Chapter 2

An Examination on the Manipulation of Hyperpolarizability in Organic EO Molecules and Its Measurement

2.1 Introduction

In nonlinear optical (NLO) materials, the application of an external electrical field results in a nonlinear polarization response. Most organic EO molecules for second order applications are of the dipolar, charge-transfer type. A polarization resulting from an externally applied electrical field is defined in part through the degree of the hyperpolarizability (β) of a molecule. Hyperpolarizability can be thought as the ease that electrons within a molecule can be perturbed from the neutral ground state to the charge separated excited state.

First, to avoid any confusion, it must be said that some terms and concepts commonly used in the nonlinear optical materials community, such as "excited state," are technically misnomers. When an electrical field is applied to an organic NLO molecule, the π-electron orbitals are actually distorted so that a majority of the electronic density shifts from the donor end to the acceptor end. No "excited state" is actually achieved as in the context of photophysics. In other words, the applied electric field **does not** elevate a single electron to a higher energy state. Rather, electrons are shifted to new increased energy levels (sometimes referred to as virtual

states) in the potential well. It is this increased energy level in the potential well that is often deemed the LUMO. The timescale of the relaxation of this electronic perturbation back to their ground state (often referred to as the HOMO) is on the order of tenths of femtoseconds. Another misconception is that the electron orbitals in *all* NLO molecules shift from ground state to the "excited state." This is a simplified model used in the two-level approximation.[1] The reality of the system, however, is that perturbation of electrons in organic NLO materials leads to a mixed array of elevated energy states (occupying many dipoles and hyperpolarizabilities) spanning the entire spectrum from the ground state to the completely charge-separated "excited state." This perturbation changes the refractive index change in the material.

A reasonable expression for molecular hyperpolarizability, β, has been the subject of intense research for many years. Finding a practical and functional expression for relating chemical structure with hyperpolarizability has been the focus of many research efforts. Typical EO chromophores have asymmetric structures in which there is an electron-rich donating portion on one end of the molecule, a π-conjugated bridge segment, and an electron-deficient acceptor on the other end. The charge-transfer axis hyperpolarizability of the chromophore, β_{zzz}, is the component that is commonly examined.

In looking at β theoretically, there have been several different approaches used toward understanding β_{zzz} and how it relates to the electronic arrangement of molecule. These approaches include models such as the additivity model and the

equivalent internal field model.[2,3] Quantum mechanically, the sum-over-states method (SOS) is perhaps the most widely used and will be the model discussed here.[4]

2.2 Hyperpolarizability and the Two-Level Model

The SOS method was originally developed by Ward for looking at how an externally applied electrical field can cause a perturbation in the electronic motions in a molecule and how this perturbation results in oscillating currents in the molecule.[1] These currents can polarize the molecule. Expressions for the molecular polarizability (α) and the first order hyperpolarizability (β) of this exposed medium can be seen in Equation 2.1, which makes a summation of all excited states.

$$\beta(-2\omega;\omega,\omega) = p\sum_{n_1 n_2}\left(\frac{e^3}{2\hbar^2}\right)\frac{r_{gn_2}r_{n_2n_1}r_{n_1g}}{(\omega-\omega_{n_1g})(2\omega-\omega_{n_2g})} \qquad (2.1)$$

In this expression, p denotes the portion of the polarization that is summed over all Cartesian indices (within the molecular framework of i, j, and k) with regard to its exposure to energies of frequency ω and 2ω. For other terms in this equation, n describes all excited states, g is the ground state, and the r terms are various dipole operators. It is within this summation that products are achieved that contain a range

of transition dipole moment terms, influenced by many dipoles produced through ground to excited state transitions and dipole transitions within different excited states.

From Equation 2.1, it can be seen how light at twice the fundamental frequency can contribute to β. This frequency term, ω and 2ω, can sometimes lead to resonant enhancement, where the electronic absorption of the chromophore overlaps with these wavelengths leading to difficulty in quantifying β.

In order to simplify the expression for hyperpolarizability, one can make the assumption that the major contributions to β come from electronic transitions in which there is a low lying ground state and an excited state dipole moment. This assumption is also known as the two-state model.[5-7] This type of model has been useful in cases involving simple chromophores such as *para*-nitroaniline. When this assumption is applied to Equation 2.1, the expression simplifies to the terms described in Equation 2.2.

$$\beta(-2\omega;\omega,\omega) \cong \frac{3e^2}{2\hbar m}\frac{\omega_{eg} f \Delta\mu}{(\omega_{eg}^2-\omega^2)(\omega_{eg}^2-4\omega^2)} \qquad (2.2)$$

From this expression, f is the oscillator strength, which is influenced by the transitional dipole moment between the ground and excited state dipole moments, ω_{eg} is the frequency of the optical transition, and $\Delta\mu$ is the difference in dipole moment between the ground state and the excited state. Using this simplified model,

chemists have established some trends relating the first hyperpolarizability of a molecule to its structural electronic arrangement.

2.3 Bond Length Alternation (BLA)

For years, chemists have pursued various approaches to increase the first order molecular hyperpolarizability. The common misconception amongst those first exploring the field was that using the best donor, bridge, and acceptor constituents would produce the best chromophore. This is not the case. A guide in conceptualizing how to construct improved nonlinear optical chromophores was formulated through the bond-length alternation (BLA) theory, initially proposed by Marder and coworkers.[8] It was shown that using the best donor, bridge, and acceptor combination currently available does not necessarily result in the best chromophore. The BLA hypothesis indicates that there is an optimal combination of donor and acceptor strengths for a given bridge that leads to a balance in electronic asymmetry and polarizability, thus maximizing hyperpolarizability (β).[9] Different donor/acceptor (D/A) strengths give the chromophore various bond-length alternations ($\langle \Delta r \rangle$), defined as the average difference between the average bond lengths of double and single carbon-carbon bonds. A theoretical analysis with a chromophore (Figure 2.1) consisting of a dimethyl amino donor, a polyene bridge and an aldehyde acceptor, revealed that in a plot of β versus $\langle \Delta r \rangle$ that β reached a maximum and then decreased in a sinusoidal fashion (Figure 2.2).[10]

Figure 2.1 Extended polyene system examined for BLA theory.

This plot was achieved by first optimizing the geometry of the chromophore in the presence of a static field. This field was then used to simulate the different polarizations induced through the bridge by different D/A strengths. For each value of the static field, the value of β was calculated by the finite-field method.[10]

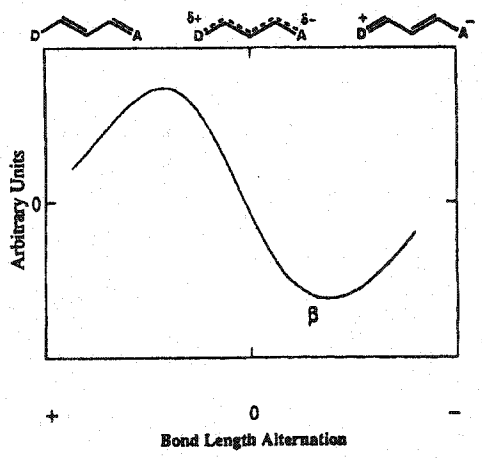

Figure 2.2 Plot of BLA versus β for $(CH_3)_2N(CH{=}CH)_4CHO$.

These calculations revealed that for chromophores with very weak donors and acceptors there was little mixing between alternating carbon double and single bonds and therefore no charge-transfer. For these chromophores, β was near zero and the BLA was so large (<Δr> ~0.1Å) that only one canonical resonance structure contributed predominantly to the ground state of the molecule. As D/A strength increased, BLA decreased and the value of β increased initially, reached a maximum value when <Δr> = 0.03 to 0.05Å and then decreased. In extreme cases, BLA values crossed beyond the zero value and became negative since the ground state became zwitterionic in nature, which is a phenomenon known as over-polarization. The zero BLA level is known as the "cyanine limit," where the donor and acceptor each transfer approximately half the charge available in both the ground and excited states. At the cyanine limit, the molecule has no change in its dipole during charge transfer. A schematic representation of these three types of polarizations is shown in Figure 2.3.

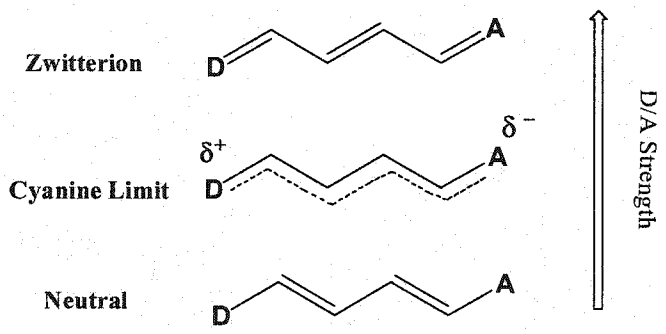

Figure 2.3. Schematic representation of the polarization types in a donor-polyene-acceptor molecule.[11]

Although the BLA theory provides us with a picture of how chromophores behave with respect to donor/acceptor strengths, this model is limited to extended polyene systems. Current state-of-the-art chromophores used in NLO prototype devices are not simple polyenes, but rather have more complex functionality addressing various issues such as stability, poling efficiency, nanoscale molecular ordering, and processability. Until systematic studies are performed to look at BLA behavior for very high $\mu\beta$ chromophores, the original model of BLA acts merely as a guideline.

On a physical level, the level of mixing between the ground and charge-separated states can also be influenced through solvent polarity, which is also known as solvatochromism. In an extremely nonpolar solvent, ether for example, the neutral ground state of the molecule predominates. As solvent polarity increases, more NLO molecules assume a certain degree of charge separation due to solvent stabilization effects on these electronically perturbed species.

2.4 Experimental improvements in molecular hyperpolarizability

Under the two-level model, molecular hyperpolarizability is dictated by a number of factors that are expressed in Equation 2.3,

$$\beta = 3\,(\mu_{ge}^2)(\mu_e - \mu_g) / (\Delta E_{eg})^2 \qquad (2.3)$$

where (μ_e - μ_g) represents the difference in dipole moment between the ground and first excited states, ΔE_{eg} is the energy gap between the HOMO and LUMO energy states, and μ_{ge} is the matrix element transition dipole moment, which can also be expressed as its Hamiltonian operator, <g |μ| e>. Quantum mechanical calculations have provided a tremendous amount of guidance in designing new chromophores with increased hyperpolarizability.[12-18]

The first modification to the chromophore backbone that resulted in a significant increase in the molecular hyperpolarizability was the simple extension of the conjugated system, as shown by Oudar.[5] This alteration can be explained from a quantum mechanical viewpoint, where extension of the polyene system effectively translates into an increase in the path length for an electron using the "particle in a box" model. Increasing the length decreases the bandgap (transitional energy, λ_{max}) by lowering the energy level of the first excited state, resulting in a higher degree of hyperpolarizability. This research launched interest in naturally occurring polyene systems as possible NLO chromophores. However, this increase in hyperpolarizability came at a price. Increased β through π- elongation was also accompanied by decreased thermal and photochemical stability.[19] Although asymmetric polyene based chromophore derivatives held some of the highest calculated values for molecular hyperpolarizability, they suffered from a number of stability problems, making them impractical for use in actual devices.

Another modification to the chromophore backbone that increased molecular hyperpolarizability was the replacement of phenyl rings with heteroaromatic groups.

Theoretical and experimental data has shown that changing the conjugated backbone from phenyl rings (used in common benchmark chromophores like Disperse Red 1 and DANS) to heteroaromatic rings (such as thiophene, furan, and thiazole) resulted in a marked increase in the hyperpolarizability in the material.[20-29] The rationale behind this strategy is that by using a component with lower aromatic stabilization energy than a phenyl ring, there would be less energy required to break the aromaticity of the ring during the charge-transfer process. However, this explanation is oversimplified.

There are other electronic factors that dictate the hyperpolarizability of a material. The use of fewer aromatic rings leads to an increase in β in most systems; however, this is not always the case. These results can perhaps be explained through the placement of the heteroaromatic ring. Heteroaromatic rings that are more electron rich in nature (pyrrole, for example) increase β when placed at the donor end of the chromophore but lead to a decrease when placed toward the acceptor end. On the other hand, with electron deficient rings (thiazole and oxazole, for example), there is a reversal of this trend.[23] Clearly, the use and placement of heteroaromatic rings plays a major role in the degree of hyperpolarizability a molecule can exhibit.

Modifications to the donor and acceptor also have led to improvements in hyperpolarizability. However, these components are not the focus of this dissertation, but rather this work will focus on the alteration of the bridge portion of organic NLO chromophores. The reader is referred to other sources that provide

background on systematic synthetic donor and acceptor modifications in examining microscopic properties, including hyperpolarizability.[30-41]

2.5 Device requirements

The pursuit of maximizing hyperpolarizability is only part of the equation in obtaining improved electro-optic compounds. There still are several issues that must be addressed to synthesize materials that will adequately fulfill device fabrication requirements. These requirements mostly pertain to the thermal, chemical, photochemical, and mechanical stability of the material, as well as its processability. These additional requirements are not the focus of this work but will be described briefly here.

Organic nonlinear optical chromophores need to have a reasonable degree of chemical and thermal stability in order with withstand the various material and device processing and operating conditions or they are of no practical commercial value. A good example of this is the aforementioned class of chromophores consisting of extended polyene functionality. Even though the hyperpolarizabilities of this category of molecules are among the highest ever recorded, they possess no commercial value due to their low chemical and thermal stability.[19] The extended polyene chain is chemically susceptible to light/heat induced cis-trans isomerization along with decomposition through radical/nucleophilic attack. Approaches to correct this flaw have included modification of the polyene backbone to form ring-locked

polyene systems that produce materials with both increased thermal and chemical stability.[4,42-45] Photochemical stability is another concern, as attack by singlet oxygen on the conjugated backbone can also diminish the electro-optic activity. Fabricating devices under an inert atmosphere and incorporating oxygen quenchers into the polymer matrix have addressed this problem.

2.6 Experimental methods for measuring hyperpolarizability

Electric-Field Induced Second-Harmonic Generation (EFISH)

One of the early methods developed for measuring microscopic nonlinearity was electric-field induced second-harmonic generation (EFISH). In this process, the NLO material is subjected to an electric field to induce noncentrosymmetric ordering. This adjustment in bulk ordering allows the second order nonlinear optical response of the molecules to be examined (Figure 2.4). Since bulk ordering is achieved in this technique, the second harmonic generation signal is much stronger than that of HRS. This technique is only applicable to dipolar NLO species because the molecules must be aligned an external electric field.

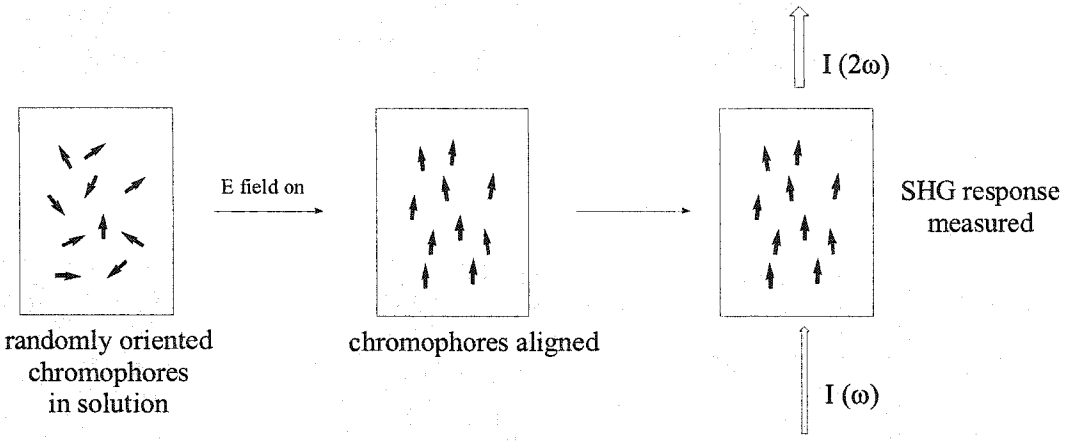

Figure 2.4 Schematic representation of the EFISH characterization method.

EFISH measures the quantity $(\mu\beta/5kT) + \gamma$, not the hyperpolarizability tensor individually. As a result, β must be determined through either estimating μ using theoretical calculations or from measuring μ directly from independent experimentation. Additionally, there are contributions to the signal arising from the third order nonlinear response (γ). First performed in the gas phase, adaptations were made so the technique could be applicable in solution. However, this technique is convoluted by local field factors. The one particular advantage to EFISH is that a large signal response is achieved, providing one with the hyperpolarizability tensor along the axis of charge transfer. A number of techniques have been employed to address these additional interactions and signal responses. [46]

Hyper-Raleigh Scattering (HRS)

Another method for determining the first order hyperpolarizability of a material is through a technique known as hyper-Raleigh scattering (HRS), which examines nonlinear light scattering at the second harmonic frequency (Figure 2.5).

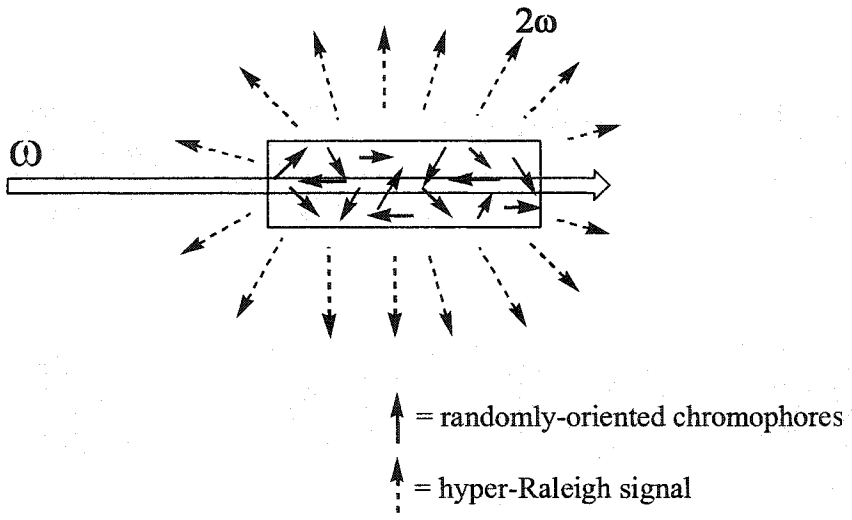

Figure 2.5 Schematic representation of the HRS characterization method.

The technique of HRS was first demonstrated in 1965, soon after the advent of the laser, but was rarely used until the early 1990s.[47,48] Since then, HRS has been used to explore the hyperpolarizabilities of a wide array of NLO compounds. HRS is a coupled electronic-vibronic process of measuring two-photon elastic light scattering arising from random fluctuations in the second-order susceptibilities of single molecules. This measurement is performed in a homogenous solution without the use of orientation aligning fields (as is the case for EFISH). As a result, HRS is

also a desirable technique for measuring the hyperpolarizabilities of apolar molecules where a center of symmetry exists. Additionally, the use of an eternal electric field in EFISH prohibits the measurement of ionic (or conductive) NLO chromophores. HRS provides a quantity of the rotational average along all components of the hyperpolarizability tensor. Since β is a dispersive quantity (i.e. varies with excitation wavelength), characterization of β at multiple wavelengths is desirable to obtain a relevant value at the desired operational wavelength. It is practical for the purpose of comparing hyperpolarizabilities between chromophores to do so at several wavelengths that are far removed the absorption maximum of the chromophore. Using an HRS wavelength that is far away from the one and two photon adsorption bands of the chromophore is often reported as an "off-resonance" frequency.

In the process of HRS, two photons at the ground state frequency ω are annihilated and a single photon is created with twice the energy (half the wavelength). The intensity of the second harmonic signal from HRS is very small due to the reduced occurrence of two-photon elastic scattering (compared to that of one-photon processes). The relation of this emitted light at 2ω to the hyperpolarizability is shown in Equation 2.4.[49]

$$I(2\omega) = G\left(N_{solvent} \langle \beta^2_{solvent} \rangle + N_{sample} \langle \beta^2_{sample} \rangle \right) \qquad (2.4)$$

In this expression, I (2ω) is the observed HRS signal intensity, G is an instrumental factor, N stands for the concentration or number density of the chromophores in solution. Comparing the two techniques of EFISH and HRS, it can be seen that EFISH is subject to many of the same problems as HRS but also holds many other quantities involved that HRS becomes a more useful technique for a reasonable quantification of β.

Notes to Chapter 2

(1) Ward, J. F. *Rev. Mod. Phys.* **1965**, *37*, 1-18.

(2) Yang, X.-L.; Anemian, R.; Zabulon, T.; Andraud, C.; Brasselet, S.; Ledoux-Rak, I. N.; Zyss, J. *Proc. SPIE* **2000**, *4106*, 222-229.

(3) Goswami, A. K.; Cross, L. E.; Buessem, W. R. *J. Phys. Soc. Jap.* **1968**, *24*, 279-281.

(4) Singer, K. D.; Kowalczk, T. C.; Nguyen, H. D.; Beuhler, A. J.; Wargowski, D. A. *Proc. SPIE* **1997**, *3006*, 326-337.

(5) Oudar, J. L.; Chemla, D. S. *J. Chem. Phys.* **1977**, *66*, 2664-2668.

(6) Levine, B. F.; Bethea, C. G. *J. Chem. Phys.* **1977**, *66*, 1070-1074.

(7) Lalama, S. J.; Garito, A. F. *Phys. Rev. A: At. Mol. Opt. Phys.* **1979**, *20*, 1179-1194.

(8) Marder, S. R.; Beratan, D. N.; Cheng, L.-T. *Science* **1991**, *245*, 103-106.

(9) Marder, S. R.; Perry, J. W.; Bourhill, G.; Gorman, C. B.; Tiemann, B. G.; Mansour, K. *Science* **1993**, *261*, 186-189.

(10) Bourhill, G.; Bredas, J.-L.; Cheng, L.-T.; Marder, S. R.; Meyers, F.; Perry, J. W.; Tiemann, B. G. *J. Am. Chem. Soc.* **1994**, *116*, 2619-2620.

(11) Zhang, C.; Ph.D. thesis, University of California: Los Angeles, CA, 1999.

(12) Bredas, J. L.; Adant, C.; Tackx, P.; Persoons, A.; Pierce, B. M. *Chem. Rev.* **1994**, *94*, 243-276.

(13) Bella, S. D.; Fragala, I.; Ratner, M. A.; Marks, T. J. *Chem. Mater.* **1995**, *7*, 400-404.

(14) Tretiak, S.; Chemnyak, V.; Mukamel, S. *Chem. Phys.* **1999**, *245*, 145-163.

(15) Painelli, A. *Chem. Phys.* **1999**, *245*, 185-197.

(16) Marder, S. R.; Gorman, C. B.; Meyers, F.; Perry, J. W.; Bourhill, G.; Bredas, J.-L.; Pierce, B. M. *Science* **1994**, *265*, 632-635.

(17) Lipinski, J.; Bartkowiak, W. *Chem. Phys.* **1999**, *245*, 263-276.

(18) Champagne, B.; Kirtman, B. *Chem. Phys.* **1999**, *245*, 213-226.

(19) Rao, V. P.; Wong, K. Y.; Jen, A. K.-Y.; Drost, K. J. *Chem. Mater.* **1994**, *6*, 2210-2212.

(20) Cho, B. R.; Son, K. N.; Lee, S. J.; Kang, T. I.; Han, M. S.; Jeon, S. J. *Tetrahedron Lett.* **1998**, *39*, 3167-3170.

(21) Chou, S.-S. P.; Hsu, G.-T.; Lin, H.-C. *Tetrahedron Lett.* **1999**, *40*, 2157-2160.

(22) Brasselet, S.; Cherioux, F.; Audebert, P.; Zyss, J. *Chem. Mater.* **1999**, *11*, 1915-1920.

(23) Rao, V. P.; Jen, A. K.-Y.; Chandrasekhar, J.; Namboothiri, I. N. N.; Rathna, A. *J. Am. Chem. Soc.* **1996**, *118*, 12443-12448.

(24) Rao, V. P.; Jen, A. K.-Y.; Wong, K. Y.; Drost, K. J. *Tetrahedron Lett.* **1993**, *34*, 1747-1750.

(25) P., S.-S.; Hsu, G.-T.; Lin, H.-C. *Tetrahedron Lett.* **1999**, *40*, 2157-2160.

(26) Song, S.; Lee, S. J.; Cho, B. R. *Chem. Mater.* **1999**, *11*, 1406-1408.

(27) Wong, K. Y.; Jen, A. K.-Y.; Rao, V. P.; Drost, K. J. *J. Chem. Phys.* **1994**, *100*, 6818-6825.

(28) Illien, B.; Jehan, P.; Botrel, A.; Darchen, A.; Ledoux, I.; Zyss, J.; L., M. P.; Lahcene, O. *New J. Chem.* **1998**, *22*, 633-641.

(29) Jen, A. K.-Y.; Rao, V. P.; Wong, K. Y.; Drost, K. J. *J. Chem. Soc., Chem. Commun.* **1993**, 90-92.

(30) Cheng, L.-T.; Tam, W.; Marder, S. R.; Steigman, A. E.; Rikken, G.; Spangler, C. W. *J. Phys. Chem.* **1991**, *95*, 10643-10652.

(31) William, D. J. *Angew. Chem. Int. Ed.* **1984**, *23*, 690-703.

(32) Singer, K. D.; Sohn, J. E.; King, L. A.; Gordon, H. M.; Katz, H. E.; Dirk, C. W. *J. Opt. Soc. Am. B: Opt. Phys.* **1989**, *6*, 1339-1350.

(33) Rao, V. P.; Cai, Y. M.; Jen, A. K.-Y. *J. Chem. Soc., Chem. Commun.* **1994**, 1689-1690.

(34) Katz, H. E.; Singer, K. D.; Sohn, J. E.; Dirk, C. W.; King, L. A.; Gordon, H. M. *J. Am. Chem. Soc.* **1987**, *109*, 6561-6563.

(35) Jen, A. K.-Y.; Rao, V. P.; Drost, K. J.; Wong, K. Y.; Cava, M. P. *J. Chem. Soc., Chem. Commun.* **1994**, 2057-2059.

(36) Jen, A. K.-Y.; Wong, K. Y.; Rao, V. P.; Drost, K. J.; Cai, Y. M. *J. Electron. Mater.* **1994**, *23*, 653-657.

(37) Cheng, L.-T.; Tam, W.; Stevenson, S. H.; Meredith, G. R.; Rikken, G.; Marder, S. R. *J. Phys. Chem.* **1991**, 10631-10643.

(38) Moylan, C. R.; Tweig, R. J.; Lee, V. Y.; Swanson, S. A.; Betterton, K. M.; Miller, R. D. *J. Am. Chem. Soc.* **1993**, *115*, 12599-12600.

(39) Burland, D. M.; Miller, R. D.; Reiser, O.; Tweig, R. J.; Walsh, C. A. *J. Appl. Phys.* **1992**, *71*, 410-417.

(40) Marder, S. R.; Cheng, L.-P.; Tiemann, B. G.; Friedli, A. C.; Blanchard-Desce, M.; Perry, J. W.; Skindhøj, J. *Science* **1994**, *263*, 511-514.

(41) Ahlheim, M.; Barzoukas, M.; Besworth, P. V.; Blanchard-Desce, F. A.; Hu, Z.-Y.; Marder, S. R.; Perry, J. W.; Runser, C.; Staehelin, M.; Zysset, B. *Science* **1996**, *271*, 335-337.

(42) Ermer, S.; Valley, L., R.; Lipscomb, G. F.; Van Eck, T. E.; Girton, D. G.; Leung, D. S.; Lovejoy, S. M. *Proc. SPIE* **1993**, *1853*, 183-192.

(43) Ermer, S.; Valley, L., R.; Lipscomb, G. F.; Van Eck, T. E.; Girton, D. G. *Appl. Phys. Lett.* **1992**, *61*, 2272-2274.

(44) Ermer, S.; Lovejoy, S. M.; Leung, D. S.; Warren, H.; Moylan, C. R.; Tweig, R. J. *Chem. Mater.* **1997**, *9*, 1437-1442.

(45) Shu, C.-F.; Tsai, W. J.; Chen, J.-Y.; Jen, A. K.-Y.; Zhang, Y.; Chen, T.-A. *J. Chem. Soc., Chem. Commun.* **1996**, 2279-2280.

(46) Singer, K. D.; Hubbard, S. F.; Schober, A.; Hayden, L. M.; Johnson, K. In *Characterization Techniques and Tabulations for Organic Nonlinear Optical Materials*; Kuzyk, M. G. D., C. W., Ed.; Marcel Dekker: New York, 1998, pp 311-513.

(47) Kajzar, F.; Horn, K.; Nahata, A.; Yardley, J. T. *MCLC S&T, Sec. B., Nonlin. Opt.* **1994**, *8*, 205-217.

(48) Karna, S. P.; Zhang, Y.; Samoc, M.; Prasad, P. N.; Reinhardt, B. A.; Dillard, A. G. *J. Chem. Phys.* **1993**, *99*, 9984-9993.

(49) Clays, K.; Persoons, A. *Phys. Rev. Lett.* **1991**, *66*, 2980-2983.

Chapter 3

Thiazole and its use in novel EO chromophores as part of a gradient bridge system

3.1 Introduction

Thiazole is a heteroaromatic compound that occurs naturally in chicken and sesame seeds. Condensation of α,β-dichloroether with barium thiocyanate by Hanstzsch and Arapides in 1888 yielded the first synthesis of thiazole, which was identified by its pyridine-like odor.[1] The atoms in the thiazole are numbered as shown in Figure 3.1, which is accepted by The Ring Index and Chemical Abstracts.[2]

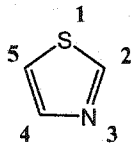

Figure 3.1 The numbering scheme for the heteroaromatic thiazole ring.

The intrinsic charge distribution of the thiazole ring gives rise to a dipole moment. This dipole moment has most of its negative charge situated near the nitrogen atom and most of its partial positive charge displaced slightly toward the sulfur atom. The dipole moment has been experimentally calculated at 1.61 +/- 0.03

D.[3] Due to this dipole moment, imparted by the electronegativity of sulfur and nitrogen, the reactivity of the hydrogens on the ring are affected. The acidicity of these hydrogens can be listed as follows: 2>5>>4. This reactivity scale explains why there are a vast amount of 2-substituted thiazole derivatives compared to that of thiazoles with substitutions at positions 5 and 4.

3.2 Early work of thiazole incorporated organic dyes

Thiazole has been used for many applications as a component of a conjugated backbone. One of its uses exists in the field of photography, where the conjugated molecule acts as a desensitizing dye.[4] As textile dyes, a class of thiazoloazamethine dyes was shown to hold an excellent affinity for polymer fibers.[5-7] Thiazole derivatives and Cu (II) complexes have demonstrated corrosion inhibition in acidic media for copper metal.[8-10]

Perhaps the most influential area in which the conjugated thiazole unit has been used is the herbicidal and pharmaceutical arena. A number of aminophenyl derivatives of thiazolium have been listed as weed-killers and as a regulator of the growth factor in plants in a number of patents.[11-13] Vinyl derivatives of 3,4,5-substituted thiazolium dyes have been known to possess both bactericidal and enzymatic action.[14] Other derivatives of thiazolium, styrylic, pyrrolic, and amino-substituted; and methane cationic dyes, hold appealing anthelmintic properties.[15,16] In particular, the amino-derivatives of thiazolium have been used as accelerators of

the catabolism and activators of cellular exchanges.[17] Finally, it should be mentioned that o- or p-hydroxystyryl thiazole dyes have been used as indicators in nonaqueous media for protolytic titrations.[18]

3.3 Thiazole used in organic NLO chromophores

Interest in synthetically incorporating thiazole into EO chromophore has surged in the last ten years.[19-23] Researchers had only examined the effect of thiazole on hyperpolarizability via various theoretical approaches. In 1990, Dirk and coworkers at AT&T Bell Laboratories compared a number of diazo dyes containing thiazole derivatives with their phenyl analogues.[24,25] As seen in Figure 3.2, chromophores A and B displayed hyperpolarizabilities of 90 and 180 (10^{-30}cm^5/esu), respectively, using EFISH at 1.579μm while their thiazole (C) and chlorothiazole (D) analogues, chromophores C and D, displayed a substantial increase in hyperpolarizability with values of 250 and 530 (10^{-30} cm^5/esu).

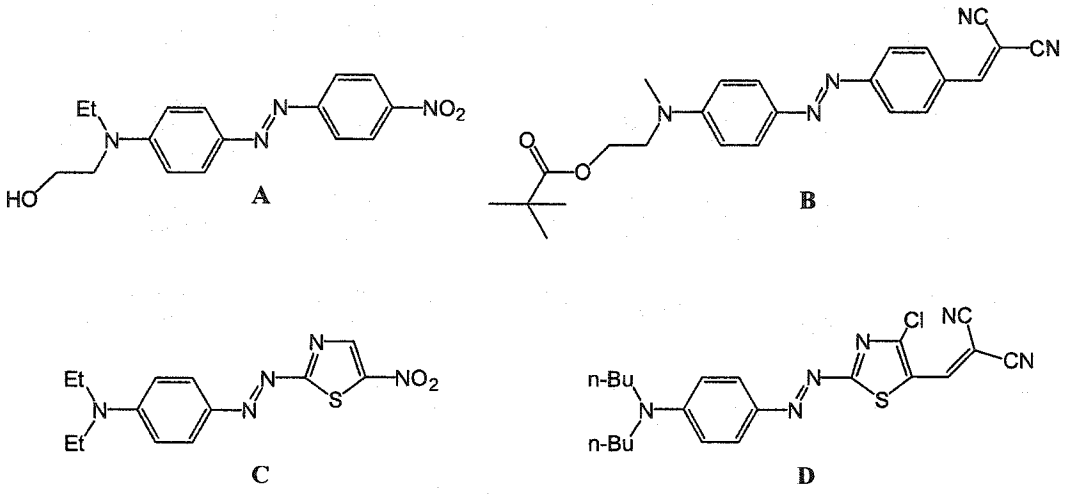

Figure 3.2 Diazo chromophores used in Dirk study.

Other thiazole containing chromophores have also been incorporated into polymethylmethacrylate (achieving an r_{33} value of 12pm/V),[26] epoxy based,[22] and polyimide based polymer systems as pendant groups. Moylan, Miller, and Wang have also experimentally demonstrated an increase in the hyperpolarizability using thiazole.[27,28]

A study by Breitung *et al.* examined β values of thiophene and thiazole-containing chromophores using theoretical calculations.[29] Molecular hyperpolarizabilities were calculated using ZINDO (sum-over-states) formalism. Examining an array of phenyl, thiophene, and thiazole-based NLO chromophore conformers, the study predicted that β (at 1.907nm) would be significantly higher in cases involving the placement of thiazole before the acceptor, which reinforced results from previous theoretical studies.[30]

The most common arguments explaining why thiazole-substituted chromophores computationally and experimentally display larger hyperpolarizabilities can be found in the concepts of aromatic delocalization energy (ADE), as well as π-electron density distribution. Through examination of ADE, it can be predicted that thiazole-containing chromophores could possess larger hyperpolarizabilities due their decreased ADE compared to that of their thiophene and aryl counterparts. The ADE of thiazole, thiophene, and phenyl are 25, 29, and 36 kcal/mol, respectively.[31] However, ADE alone cannot explain the differences in the regiochemical orientation of the thiazole-containing chromophores found in the Varansi study.

With all the experimental work that has been done concerning thiazole containing EO chromophores, one major aspect sill has not been explored – the orientation of the thiazole ring in conjugated system (Figure 3.3). The intrinsic dipolar charge distribution of the thiazole ring offers the possibility that it may act as an active bridging molecule. When carbon-2 is attached to the donor end and carbon-5 attached to the acceptor end of the molecule, it is referred to in this dissertation as thiazole "backward," since the charge distribution of thiazole opposes the charge distribution of the overall dipolar chromophore. Alternatively, when carbon-5 is attached to the donor end and carbon-2 attached to the acceptor end of the molecule, it will be referred to here as thiazole "forward," since the charge distribution of thiazole coincides with the direction of the charge distribution of the overall dipolar chromophore.

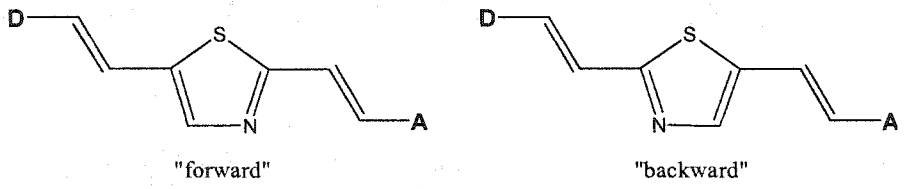

Figure 3.3 Structural representations of thiazole "forward" and "backward." **D** represents the donor end and **A** the acceptor end of the molecule.

The Breitung study illustrated the importance of the orientation of thiazole with respect to the chromophore backbone.[29] The "forward" chromophore (Figure 3.4) predicted a nearly two-fold enhancement in the β_μ value (defined as the hyperpolarizability along the dipole moment vector), compared to that of its "backward" analogue.

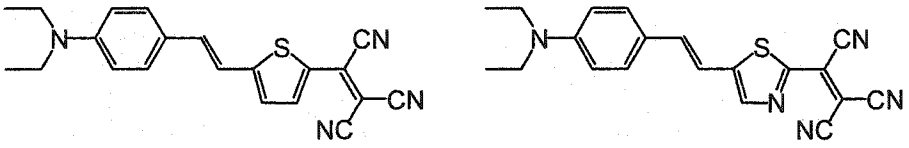

$\beta = 90 \times 10^{-30}$ cm^5 esu^{-1} $\beta = 177 \times 10^{-30}$ cm^5 esu^{-1}

Figure 3.4 Thiazole chromophores from the computational Breitung study. Values were calculated at 1907 nm.

The Breitung study computationally demonstrates that the conformational orientation of the thiazole ring holds a potentially powerful tool in dictating the degree of hyperpolarizability in an organic EO material. No study up to this point has

experimentally verified the predicted superiority of thiazole in this particular "forward" orientation. Only the hyperpolarizability of various chromophores containing thiazole in a "backward" orientation has been explored experimentally.

3.4 The Gradient Bridge Concept

Bridge components in nonlinear optical chromophores are designed to be electron conduits in charge transfer between the donor and acceptor groups. During electric field induced perturbation of the electronic distribution, a desirable bridge component will present virtually no energetic barrier or even promote such a transfer. As noted earlier, the use of a thiophene unit is preferred over that of phenyl ring since studies have shown that the reduced aromaticity of thiophene leads to increased hyperpolarizability. Thiophene represents an example of a bridge that presents a low energetic barrier. An example of a bridge that promotes such a transfer is the quinoidal component. Acquiring the aromatic stabilization energy of benzene during charge transfer acts as the driving force behind the perturbation of electronic charge from donor to acceptor. However, quinoidal bridges are synthetically difficult to incorporate into chromophore structures and also have poor chemical and thermal stability.

The motivation of the research presented in this dissertation is to incorporate bridge components that actively participate in electron transfer, rather than act as passive electron conduits. It could be possible to find an improved bridge through

the use of novel structural components or systematic placement of bridge components along the conjugated system. The model being explored through the work presented in this dissertation is the concept of a gradient bridge. A gradient bridge can be visualized as an "electron waterfall." This representation is illustrated in Figure 3.5, where the different portions of a chromophore decrease in electron donating ability (or alternatively, increasing electron acceptability). Each segment of the chromophore aids in transferring the charge towards the acceptor upon application of an external electric field.

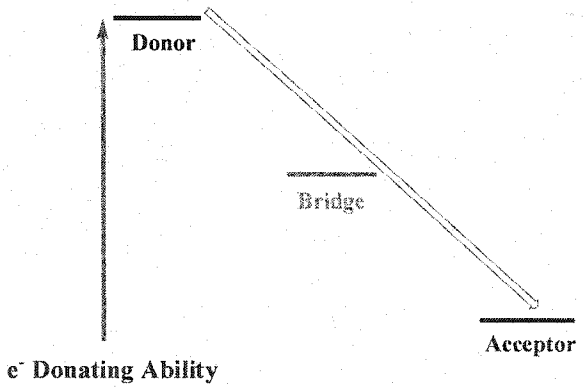

Figure 3.5 A schematic representation of the gradient bridge concept.

This concept could be used to dictate the use of certain moieties along the chromophore backbone. Phenyl components have been used in several NLO chromophores that have given some of the highest μβ values ever reported. For example, some high μβ chromophores use an amino benzene-type donor.[32]

However, in order to compensate for the poor electron transfer ability of the phenyl ring, the other components of the chromophore must help to donate and accept electron density from either side of the phenyl ring. Again, it is useful to envision the "electron waterfall" analogy, where a strong electron donor donates into the phenyl ring while another component can help pull electron density towards the acceptor during charge transfer.

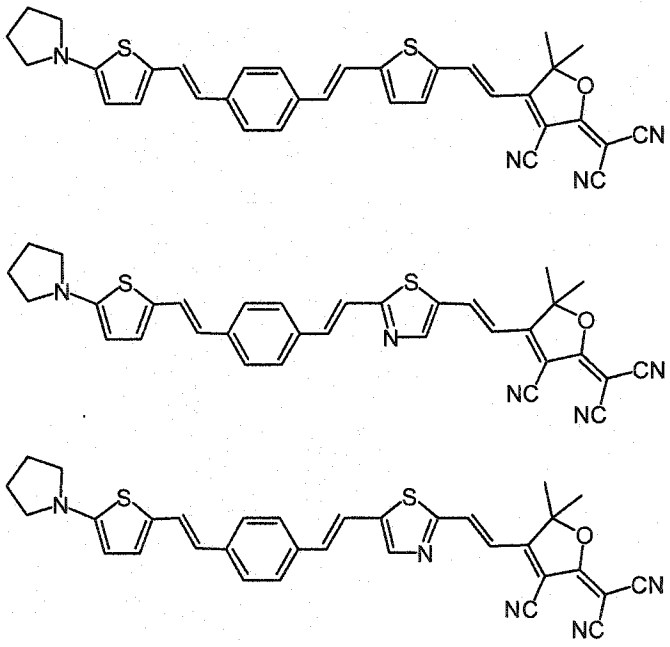

Figure 3.6 Proposed 3-ring gradient bridge chromophores.

To fully investigate this gradient bridge concept, a series of chromophores that possess this gradient bridge type of backbone were originally examined. The structures of the chromophores involved in this initial 3-ring gradient bridge system are displayed in Figure 3.6.

The systematic synthesis and examination of the hyperpolarizability of these compounds through HRS could provide evidence that a gradient bridge exists. This also could lead to a better understanding of the electron transfer across the bridge of chromophores. Furthermore, the results could dictate the synthesis of future EO chromophores that could be incorporated into polymers for device applications.

Notes to Chapter 3

(1) Hantzsch, A.; Arapides, L. *Berichte*, 1888; Vol. 21.

(2) Patterson, A. M.; Campbell, L. T.; Walker, D. F. *The Ring Index*; 2nd ed.; American Chemical Society, 1960.

(3) Bak, B.; Christensen, D.; Hansen-Nygaard, L.; Rastrup-Andersen, J. *J. Mol. Spectrosc.* **1962**, *9*, 222-224.

(4) Knott, E. B. *J. Chem. Soc.* **1952**, 4099-4106.

(5) Rangnekar, D. W.; Maladkar, G. J. *Phosphorus, Sulfur, and Silicon and the Related Elements* **2000**, *164*, 199-205.

(6) Elkholy, Y. M.; wahba Erian, A.; Helal, M. H. *Pigment & Resin Technology* **2001**, *30*, 168-170.

(7) Maradiya, H. R.; Patel, V. S. *Chem. Heterocycl. Compd.* **2003**, *39*, 357-363.

(8) Vastag, G.; Szocas, E.; Shaban, A.; E., K. *Pure Appl. Chem.* **2001**, *73*, 1861-1869.

(9) Quraishi, M. A.; Wajid Khan, M.; Ajmal, M.; Muralidharan, S.; Iyer, S. V. *Anti-Corrosion Methods and Materials* **1996**, *43*, 5-8.

(10) El-Mossalomy, E. H.; Ibahim, A. A. *Pigment & Resin Technology* **2002**, *31*, 375-380.

(11) Takahashi, T.; Satake, K. *Yakugaku Zasshi* **1951**, *71*, 905-911.

(12) Reifschneider, W.; US 3511850, 1970, p p5.

(13) Reifschneider, W.; US 3682879, 1972, p p5.

(14) Takahashi, T.; Hayami, M. *Jpn. J. Pharmacol.* **1961**, *81*, 1419-1426.

(15) Phillips, A. P.; Burrows, R. B.; ZA6805975, 1969, p p22.

(16) Co, B. W. a.; GB 1246649, 1971, p p 7.

(17) Banno, M.; Yasui, S.; JP45033887, 1970, p p 4.

(18) Blazsek-Bodo, A.; Vernes, M.; Szurkos, A. *Farmacia Bucharest* **1974**, *22*, 345-252.

(19) Jug, K.; Chiodo, S.; Janetzko, F. *Chem. Phys.* **2003**, *287*, 161-168.

(20) Karna, S. P.; Keshari, V.; Prasad, P. N. *Chem. Phys. Lett.* **1995**, *234*, 390-394.

(21) Lee, S.-H.; Otomo, A.; Nakahama, T.; Yamanda, T.; Kamikado, T.; Yokoyama, S.; Mashiko, S. *J. Mater. Chem.* **2002**, *12*, 2187-2188.

(22) Leng, W.; Zhou, Y.; Xu, Q.; Liu, J. *Macromolecules* **2001**, *34*, 4774-4779.

(23) Shu, C.-F.; Wang, Y.-K. *J. Mater. Chem.* **1998**, *8*, 833-835.

(24) Dirk, C. W.; Katz, H. E.; Schilling, M. L. *Chem. Mater.* **1990**, *2*, 700-705.

(25) Dirk, C. W.; Caballerro, N.; Kuzyk, M. G. *Chem. Mater.* **1993**, *5*, 733-737.

(26) Watanabe, T.; Amano, M.; Tomaru, S. *Jpn. J. Appl. Phys.* **1994**, *33*, 1683-1685.

(27) Wang, Y.-K.; Shu, C.-F.; Breitung, E. M.; McMahon, R. J. *J. Mater. Chem.* **1999**, *9*, 1449-1452.

(28) Wang, X.; Yang, K.; Kumar, J.; Tripathy, S. K.; Chittibabu, K. G.; Li, L.; Lindsay, G. *Macromolecules* **1998**, *31*, 4126-4134.

(29) Breitung, E. M.; Shu, C.-F.; McMahon, R. J. *J. Am. Chem. Soc.* **2000**, *122*, 1154-1160.

(30) Varanasi, P. R.; Jen, A. K.-Y.; Chandrasekhar, J.; Namboothiri, I. N. N.; Rathna, A. *J. Am. Chem. Soc.* **1996**, *118*, 12443-12448.

(31) Gilchrist, T. L. *Heterocyclic Chemistry*; John Wiley & Sons: New York, 1985.

(32) Bourhill, G.; Bredas, J.-L.; Cheng, L.-T.; Marder, S. R.; Meyers, F.; Perry, J. W.; Tiemann, B. G. *J. Am. Chem. Soc.* **1994**, *116*, 2619-2620.

Chapter 4

The design and synthesis of gradient bridge EO chromophores

4.1 Synthetic rationale

Bridges act as electron conduits in the charge transfer process between the donor and acceptor groups. It could be possible to find an improved bridge through the use of novel structural components or systematic placement of bridge components along the conjugated system. The model explored in this dissertation is that of a gradient bridge. A gradient bridge can be visualized as an "electron waterfall," where the different portions of a chromophore decrease in electron donating ability (or alternately, increasing electron accepting ability). Each segment of the chromophore aids in transferring the charge towards the acceptor upon application of an external electric field.

The ability to attach additional functional groups on the phenyl ring of the gradient bridge chromophore would allow attachment of bulky inactive substituents, such as crosslinkable dendrimers (Figure 4.1). This feature on the gradient bridge may provide a useful approach in minimizing electrostatic interactions between chromophores. Indeed, a phenyl ring is a good candidate due to its potential ease in functionalization. However, the phenyl ring is considered a poor π-electron bridge.

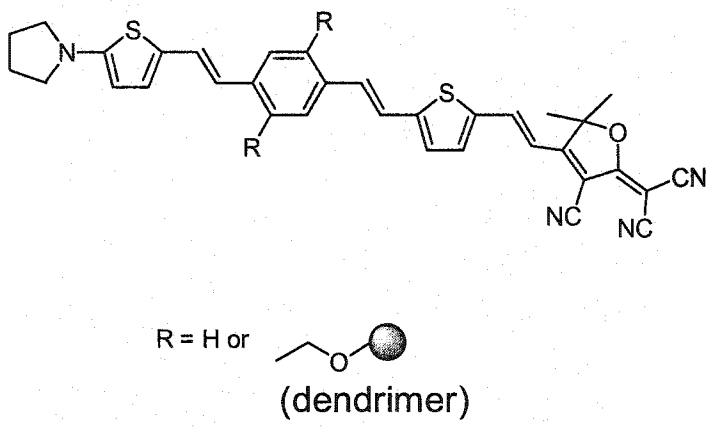

Figure 4.1 Gradient bridge chromophore initially examined.

A good bridge should provide a small or negligible energy barrier during charge transfer. A charge transfer through benzene would have a large energy barrier (larger bandgap) since it undergoes a benzoidal to quinoidal transformation and therefore loses aromaticity. The use of a gradient bridge works to compensate for this energetic barrier and provide a more efficient electron-transfer mechanism when this material is exposed to strong electrical fields.

4.2 Gradient Bridge Chromophore Synthesis

For the synthesis of gradient bridge chromophore **9**, as shown in Figure 4.2, the donor aldehyde intermediate **1** was synthesized as previously described.[1] This intermediate was coupled via Horner-Emmons with the bridge phosphonate intermediate **2** to produce the donor bridge bromide intermediate **3** in good yield (87%). The intermediate **2** was synthesized as previously described.[2] Subsequent formylation of **2** with *n*BuLi and N,N-dimethylformamide (DMF) produced the donor bridge aldehyde intermediate **4** in excellent yield. The addition of the third aromatic ring was accomplished through Horner-Emmons coupling of the aldehyde **4** with the bromothiophenephosphonate intermediate **5**. The synthesis of this phosphonate building block (bromo derivative) has been described previously.[3] The intermediate **6** was formylated with *n*BuLi and DMF to produce the aldehyde intermediate **7**, which held poor solubility in organic solvents, resulting in poor yield following purification by silica gel chromatography. The intermediate **7** was coupled in a Knoevenagel condensation with the tricycanofuran (TCF) acceptor **8** to produce the gradient bridge chromophore **9**. The isolation of the TCF acceptor was accomplished through procedures previously described by Ermer and coworkers.[4]

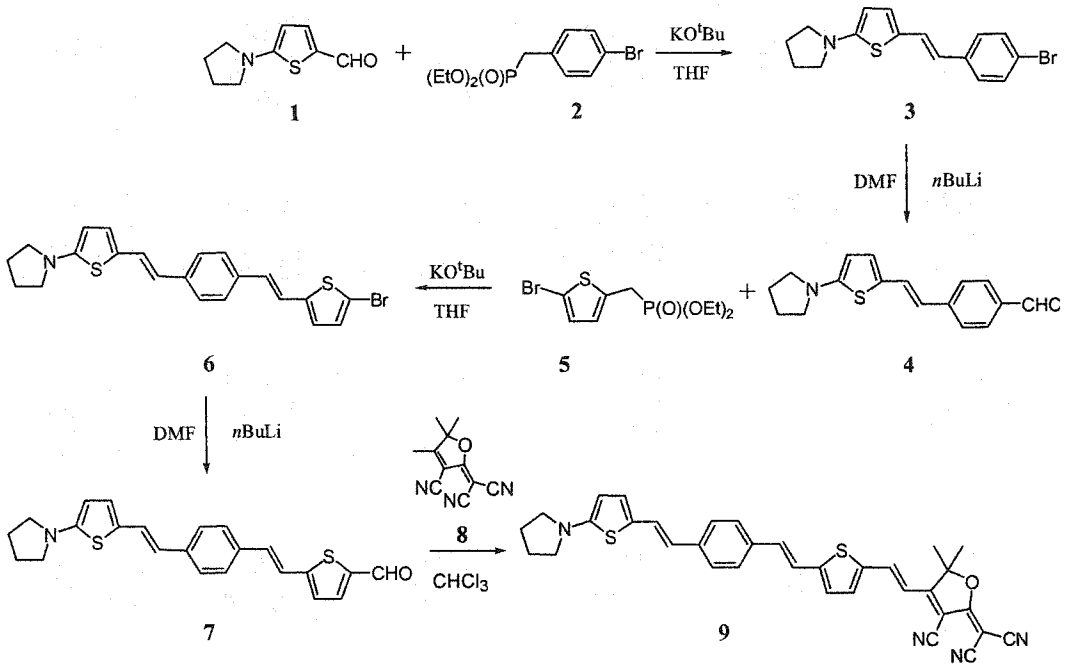

Figure 4.2 Structure and synthesis of 3-ring gradient bridge chromophore **9**.

Chromophore **9** had a significantly reduced solubility in common organic solvents, mainly due to its three conjugated aromatic units. Chromophore **9** was only soluble on a sub-millimolar scale in chloroform. In addition, the HRS results at 1.3μm showed unusual results that suggested that these three-ring system chromophores could be aggregating and rotating in solution in ways that make intercomparison of these chromophores particularly difficult. Therefore, it became necessary to reduce the number of aromatic rings in the system, as a three ring system would not only be difficult to characterize but also become impractical to apply its results to the bulk material due to its extremely poor processability. It became evident from these initial results that the gradient bridge system would have

be altered in order to ensure that the resulting series of chromophores could be effectively probed to determine the success or failure of the gradient bridge concept.

The switch to a two-ring gradient bridge system could still demonstrate the feasibility of the concept and would more closely model the theoretical study by Breitung and coworkers.[5] In this study, a number of two-ring system gradient chromophores (Figure 4.3) were synthesized.

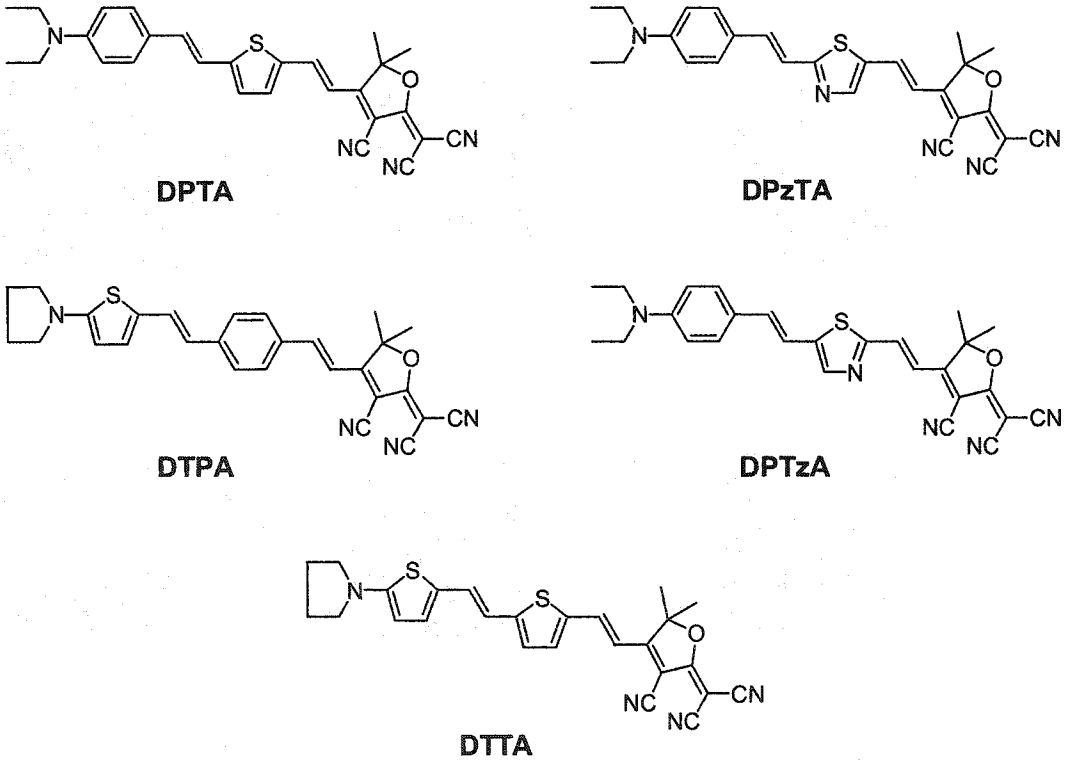

Figure 4.3 Two-ring gradient chromophores for systematic study.

The notation system for these gradient bridge chromophores are as follows: D designates the diethyl- or pyrrolidine- amino-based donor portion, P stands for the phenyl ring, T represents the thiophene ring, and A stands for the TCF acceptor component. Tz stands for thiazole oriented so the nitrogen on the ring is faced toward the acceptor end, also known as thiazole "forward." The zT term stands for thiazole oriented so the nitrogen on the ring is faced toward the donor end, also known as thiazole "backward."

As with the three-ring system, the aim of this investigation is to examine the hyperpolarizabilities of these compounds through HRS to provide evidence whether or not a gradient bridge is successful. Furthermore, the results could dictate the synthesis of future EO chromophore backbones that could easily be incorporated into polymers for device applications. Unlike the di- or tri-cyano vinyl-based acceptor used in the Breitung study, the major difference in the chromophore design would be in the use of the stronger 2-dicyanomethylene-3-cyano-4,5,5-trimethyl-2,5-dihydrofuran acceptor (TCF). The TCF acceptor provides increased chemical stability compared to that of di- and tri-cyano vinyl-based acceptors. This study would also attempt to become the first example of thiazole used as a bridge in what the Breitung paper referred to as the "matched" case, or what this study denotes as thiazole "forward." The only examples of thiazole incorporated into NLO chromophores have been with the thiazole in a "backward" configuration.[6-18]

The gradient chromophore DPTA was synthesized in the Dalton group by Dr. Olivier Clot and its synthesis has been described previously.[19] The synthesis of

DTPA was accomplished in one step using the donor bridge intermediate **4** from the 3-ring gradient system and subjecting it to Knoevenagel condensation with the TCF acceptor (Figure 4.4).

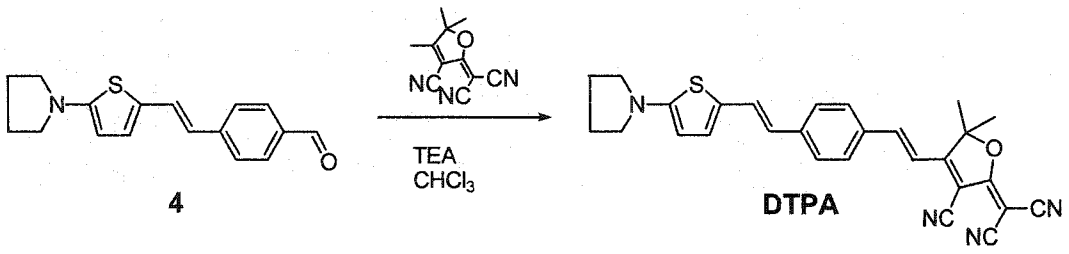

Figure 4.4 Synthesis of the DTPA gradient bridge chromophore.

The synthesis of gradient bridge chromophore DTTA was achieved by synthesizing the pyrrolidine-based amino donor bridge intermediate **12** using a modified procedure from Hudson, where the piperidine-based amino donor bridge intermediate was previously reported.[20] The TCF acceptor coupled with intermediate **12** via Knoevenagel condensation produced the DTTA chromophore.

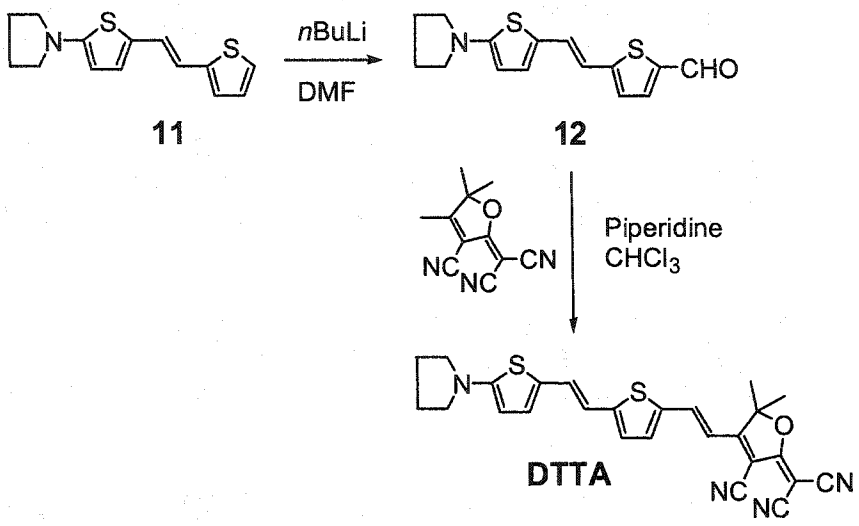

Figure 4.5 Synthesis of the DTTA gradient bridge chromophore.

For the synthesis of chromophore DPzTA (Figure 4.6), the commercially available starting material N,N-diethyl-4-benzaldehyde, **14**, was subjected to Horner-Emmons coupling with the thiazole "backward" phosphonate intermediate **15** to produce the donor bridge product. The intermediate **15** was synthesized as previously described.[21] Subsequent formylation produced the donor bridge aldehyde intermediate **17** in good yield (80%). Attachment of the TCF acceptor was successful through Knoevenagel condensation using a catalytic amount of triethylamine to produce the thiazole "backward" chromophore DPzTA.

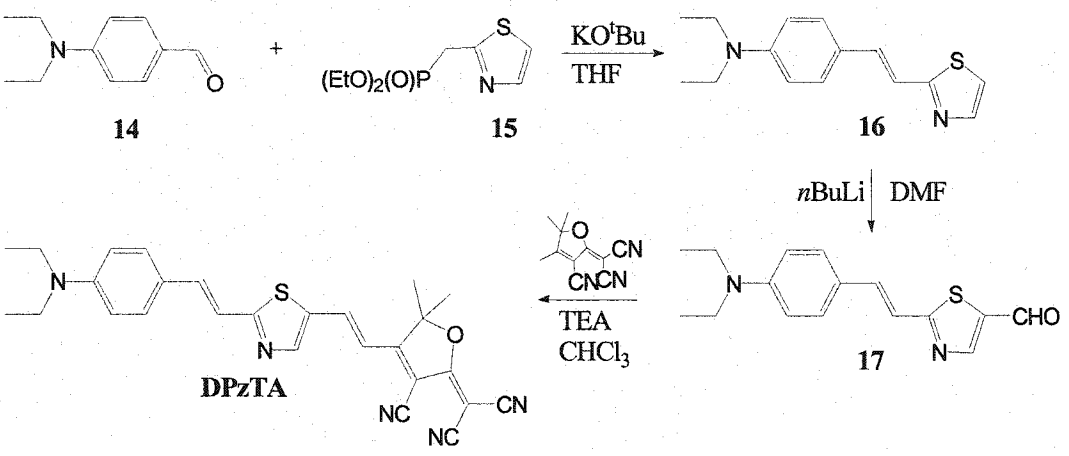

Figure 4.6 Synthesis of the DPzTA gradient bridge chromophore.

The incorporation of thiazole "forward" in the π-electron backbone proved to be the most synthetically challenging. To couple the donor and bridge component, the initial reaction of choice was a Horner-Emmons coupling due to its ease of work-up and purification. Using a triphenylphosphonium salt in a standard Wittig reaction produces triphenylphosphineoxide as a by-product, which is soluble in common organic solvents and difficult to separate from the desired product. On the other hand, the use of the phosphonate functionality in a Horner-Emmons coupling results in a phosphonate ester salt by-product, which is water-soluble and can be readily separated from the desired product. The phosphonate functionality was then attached on the thiazole component. Its synthesis (Figure 4.7) started from 5-hydroxymethylthiazole, **19**, which was chlorinated from 5-hydroxymethylthiazole using mild conditions of carbon tetrachloride and triphenylphosphine in benzene.

The 5-chloromethylthiazole intermediate **20** was then quantitatively converted to the thiazole "forward" phosphonate **21** via an Arbuzov mechanism using triethylphosphite.

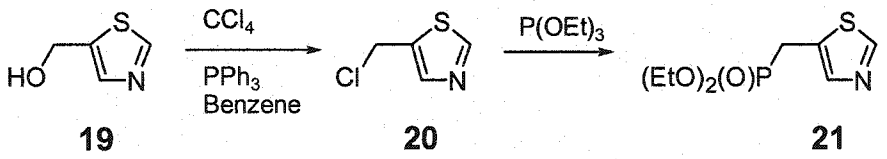

Figure 4.7 Synthesis of the thiazole "forward" phosphonate building block.

The coupling between the thiazole "forward" phosphonate and the diethylaminobenzaldehyde donor was attempted several times (Figure 4.8).

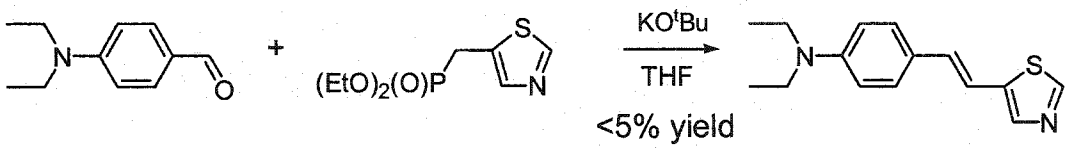

Figure 4.8 Initial coupling between donor and thiazole "forward."

^{1}H NMR revealed the resulting crude product consisted of a mixture of the intended product and unreacted donor aldehyde, with the coupled product comprising less than five percent of the crude mixture.

These two components of the crude mixture could not be separated via silica gel chromatography due to their remarkably similar R_f values. In addition, the thiazole "forward" phosphonate appeared to have decomposed during the course of the reaction. The explanation for this can be found in looking at the electronic configuration of the resulting anion. As shown in Figure 4.9, there is a distinction between the inherent electronic stability between the anion of thiazole "forward" and "backward." In the case of the thiazole "backward" phosphonate, the predominate anion that forms is at the phosphonate methylene group. In the case of thiazole "forward" phosphonate, however, the anion that forms is a competition could be either from the phosphonate methylene group or from the hydrogen at carbon-2. where the experimental results suggest that H-2 deprotonation is favored over the formation of the phosphonate ylide.

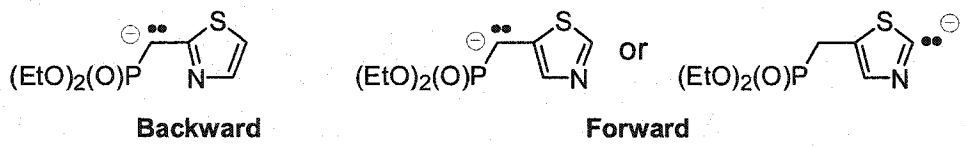

Figure 4.9 Electronic configuration of the anionic thiazole phosphonate isomers.

These results then motivated the reversal of the reactive functionalities on the donor and bridge. In this new scheme, the phosphonate would be on the amino donor and the aldehyde on the thiazole (Figure 4.11). 5-Thiazolecarboxaldehyde was obtained via literature procedures (Figure 4.10) starting from the unsubstituted

thiazole ring, blocking the 2-position with the trimethylsilyl (TMS) group through lithiation of position-2, followed by quenching with trimethylsilylchloride. [22] This intermediate was then formylated at the 5-position with *n*BuLi and quenched with N-formylmorpholine to form the TMS-protected thiazolecarboxaldehyde intermediate. Finally, the intended thiazole derivative was formed through deprotection of the TMS group with dilute hydrochloric acid.

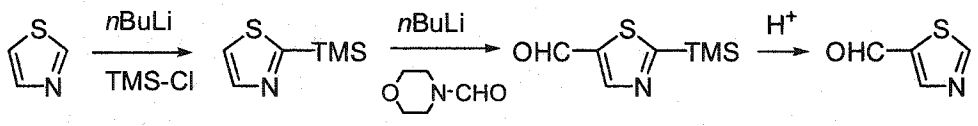

Figure 4.10 Synthesis of the 5-formylthiazole building block.

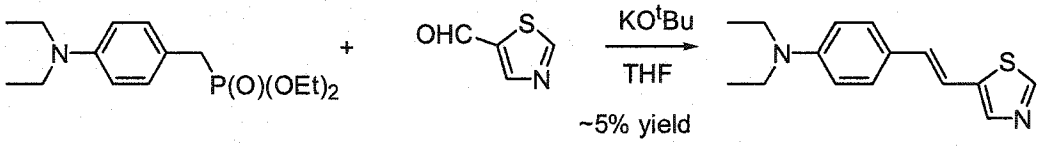

Figure 4.11 Proposed coupling between donor phosphonate and thiazole aldehyde.

The attempted coupling between these new reagents resulted in only ~5% product formation (Figure 4.11). However, ^{1}H NMR revealed that the 5-thiazolecarboxaldehyde had been completely consumed and there was still quite a bit of unreacted donor phosphonate. To ensure that the potassium *tert*-butoxide base is not reacting directing with the 5-thiazolecarboxaldehyde substrate, this base was added to the donor phosphonate directly in dry THF and allowed to stir for 40

minutes before the addition of the thiazole derivative. These conditions produced the same results as the addition of the base to both substrates in the same reaction pot. TLC indicated the complete consumption of the 5-thiazolecarboxaldehyde and ^{1}H NMR showed a substantial amount of apparent "unreacted" donor phosphonate. These results from these different reaction conditions suggested the possibility that the anion of the donor phosphonate is so "hot," or reactive, that this anion actually underwent an acid-base reaction with 5-thiazolecarboxaldehyde. The proposed reaction to explain the resulting NMR spectrum is shown in Figure 4.12. The anion of the donor phosphonate preferentially attacks the hydrogen on position-4 or position-2.

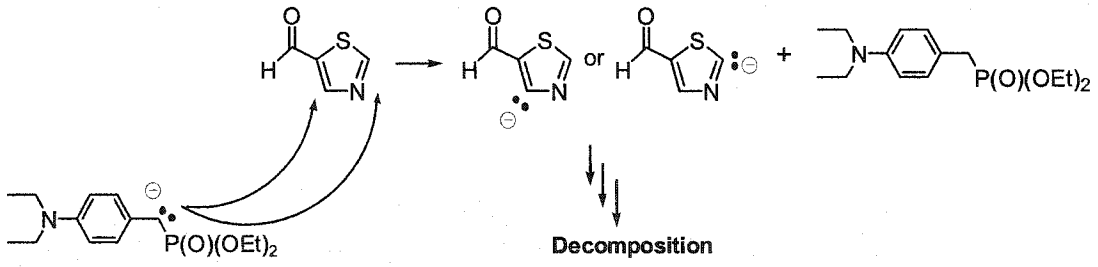

Figure 4.12 Proposed mechanism between donor phosphonate and thiazole aldehyde.

Other than pKa values for thiazole, thiazolium salts, and substituent effects on the highly reactive position-2 hydrogen (in DMSO), there are **no** published pKa values for the thiazole hydrogen at position-4 or position-2, especially with an

electron-withdrawing substituent at position-5.[23-25] This acid-base reaction regenerates the original donor phosphonate that is still evident by ^{1}H NMR and also produces an anionic 5-formylthiazole, which then undergoes decomposition. Additional couplings were attempted at –78 °C to examine if this proposed thiazole anion would be more stabilized. However, after quenching the reaction at –78 °C, the resulting reaction mixture was identical to that conducted originally at 0 °C.

This revelation in thiazole-5-carboxaldehyde reactivity prompted the use of a less basic donor anion, which was found in the Wittig salt functionality (Figure 4.13).[26,27] With the use of this particular functionality, the anion of the donor Wittig salt is stabilized by the neighboring formal positive charge on the phosphorus atom, resulting in a less basic anion. This stabilization results in a drop in the basicity of the anion, where the acid-base reaction of the donor anion with 5-thiazolecarbozaldehyde becomes unfavorable and now the nucleophilic attack with the carbonyl group on thiazole will occur with greater frequency. The donor Wittig salt was produced directly from the benzyl alcohol functionality with triphenylphosphonium bromide per methods reported previously by Zhang, *et al.*[28]

Reacting the amino donor Wittig salt **22** with 5-formylthiazole **23** in ethanol with sodium ethoxide produced the desired coupled product in 60% yield. The reaction, due to the stability of both the threo and erythro oxaphosphetane intermediates produced the desired donor-bridge component as a mixture of cis and trans isomers in a ratio of roughly 1:2.

This mixture was then isomerized to the all-trans product **24** by refluxing the mixture in THF using a few crystals of iodine. Formylation of the donor-bridge product was straightforward using *n*BuLi/DMF to produce intermediate **25**. Coupling of this donor bridge aldehyde with the TCF acceptor was achieved through the use of ammonium acetate as the base. This method proved to isolate the first thiazole "forward" containing chromophore DPTzA in 78% yield. The added advantage of using this base is the precipitation of the analytically pure product, without the need for purification since the byproducts are alcohol soluble.

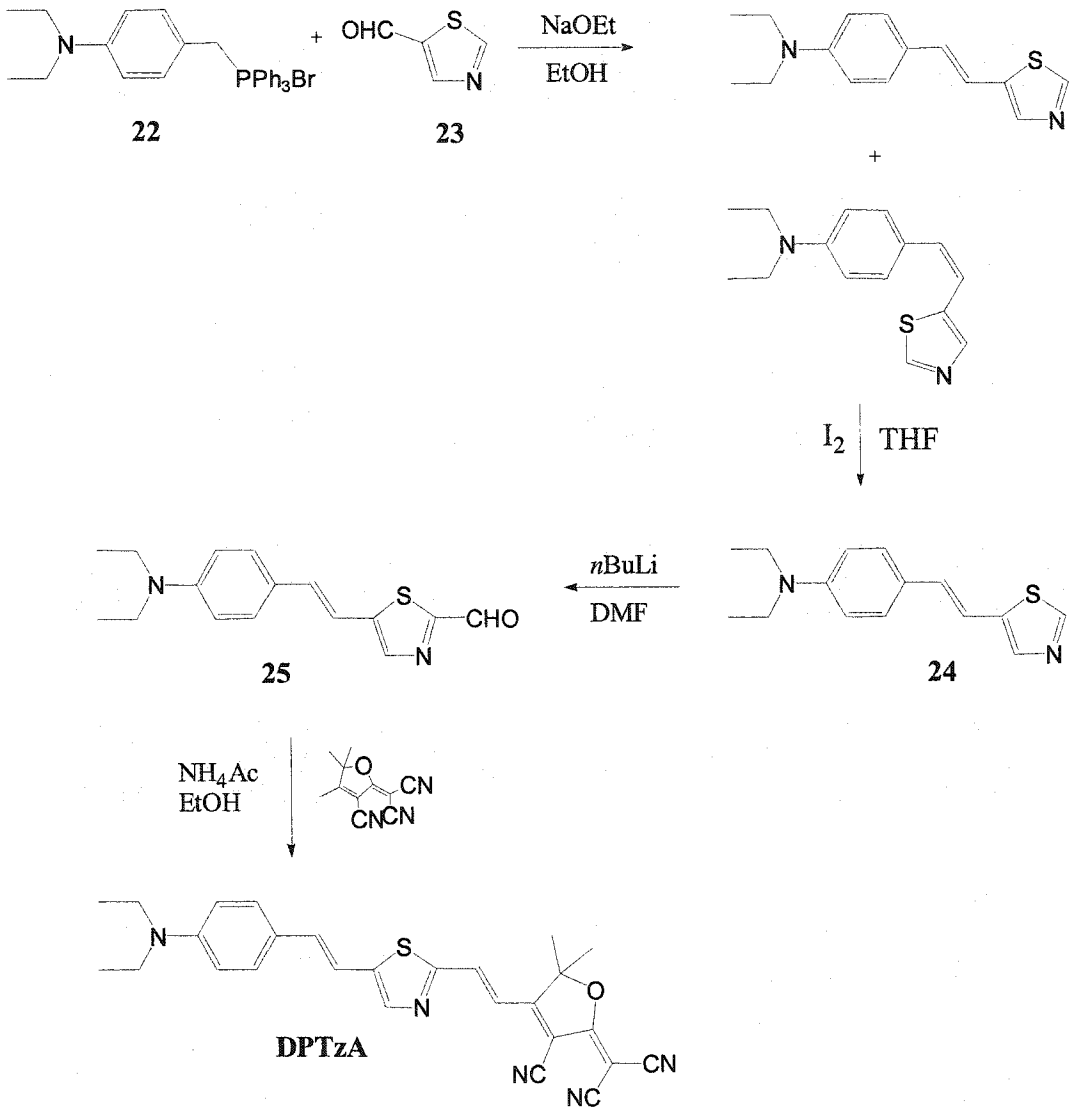

Figure 4.13 Synthesis of the first thiazole "forward" chromophore DPTzA.

4.3 Gradient bridge chromophores for Electro-Optic (EO) activity

Besides the central focus of determining the first order hyperpolarizability of the gradient bridge chromophores, examining the bulk nonlinear optical response of

some of these novel chromophores was explored. The initial chromophores do not possess the necessary functionality to be incorporated into a polymer matrix satisfactorily in order to determine their nonlinear optical response (r_{33}). The chromophores chosen were derivatives of the DPTA chromophore, which would act as a "control" in comparison with a derivative of the DPTzA chromophore (Figure 4.14). These new chromophores would provide a direct comparison between a novel thiazole "forward" chromophore with its thiophene analogue. For ease of designation, these derivatives are denoted as bDPTA and bDPTzA, respectively, with "b" standing for the dibutyl chain located on the donor end of the molecule.

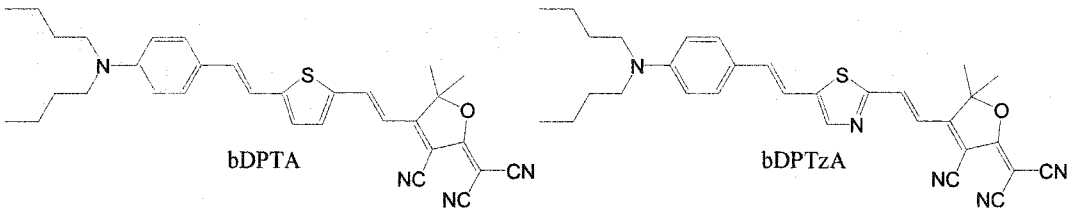

Figure 4.14 bDPTA and bDPTzA chromophores for EO activity study.

The chosen alteration to the principle family of gradient bridge chromophores that was chosen was an expansion of the alkyl chains on the donor end to n-butyl chains. This change provided the resulting chromophores with the necessary functionality to make them appreciably soluble in common organic spin-casting solvents. The methodologies used to synthesize these gradient bridge chromophore

derivatives were the same as isolating the original diethyl donor-containing chromophores (Figures 4.15 and 4.16).[19]

In the synthesis of chromophore bDPTA the thiophene phosphonate intermediate, **28**, was made according to previously described procedures,[3] starting from thiophene-2-methanol. The synthesis of chromophore bDPTzA involved similar methodology employed in synthesizing the diethylamino donor version.

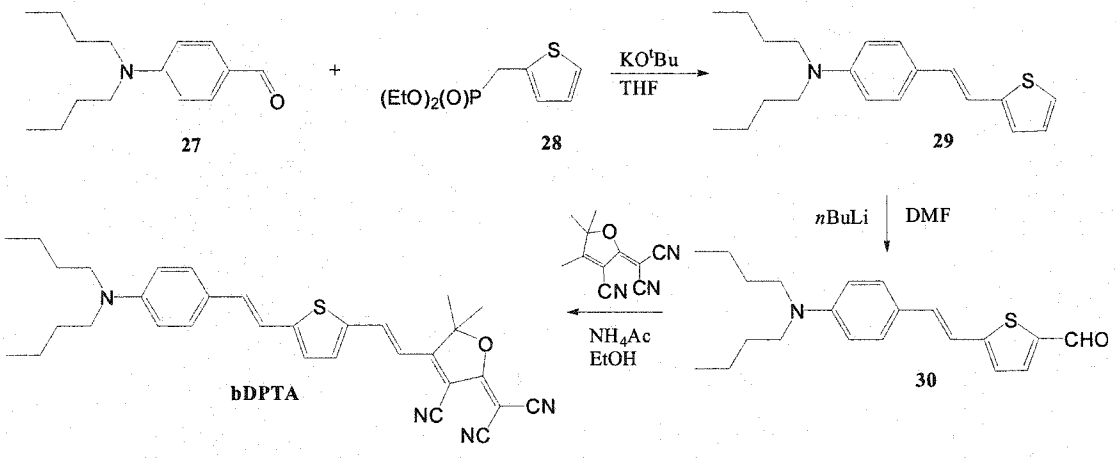

Figure 4.15 Synthetic scheme for the bDPTA chromophore.

4.4 Conclusions

A new class of thiazole-containing EO chromophores was synthesized successfully. The key behind the thiazole "forward" synthesis resided in the use of the correct donor functionality in the initial coupling reaction, which was dictated by the reactivity of the thiazole carboxaldehyde reactant. Though more fundamental

research behind the chemical reactivity of these thiazole derivatives needs to be investigated, a methodology has been developed that will allow chemists to incorporate thiazole "forward" into future EO materials. The performance of these thiazole-based chromophores is evaluated in the following chapter.

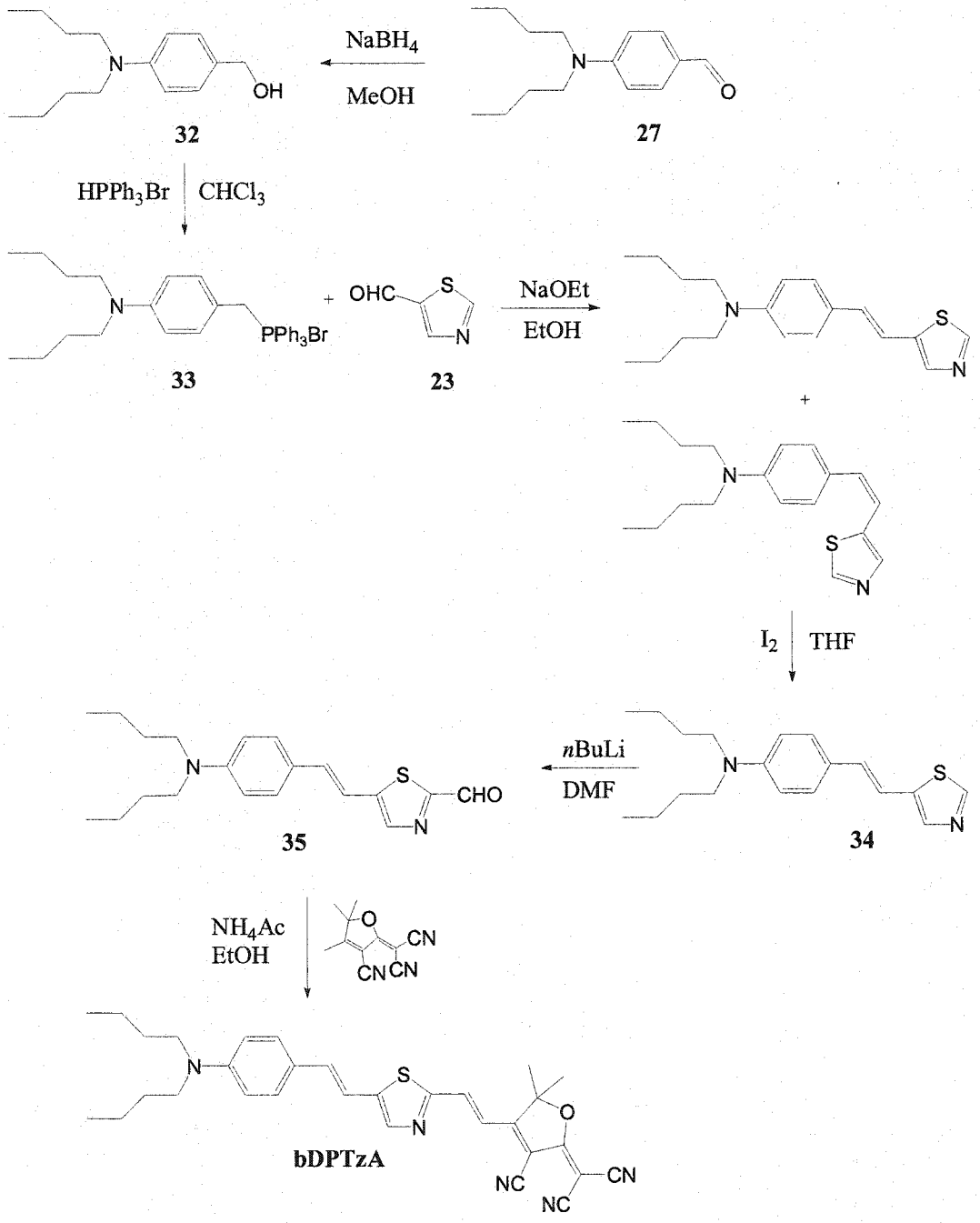

Figure 4.16 Synthetic scheme for the bDPTzA chromophore.

4.5 Experimental Section

General methods of material characterization

All chemicals were purchased from Aldrich unless otherwise specified. All reactions were carried out under a nitrogen atmosphere unless otherwise specified. Tetrahydrofuran (THF) and diethyl ether solvents were dried over Na/benzophenone and distilled before use in all air/water sensitive reactions. ^{1}H NMR spectra were obtained on a Buker-200 or 300 FT-NMR spectrometer. UV-Vis spectra were obtained from a Shimadzu UV-1601 spectrophotometer using a 1-cm path length quartz cell. Elemental Analysis data was obtained through Prevalere Life Sciences Inc. (Whitesboro, NY). Mass spectrometry data was obtained through the Medicinal Chemistry Department, Mass Spectrometry at the University of Washington using electrospray ionization in positive ion mode under normal resolution unless other noted. Thermal analyses were performed on a Shimadzu DSC-60 differential scanning calorimeter under nitrogen atmosphere (100mL/min) at a heating rate of 10 °C/min.

2-[(1E)-2-(4-bromophenyl)vinyl]-5-pyrrolidinylthiophene (3): To a solution of 5-pyrrolidino-2-thiophenecarboxaldehyde (1.0g, 0.05mol) and (4-bromobenzyl)-phosphonic acid diethyl ester (1.86g, 0.06mol) in a minimal amount of dry THF stirring at 0 °C was added dropwise slowly 1M solution of potassium *tert*-butoxide in

THF (6.07mL, 0.006mol). Upon addition, the solution turned to a yellowish color. After addition, the solution was allowed to gradually warm to RT for 3h. Upon addition of deionized water, a dark yellowish precipitate crashed out of solution. This precipitate was filtered and washed several times with water. This crude product was recrystallized either from EtOH/water or THF/water to give the pure product as yellow needles (1.6g, 87%). ^{1}H NMR ($CDCl_3$, 200MHz) δ7.42 (d, J = 7.8Hz, 2H), 7.28 (d, J = 8.1Hz, 2H), 7.10 (d, J = 15.8Hz, 1H), 6.81 (d, J = 3.7Hz, 1H), 6.42 (d, J = 16.1Hz, 1H), 5.65 (d, J = 3.7Hz, 1H) 3.34 (m, 4H), 2.08 (m, 4H).

4-[(1E)-2-(5-pyrrolidinyl(2-thienyl)vinyl]benzaldehyde (4): To a solution of 2-[(1E)-2-(4-bromophenyl)vinyl]-5-pyrrolidinylthiophene (0.230g, 0.688 mmol) in dry THF stirring at –78 °C under N_2 purge was added *n*BuLi (0.303mL, 0.06mol of a 1.6M solution in hexanes) dropwise. The solution turned from a bright yellow to a burnt red color upon lithiation. The lithiated species appears to be an orange cream precipitate in THF. The solution was allowed to stir for 1h at –78 °C, at which time the reaction was quenched with 1mL of dry N,N-dimethylformamide (DMF). Upon addition of DMF, the solution turned a transparent orange color. The mixture was then allowed to warm gradually to room temperature. Saturated NH_4Cl was added to the reaction and allowed to stir vigorously for 1h. The crude product was extracted with CH_2Cl_2, washed three times with water, dried over sodium sulfate, and the solvent removed *in vacuo*. The product was used without further purification (0.190g, 97%). ^{1}H NMR ($CDCl_3$, 300MHz) δ9.90 (s, 1H), 7.75 (d, J = 8.6Hz, 2H),

7.46 (d, J = 8.6Hz, 2H), 7.23 (d, J = 15.1Hz, 1H), 6.84 (d, J = 3.7Hz, 1H), 6.43 (d, J = 15.4Hz, 1H), 5.63 (d, J = 3.7Hz, 1H), 3.32 (m, 4H), 2.04 (m, 4H); (d_6-DMSO, 200MHz) δ9.90 (s, 1H), 7.78 (d, J = 8.4Hz, 1H), 7.60 (d, J = 8.4Hz, 2Hz), 7.46 (d, J = 15.8Hz, 1H), 6.96 (d, J = 3.8Hz, 1H), 6.42 (d, J = 15.8, 1H), 5.72 (d, J = 4.0Hz, 1H), 3.28 (m, 4H), 2.00 (m, 4H). Anal. Calcd for $C_{17}H_{17}NOS$: C, 72.05; H, 6.05; N, 4.94; found: C, 71.90; H, 5.87; N, 4.75.

2-((1E)-2-{4-[(1E)-2-(5-pyrrolindinyl(2-thienyl)vinyl]phenyl}vinyl)-5-bromothiophene (6): To a solution of 4-[(1E)-2-(5-pyrrolidinyl(2-thienyl)vinyl]benzaldehyde (**4**) (3.15g, 11.0mmol) and phosphonic acid[(5-bromo-2-thienyl)methyl]-,diethyl ester (**5**) (3.48g, 11.0mmol) in a minimum amount of dry THF stirring at 0 °C was added dropwise slowly 1M solution of potassium *tert*-butoxide in THF (11.1mL, 11.1mmol). Upon addition, a precipitate formed in the reaction solution. The solution was allowed to stir at room temperature for 3h. The reaction was quenched with water, extracted with chloroform, and dried over sodium sulfate. Removal of solvent yielded a metallic red solid. Recrystallization of the crude material with benzene/hexanes gave a pure product (4.4g, 80%). ^{1}H NMR ($CDCl_3$, 200MHz): δ7.34 (s, 4H), 7.10 (d, J = 15.8Hz, 1H), 7.05 (d, J = 16.1Hz, 1H), 6.92 (d, J = 3.6Hz, 1H), 6.75 (d, J = 3.6, 1H), 6.73 (d, J = 16.3Hz, 1H), 6.45 (d, J = 15.6Hz, 1H), 5.64 (d, J = 3.8Hz, 1H), 3.31 (m, 4H), 2.03 (m, 4H). Anal. Calcd for $C_{22}H_{20}BrNS_2$: C, 59.72; H, 4.56; N, 3.17; found: C, 59.42; H, 4.36; N, 3.22.

5-((1E)-2-{4-[(1E)-2-(5-pyrrolidinyl(2-thienyl))vinyl]phenyl}vinylthiophene-2-carboxaldehyde (7): To a solution of 2-((1E)-2-{4-[(1E)-2-(5-pyrrolindinyl(2-thienyl)vinyl]phenyl}vinyl)-5-bromothiophene (**6**) (0.750g, 0.0017mol) in dry THF stirring at –78 °C under N_2 purge was added *n*BuLi (0.71mL, 0.0018mol of a 2.5M solution in hexanes) dropwise. The solution turned a brown/black color upon lithiation. The solution was allowed to stir for 1h at –78 °C, at which time the reaction was quenched with 1mL of dry DMF. The solution was then allowed to warm gradually to room temperature. Saturated NH_4Cl was added to the reaction and allowed to stir vigorously for 1h. The crude product was extracted with chloroform, washed three times with water, and dried over sodium sulfate. Solvent was removed *in vacuo* to reveal 800mg of a crude black solid. Column chromatography on silica gel with 1:1 (v/v) benzene/hexanes on a small sample revealed 40mg of a black metallic solid (6%). ^{1}H NMR (d_6-DMSO, 200MHz): δ9.88 (s, 1H), 7.95 (d, J = 4.0Hz, 1H), 7.55 (d, J = 7.9Hz, 2H), 7.48 (d, J = 15.1Hz, 1H), 7.44 (d, J = 7.5Hz, 2H), 7.39 (d, J = 4.0Hz, 1H), 7.30 (d, J = 16.3Hz, 1H), 7.21 (d, J = 16.3Hz, 1H), 6.88 (d, J = 4.2Hz, 1H), 6.37 (d, J = 16.1Hz, 1H), 5.68 (d, J = 3.8Hz, 1H), 3.26 (m, 4H), 1.99 (m, 4H).

4-{(1E)-2-[5-((1E)-2-{4-[(1E)-2-(5-pyrrolidinyl(2-thienyl))vinyl]phenyl}vinyl)(2-thienyl)]vinyl}-2-dicyanomethylene-5,5-dimethyl-5-hydrofuran-3-carbonitrile (9): To a solution of 5-((1E)-2-{4-[(1E)-2-(5-pyrrolidinyl(2-thienyl))vinyl]phenyl}vinylthiophene-2-carboxaldehyde (**7**) (0.393g, 1.00mmol) and

2-dicyanomethylene-3-cyano-4,5,5-trimethyl-2,5-dihydrofuran (**8**) (0.260g, 1.00mmol) in chloroform (~50mL) was fitted with a condenser and heated to a gentle reflux. Piperidine (2 drops) was then added and the reaction allowed to stir at reflux under N_2 purge. The reaction was monitored by TLC until the starting material 2-dicyanomethylene-3-cyano-4,5,5-trimethyl-2,5-dihydrofuran was completely consumed. Upon completion, the reaction mixture was washed with saturated ammonium chloride solution and extracted with chloroform. The product had a limited solubility in chloroform and precipitated out as a dark purple solid. This crude material was filtered on a Büchner funnel and washed repeatedly with methanol (250mg, 43%). ^{1}H NMR (d_6-DMSO, 300MHz, 8192scans): δ8.10 (d, J = 15.8Hz, 1H), 7.77 (d, J = 3.7Hz, 1H), 7.56 (d, J = 8.3Hz, 2H), 7.52 (d, J = 16.1Hz, 1H), 7.46 (d, J = 8.1Hz, 2H), 7.36 (d, J = 4.1Hz, 1H), 7.32 (d, J = 15.6Hz, 1H), 7.25 (d, J = 16.1Hz, 1H), 6.88 (d, J = 3.8Hz, 1H), 6.72 (d, J = 15.9Hz, 1H), 6.40 (d, J = 15.9Hz, 1H), 5.68 (d, J = 4.2Hz, 1H), 3.26 (m, 4H), 2.00 (m, 4H), 1.80 (s, 6H). Anal. Calcd for $C_{34}H_{28}N_4OS_2$: C, 71.30; H, 4.93; N, 9.78; found: C, 70.62; H, 4.74; N, 9.72.

4-((1E)-2-{4-[(1E)-2-(5-pyrrolidinyl(2-thienyl))vinyl]phenyl}vinyl)-2-(dicyanomethylene)-5,5-dimethyl-5-hydrofuran-3-carbonitrile (DTPA): A solution of 4-[(1E)-2-(5-pyrrolidinyl(2-thienyl)vinyl]benzaldehyde (**9**) (1.000g, 0.0035mol) and 2-dicyanomethylene-3-cyano-4,5,5-trimethyl-2,5-dihydrofuran (0.879g, 0.0044mol) in chloroform (~50mL) was heated to a gentle reflux.

Triethylamine (3 drops) was then added and the reaction allowed to stir at reflux under N_2 purge while monitoring TLC (~26h). Upon completion, the solvent was removed *in vacuo*. The crude product was washed several times with MeOH. Silica gel chromatography with CH_2Cl_2 revealed purified product (200mg, 43%). ^{1}H NMR (d_6-DMSO, 300MHz): δ7.88 (d, J = 16.5Hz, 1H), 7.81 (d, 8.7Hz, 2H), 7.54 (d, J = 8.5Hz, 2H), 7.49 (d, J = 15.5Hz, 1H), 7.13 (d, J = 15.5Hz, 1H), 6.99 (d, J = 4.2Hz, 1H), 5.75 (d, J = 4.3Hz, 1H), 3.29 (m, 4H), 2.00 (m, 4H), 1.79 (s, 6H). Anal. Calcd for $C_{28}H_{24}N_4OS$: C, 72.93; H, 5.21; N, 12.06; found: C, 72.80; H, 5.20; N, 11.67.

5-[2-(5-Pyrrolidin-1-yl-thiophen-2-yl)-vinyl]-thiophene-2-carbaldehyde (12): To a solution of [5-((1E)-2-thienyl)vinyl)(2-thienyl)]diethylamine (**11**) (1.25g, 4.75 mmol) in dry THF stirring at –78 °C under N_2 purge was added *n*BuLi (1.61mL, 0.03mol of a 1.6M solution in hexanes) dropwise. The solution turned a dark green color upon lithiation. The solution was allowed to stir for 45 minutes at –78 °C, at which time the reaction was quenched with 1mL of dry DMF and allowed to warm gradually to room temperature. Saturated NH_4Cl solution was then added to the reaction and allowed to stir overnight. The crude product was extracted with chloroform, washed three times with water, and dried over sodium sulfate. The crude product was purified via silica gel chromatography with methylene chloride. The eluted product revealed red crystals (0.800g, 58%). ^{1}H NMR ($CDCl_3$, 300MHz): δ9.77 (s, 1H), 7.58 (d, J = 3.8Hz, 1H), 7.13 (d, J = 15.8Hz, 1H), 6.94 (d, J

= 3.8Hz, 1H), 6.85 (d, J = 3.8Hz, 1H), 6.52 (d, J = 15.7Hz, 1H), 5.74 (d, J = 3.9Hz, 1H), 3.36 (q, J = 7.1Hz, 4H), 1.23 (t, J = 7.1Hz, 6H).

4-((1E)-2-{5-[(1E)-2-(5-pyrrolidinyl(2-thienyl))vinyl](2-thienyl)}vinyl-2-(dicyanomethylene)-5,5-dimethyl-5-hydrofuran-3-carbonitrile (DTTA): A solution of 5-[2-(5-Pyrrolidin-1-yl-thiophen-2-yl)-vinyl]-thiophene-2-carbaldehyde (**12**) (1.51g, 5.22mmol), 2-dicyanomethylene-3-cyano-4,5,5-trimethyl-2,5-dihydrofuran (**8**) (1.30g, 6.52mmol), and ~ 5 drops of piperidine were added to a 50mL RB flask, dissolved in 20mL chloroform, and attached to Soxhlet apparatus charged with 4Å molecular sieves. The solution was allowed to stir at reflux under N_2 purge for 12h. After allowing the solution to cool to RT, the solvent was removed *in vacuo*. MeOH was added to the resulting solid and a dark semi-solid ("goo") was collected by filtering and washed several times with MeOH. This solid was dried overnight in a RT vacuum dessicator. The crude solid was recrystallized in methanol. The resulting solid was filtered and washed several times with RT MeOH. The crude solid was then loaded on a plug of silica and eluted as a green solution using 100% CH_2Cl_2 as the mobile phase to reveal 160mg (7%) of the intended product. ^{1}H NMR (d_6-DMSO, 300MHz): δ8.03 (d, J = 15.3Hz, 1H), 7.70 (d, J = 4.5Hz, 1H), 7.41 (d, J = 15.3Hz, 1H), 7.18 (d, J = 4.5Hz, 1H), 7.16 (d, J = 4.2Hz, 1H), 6.65 (d, J = 15.3Hz, 1H), 6.47 (d, J = 15.6Hz, 1H), 5.88 (d, J = 3.9Hz, 1H), 3.34 (m, 4H), 2.02 (m, 4H), 1.77 (s, 6H). Anal. Calcd for $C_{26}H_{22}N_4OS_2$: C, 66.36; H, 4.71; N, 11.91; found: C, 65.77; H, 4.73; N, 12.08.

[4-((1E)-2-(1,3-thiazol-2-yl)vinyl)phenyl]diethylamine (16): To a solution of N,N-diethylamino-4-benzaldehyde (**14**) (2.00g, 0.011mol) and diethoxyphosphino(1,3-thiazol-5-5-ylmethyl)-1-one (**15**) (2.914g, 0.0124mol) in a minimum amount of dry THF stirring at 0 °C was added dropwise slowly 1M solution of potassium *tert*-butoxide in THF (13.54mL, 13.54mmol). Upon addition, the solution turned to a yellow color. The solution was allowed to gradually warm to room temperature overnight. Upon addition of deionized water, an orange-yellow precipitate fell out of solution. This precipitate was filtered and washed several times with water. This solid was used for subsequent reactions without further purification (0.770g, 26%). ^{1}H NMR ($CDCl_3$, 300MHz): δ7.38 (d, J = 8.6Hz, 2H), 7.30 (d, J = 16.0Hz, 1H), 7.13 (d, J = 2.9Hz, 1H) 7.07 (d, J = 16.1Hz, 1H), 6.63 (d, J = 8.8Hz, 2H), 3.38 (q, J = 6.7Hz, 4H), 1.17 (t, J = 6.9Hz, 6H). Anal. Calcd for $C_{15}H_{18}N_2S$: C, 69.73; H, 7.02; N, 10.84; found: C, 69.47; H, 6.64; N, 10.41.

2{(1E)-2-[4-(diethylamino)phenyl]vinyl}1,3-thiazole-5-carbaldehyde (17): To a solution of [4-((1E)-2-(1,3-thiazol-2-yl)vinyl)phenyl]diethylamine (**16**) (0.770g, 0.002 mol) in dry THF stirring at –78 °C under N_2 purge was added *n*BuLi (1.61mL, 0.003mol of a 1.6M solution in hexanes) dropwise. The bright yellow solution formed a gray precipitate upon lithiation. The solution was allowed to stir for 45 minutes at –78 °C, at which time the reaction was quenched with 1mL of dry DMF. The solution was then allowed to warm gradually to room temperature. Saturated

NH_4Cl solution was added to the reaction and allowed to stir overnight. The crude product was extracted with chloroform, washed three times with water, dried over sodium sulfate and the solvent removed *in vacuo*. The product was used without further purification (0.678g, 80%). ^1H NMR ($CDCl_3$, 300MHz): δ9.97 (s, 1H), 8.58 (s, 1H), 7.61 (d, J = 15.8Hz, 1H), 7.54 (d, J = 8.6Hz, 1H), 7.23 (d, J = 16.1Hz, 1H), 6.68 (d, J = 9.5Hz, 2H), 6.68 (d, J = 9.5Hz, 2H), 1.11 (t, J = 7.1Hz, 6H). Anal. Calcd for $C_{16}H_{18}N_2OS$: C, 67.10; H, 6.33; N, 9.78; found: C, 67.18; H, 6.59; N, 9.75.

4-[((1E)-2-(2{(1E)-2-[4-(diethylamino)phenyl]vinyl}(1,3-thiazol-5-yl)vinyl]-2-dicyanomethylene-5,5-dimethyl-5-hydrofuran-3-carbonitrile (DPzTA): A flask holding a solution of 2{(1E)-2-[4-(diethylamino)phenyl]vinyl}1,3-thiazole-5-carbaldehyde (**16**) (0.510g, 0.002mol) and 2-dicyanomethylene-3-cyano-4,5,5-trimethyl-2,5-dihydrofuran (**8**) (0.426g, 0.002mol) in chloroform (~50mL) was fitted with a Soxhlet apparatus charged with 4Å molecular sieves and the solution heated to a gentle reflux. Triethylamine (3 drops) was then added and the reaction allowed to stir at reflux under N_2 purge while being monitored by TLC (~22h). The solvent was then removed *in vacuo*. Upon addition of a small amount of MeOH, a green metallic solid precipitated out of solution, which was subsequently filtered and washed a few times with methanol (280mg, 34%). ^1H NMR (d_6-DMSO, 300MHz): δ8.35 (s, 1H), 8.15 (d, J = 15.7Hz, 1H), 7.61 (d, J = 15.7Hz, 1H), 7.55 (d, J = 8.3Hz, 2H), 7.24 (d, J = 15.7Hz, 1H), 6.64 (d, J = 15.7Hz, 1H), 3.41 (q, J = 6.7Hz, 4H), 1.80

(s, 6H), 1.12 (t, J = 6.6Hz, 6H). Anal. Calcd for $C_{27}H_{25}N_5OS$: C, 69.35; H, 5.39; N, 14.98; found: C, 68.52; H, 5.84; N, 14.47.

5-chloromethylthiazole (20): To a solution of 30mL carbon tetrachloride and 40mL benzene was added 5-hydroxymethylthiazole (**19**) (CAS#38585-74-9, available commercially from Austin Chemical Company Inc. Phone: (847)520-9600 Fax: (847)520-9160) (1.00g, 0.009mol) and triphenylphosphine (3.92g, 0.015mol). The mixture was heated to reflux for 4h. After cooling, the solvents were removed *in vacuo* and the resulting crude product was purified on silica gel with hexanes/ethyl acetate (60:40, v:v) as the mobile phase to reveal 0.7g (60%) as a pale oil. ^{1}H NMR ($CDCl_3$, 200MHz): δ8.80 (s, 1H), 7.83 (s, 1H), 4.82 (s, 2H).

Diethoxyphosphino(1,3-thiazol-5-5-ylmethyl)-1-one (21): 5-chloromethylthiazole (**20**) (5.483g, 0.0410mol) and triethylphosphite (~8.8mL, 0.05mol) were heated to 120 °C and allowed to stir overnight. The excess triethylphosphite was removed via vacuum distillation. The product was obtained in quantitative yield and stored in the freezer. ^{1}H NMR ($CDCl_3$, 200MHz): δ8.68 (s, 1H), 7.69 (d, J = 3.7Hz, 1H), 4.07 (q, J = 7.4Hz, 4H), 3.29 (d, J = 20.6Hz, 2H), 1.25 (t, J = 7.1Hz, 6H).

[4-((1E)-2-(1,3-thiazol-5-yl)vinyl)phenyl]diethylamine (24): N,N-diethyl-4-aminotriphenylphosphonium bromide (0.490g, 0.972mmol) and thiazole-5-carboxaldehyde (0.100g, 0.884mmol) were dissolved in 20mL of dry EtOH. A

prepared 5mL solution of NaOEt from 0.035g (1.47mmol) of NaH was then added dropwise. After the addition, the solution was heated to reflux under N_2 purge for 2.5h. As the solution warmed, its color turned from straw yellow to deep red. The reaction was quenched with water, the ethanol removed *in vacuo*, the product was extracted with ether, and dried over sodium sulfate. Crude product was purified through a silica gel plug first adding hexanes, then 10/90 (v/v) hexanes/methylene chloride. The resulting product was a 1:2 mixture of cis:trans isomers. This mixture was isomerized to an all-trans product by refluxing the product in dry THF with a few crystals of iodine until TLC indicated the isomerization was complete. The pure product forms faint yellow cubic crystals while the amorphous solid was bright yellow in color. ^{1}H NMR (d_6-DMSO, 300MHz): δ8.89 (s, 1H), 7.85 (s, 1H), 7.36 (d, J = 8.7Hz, 2H), 7.15 (d, J = 15.3Hz, 1H), 6.82 (d, J = 16.2Hz, 1H), 6.64 (d, J = 9.0Hz, 1 H), 3 .36 (q, 4 H), 1 .10 (t, 6 H). A nal. Calcd for $C_{15}H_{18}N_2S$: C , 6 9.73; H , 7.02; N, 10.84; found: C, 70.08; H, 6.84; N, 10.39.

5-{(1E)-2-[4-(diethylamino)phenyl]vinyl}1,3-thiazole-2-carboxaldehyde (25): To a solution of [4-((1E)-2-(1,3-thiazol-5-yl)vinyl)phenyl]diethylamine (**24**) (1.156g, 4.474mmol) in dry THF (20mL) stirring at –78 °C under N_2 purge was added *n*BuLi (1.61mL, 0.003mol of a 1.6M solution in hexanes) dropwise. The solution was allowed to stir for 45 minutes at –78 °C, at which time the reaction was quenched with 1mL of dry DMF. The solution was then allowed to warm gradually to room temperature. Saturated NH_4Cl solution was then added to the reaction and allowed

to stir for 30 minutes. The crude product was extracted with ethyl acetate, washed three times with water, dried over sodium sulfate, and the solvent removed *in vacuo*. Some orange precipitate fell out of the ethyl acetate solution, which was filtered before adding the drying agent. The crude product was run on silica gel column chromatography using methylene chloride as the mobile phase to elute a red colored solid (0.650g, 80%). ^{1}H NMR (d_6-DMSO, 300MHz): δ9.86 (s, 1H), 8.19 (s, 1H), 7.44 (d, J = 9.0Hz, 2H), 7.24 (d, J = 15.9Hz, 1H), 7.18 (d, J = 16.2Hz, 1H), 6.67 (d, J = 9.0Hz, 2H), 3.38 (q, 4H), 1.09 (t, 6H). Anal. Calcd for $C_{16}H_{18}N_2OS$: C, 67.10; H, 6.33; N, 9.78; found: C, 67.84; H, 6.63; N, 9.32.

4-[(1E)-2-(5-{(1E)-2-[4-(diethylamino)phenyl]vinyl}(1,3-thiazol-2-yl))vinyl]-2-(dicyanomethylene)-5,5-dimethyl-5-hydrofuran-3-carbonitrile (DPTzA): To a solution of 5-{(1E)-2-[4-(diethylamino)phenyl]vinyl}1,3-thiazole-2-carboxaldehyde (**25**) (0.100g, 0.349mmol) and 2-dicyanomethylene-3-cyano-4,5,5-trimethyl-2,5-dihydrofuran (**8**) (0.083g, 0.419mmol) in ethanol (~5mL) was added a few crystals (<1mg) of ammonium acetate. The solution was heated to 60°C overnight. After cooling, the ethanol was removed *in vacuo* and the solid was washed several times with methanol to reveal a metallic dark red solid (0.127g, 78%). ^{1}H NMR (d_6-DMSO, 300MHz): δ8.15 (s, 1H), 7.99 (d, J = 16.2Hz, 1H), 7.43 (d, J = 8.2Hz, 2H), 7.30 (d, J = 15.6Hz, 1H), 7.26 (d, J = 15.0Hz, 1H), 7.09 (d, J = 16.3Hz, 1H), 6.67 (d, J = 8.4Hz, 2H), 3.39 (q, 4H), 1.81 (s, 6H), 1.11 (t, 4H). Anal. Calcd for $C_{27}H_{25}N_5OS$: C, 69.35; H, 5.39; N, 14.98; found: C, 69.48; H, 5.17; N, 14.85.

[4-((1E)-2-(2-thienyl)vinyl)phenyl]dibutylamine (29): To a solution of N,N-dibutylamino-4-benzaldehyde (**27**) (5.00g, 21.4mmol) and thiophene-2-methylphosphonic acid diethyl ester (**28**) (5.58g, 23.8mmol) in 50mL of dry THF stirring at 0 °C was added dropwise slowly 1M solution of potassium *tert*-butoxide in THF (26.2mL, 26.2mmol). After addition, the solution was allowed to gradually warm to room temperature overnight. The reaction was then quenched with water, extracted with ether, and dried over sodium sulfate. The crude sample was passed through a plug of silica with methylene chloride as the mobile phase to reveal 3.50g (63%) of a dark yellow oil product. ^{1}H NMR (d_6-DMSO, 300MHz): δ7.33 (d, J = 8.8Hz, 2H), 7.08 (d, J = 16.3Hz, 1H), 7.06 (d, J = 4.0Hz, 1H), 7.01 (d, J = 5.0Hz, 1H), 7.00 (dd, J = 5.0Hz, 1H), 6.76 (d, J = 16.1Hz, 1H), 6.60 (d, J = 8.9Hz, 2H), 3.39 (q, 4H), 1.81 (s, 6H), 1.11 (t, 4H). *m/z: Found* – 257.1 (M^+ - 2Et), 314.2 (M^+ + H).

5-{(1E)-2-[4-(dibutylamino)phenyl]vinyl}thiophene-2-carboxaldehyde (30): To a solution of [4-((1E)-2-(2-thienyl)vinyl)phenyl]dibutylamine (**29**) (3.50g, 11.1mmol) in dry THF (50mL) stirring at –78 °C under N_2 was added *n*BuLi (7.65mL, 12.2mol of a 1.6M solution in hexanes) dropwise. The solution was allowed to stir for 45 minutes at –78 °C, at which time the reaction was quenched with 3mL of dry DMF. The solution was then allowed to warm gradually to room temperature. Saturated NH_4Cl solution was then added to the reaction and allowed

to stir for 30 minutes. The crude product was extracted with methylene chloride, washed three times with water, and dried over sodium sulfate. The crude product was purified on silica gel column chromatography using methylene chloride as the mobile phase to reveal a red oil (2.25g, 59%). ^{1}H NMR (d_6-DMSO, 300MHz): δ9.81 (s, 1H), 7.90 (d, J = 3.9Hz, 1H), 7.42 (d, J = 8.9Hz, 1H), 7.27 (d, J = 4.0Hz, 1H), 7.17 (d, J = 16.1Hz, 1H), 7.10 (d, J = 16.1Hz, 1H), 6.63 (d, J = 9.0Hz, 1H), 3.28 (t, J = 7.7Hz, 4H), 1.46 (m, 4H), 1.27 (m, 4H), 0.90 (t, J = 7.3Hz, 6H). *m/z: Found* – 314.2 (M^+ - Et), 342.2 (M^+ + H).

4-[(1E)-2-(5-{(1E)-2-[4-(dibutylamino)phenyl]vinyl}(2-thienyl))vinyl]-2-(dicyanomethylene)-5,5-dimethyl-5-hydrofuran-3-carbonitrile (bDPTA): To a solution of 5-{(1E)-2-[4-(dibutylamino)phenyl]vinyl}thiophene-2-carboxaldehyde (**30**) (2.25g, 6.60mmol) and 2-dicyanomethylene-3-cyano-4,5,5-trimethyl-2,5-dihydrofuran (**8**) (1.57g, 7.90mmol) in ethanol (~40mL) was added a few crystals (<1mg) of ammonium acetate. The solution was heated to 70 °C for 16h. After cooling, the ethanol was removed *in vacuo* and the solid was washed several times with methanol to reveal a metallic green solid (2.76g, 80%). ^{1}H NMR (d_6-DMSO, 300MHz): δ8.07 (d, J = 15.7Hz, 1H), 7.73 (d, J = 4.1Hz, 1H), 7.44 (d, J = 9.0Hz, 2H), 7.25 (d, J = 4.0Hz, 1H), 7.21 (d, J = 15.8Hz, 1H), 7.15 (d, J = 15.9Hz, 1H), 6.64 (d, J = 8.6Hz, 2H), 6.61 (d, J = 15.9Hz, 1H), 3.32 (t, J = 7.0Hz, 4H), 1.79 (s, 6H), 1.46 (m, 4H), 1.27 (m, 4H), 0.90 (t, J = 7.3Hz, 6H). Anal. Calcd for $C_{32}H_{34}N_4OS$: C, 73.53; H, 6.56; N, 10.72; found: C, 73.93; H, 6.33; N, 10.65.

N,N-dibutyl-4-aminobenzylalcohol (32): To a stirred solution of N,N-dibutylamino-4-benzaldehyde (**27**) (13.2g, 56.6mmol) in 125mL methanol was added $NaBH_4$ (1.07g, 28.3mmol) portionwise and the solution was allowed to stir for 1h under nitrogen purge at RT. The mixture was then acidified with 1M HCl solution and then neutralized with $NaHCO_3$ solution. The methanol was then removed *in vacuo* and the resulting oil was extracted with methylene chloride, washed with brine and dried over sodium sulfate. Removal of the solvent revealed 13.3g (100%) of a pale yellow oil. ^1H NMR ($CDCl_3$, 300MHz): δ7.19 (d, J = 8.6Hz, 2H), 6.61 (d, J = 8.7Hz, 2H), 4.54 (d, J = 5.4Hz, 2H), 3.24 (t, J = 7.6Hz, 4H), 1.51 (m, 4H), 1.29 (m, 4H), 0.93 (t, J = 7.3Hz, 6H).

N,N-Dibutyl-4-aminotriphenylphosphonium b romide (33): A mixture of N,N-dibutyl-4-aminobenzylalcohol (**32**) (13.30g, 56.5mmol) and triphenylphosphonium bromide (17.45g, 50.9mmol) was dissolved in 125mL chloroform and heated to reflux for 1.5h in a Dean-Stark apparatus. After cooling, the chloroform was concentrated *in vacuo*, diethyl ether was added dropwise to the stirred solution until a white precipitate formed. This precipitate was filtered through a Büchner funnel and washed several times to reveal 20.72g (65%) of a white solid. ^1H NMR ($CDCl_3$, 300MHz): δ7.60 (m, 15H), 6.62 (d, J = 8.6Hz, 2H), 6.35 (d, J = 8.5Hz, 2H), 5.10 (d, J = 12.9Hz, 2H) 3.17 (t, J = 7.6Hz, 4H), 1.46 (m, 4H), 1.23 (m, 4H), 0.90 (t, J = 7.3Hz, 6H). *m/z: Found* – 480.3 (M^+ - HBr), 218 (M^+ - PPh_3Br).

[4-((1E)-2-(1,3-thiazol-5-yl)vinyl)phenyl]dibutylamine (34): A mixture of N,N-Dibutyl-4-aminotriphenylphosphonium bromide (**33**) (11.01g, 19.60mmol) and thiazole-5-carboxaldehyde (2.00g, 17.6mmol) was dissolved in 15mL of dry EtOH. A prepared 5mL solution of NaOEt from 0.707g (29.5mmol) of NaH was then added dropwise. After the addition, the solution was heated to reflux under N_2 purge for 2.5h. As the solution warmed, its color turned from straw yellow to deep red. The reaction mixture was filtered to remove the byproduct precipitate. The reaction was quenched with water, ethanol removed *in vacuo*, extracted with ether, washed with brine, and dried over sodium sulfate. Crude product was purified through a silica gel plug first adding 90/10 (v/v) hexanes/methylene chloride, then 100% ethyl acetate. The first eluent revealed a mixture of 2:1 cis/trans product mixture, while the second eluent revealed a 4:1 trans/cis product mixture. This mixture was isomerized to an all-trans product by refluxing the product in dry THF with a few crystals of iodine until TLC indicated the isomerization was complete (3.50g, 63%). ^{1}H NMR (d_6-DMSO, 300MHz): δ8.88 (s, 1H), 7.84 (s, 1H), 7.35 (d, J = 8.9Hz, 2H), 7.14 (d, J = 16.3Hz, 1H), 6.81 (d, J = 16.6Hz, 1H), 6.60 (d, J = 8.4Hz, 2H), 3.28 (t, J = 7.1Hz, 4H), 1.50 (m, 4H), 1.33 (m, 4H), 0.92 (t, J = 7.3Hz, 6H). *m/z: Found* – 315.2 (M^+ + H + Na), 337.2 (M^+ + H).

5-{(1E)-2-[4-(dibutylamino) phenyl]vinyl}-1,3-thiazole-2-carboxaldehyde (35): To a solution of [4-((1E)-2-(1,3-thiazol-5-yl)vinyl)phenyl]dibutylamine (**34**) (3.00g,

9.54mmol) in dry THF (50mL) stirring at –78 °C under N_2 purge was added *n*BuLi (6.60mL, 10.5mol of a 1.6M solution in hexanes) dropwise. The solution was allowed to stir for 45 minutes at –78 °C, at which time the reaction was quenched with 3mL of dry DMF. The solution was then allowed to warm gradually to room temperature. Saturated NH_4Cl solution was then added to the reaction and allowed to stir for 30 minutes. The crude product was extracted with methylene chloride, (note: heavy emulsion can form) washed three times with water, and dried over sodium sulfate. The crude product was run on silica gel column chromatography using methylene chloride as the mobile phase to elute a dark red colored solid (1.03g, 32%). ^{1}H NMR (d_6-DMSO, 300MHz): δ9.85 (s, 1H), 8.18 (s, 1H), 7.42 (d, J = 9.0Hz, 1H), 7.23 (d, J = 16.1Hz, 1H), 7.17 (d, J = 16.0Hz, 1H), 6.64 (d, J = 9.0Hz, 1H), 3.28 (t, J = 7.6Hz, 4H), 1.46 (m, 4H), 1.26 (m, 4H), 0.90 (t, J = 7.3Hz, 6H). *m/z: Found* – 343.2 (M^+ + H), 365.2 (M^+ + Na), 375.2 (M^+ + H + MeOH).

4-[(1E)-2-(5-{(1E)-2-[4-(dibutylamino)phenyl]vinyl}(1,3-thiazol-2-yl))vinyl]-2-(dicyanomethylene)-5,5-dimethyl-5-hydrofuran-3-carbonitrile (bDPTzA): To a solution of 5-{(1E)-2-[4-(dibutylamino) phenyl]vinyl}-1,3-thiazole-2-carboxaldehyde (**35**) (1.03g, 3.28mmol) and 2-dicyanomethylene-3-cyano-4,5,5-trimethyl-2,5-dihydrofuran (**8**) (0.783g, 3.93mmol) in ethanol (~40mL) was added a few crystals (<1mg) of ammonium acetate. The solution was heated to 70 °C for 16h. After cooling, the ethanol was removed *in vacuo* and the solid was washed several times with methanol to reveal a metallic light red solid (0.763g, 44%). ^{1}H

NMR (d_6-DMSO, 300MHz): δ8.15 (s, 1H), 7.98 (d, J = 16.0Hz, 1H), 7.42 (d, J = 8.9Hz, 2H), 7.30 (d, J = 16.0Hz, 1H), 7.24 (d, J = 16.2Hz, 1H), 7.08 (d, J = 16.0Hz, 1H), 6.64 (d, J = 9.0Hz, 2H), 3.32 (t, J = 7.0Hz, 4H), 1.81 (s, 6H), 1.46 (m, 4H), 1.27 (m, 4H), 0.90 (t, J = 7.3Hz, 6H). Anal. Calcd for $C_{31}H_{33}N_5OS$; C, 71.10; H, 6.35; N, 13.37; found: C, 71.44; H, 6.26; N, 13.41.

Notes to Chapter 4

(1) Prim, D.; Kirsch, G.; Nicoud, J. F. *Synlett* **1998**, 383-384.

(2) Hum, G.; Grzyb, J.; Taylor, S. D. *J. Comb. Chem.* **2000**, *2*, 234-242.

(3) Zhang, C.; Ren, A. S.; Dalton, L. R. *Polym. Prepr. (Am. Chem. Soc., Div. Polym. Chem.)* **1999**, *40*, 156-157.

(4) Ermer, S.; Lovejoy, S. M.; Bedworth, P. V.; Leung, D. S.; Warren, H. B.; Epstein, J. A.; Girton, D. G.; Dries, L. S.; Taylor, R. E.; Barto, R. R. J.; Eades, W.; Van Eck, T. E.; Moss, A. S.; Anderson, W. M. *Adv. Funct. Mater.* **2002**, *12*, 605-610.

(5) Breitung, E. M.; Shu, C.-F.; McMahon, R. J. *J. Am. Chem. Soc.* **2000**, *122*, 1154-1160.

(6) Dirk, C. W.; Katz, H. E.; Schilling, M. L. *Chem. Mater.* **1990**, *2*, 700-705.

(7) Dirk, C. W.; Caballerro, N.; Kuzyk, M. G. *Chem. Mater.* **1993**, *5*, 733-737.

(8) Lee, S.-H.; Otomo, A.; Nakahama, T.; Yamanda, T.; Kamikado, T.; Yokoyama, S.; Mashiko, S. *J. Mater. Chem.* **2002**, *12*, 2187-2188.

(9) Leng, W.; Zhou, Y.; Xu, Q.; Liu, J. *Macromolecules* **2001**, *34*, 4774-4779.

(10) Miller, R. D.; Lee, V. Y.; Moylan, C. R. *Chem. Mater.* **1994**, *6*, 1023-1032.

(11) Moylan, C. R.; Tweig, R. J.; Lee, V. Y.; Swanson, S. A.; Betterton, K. M.; Miller, R. D. *J. Am. Chem. Soc.* **1993**, *115*, 12599-12600.

(12) Moylan, C. R.; Miller, R. D.; Twieg, R. J.; Betterton, K. M.; Lee, V. Y.; Matray, T. J.; Nguyen, C. *Chem. Mater.* **1993**, *5*, 1499-1508.

(13) Nakayama, H.; Sugihara, O.; Fujimura, H.; Matsushima, R.; Okamoto, N. *Opt. Rev.* **1995**, *2*, 236-238.

(14) Shu, C.-F.; Wang, Y.-K. *J. Mater. Chem.* **1998**, *8*, 833-835.

(15) Wang, X.; Yang, K.; Kumar, J.; Tripathy, S. K.; Chittibabu, K. G.; Li, L.; Lindsay, G. *Macromolecules* **1998**, *31*, 4126-4134.

(16) Watanabe, T.; Amano, M.; Tomaru, S. *Jpn. J. Appl. Phys.* **1994**, *33*, 1683-1685.

(17) Wurthner, F.; Thalacker, C.; Matschiner, R.; Lukaszuk, K.; Wortsmann, R. *Chem. Commun.* **1998**, 1739-1740.

(18) Yamamoto, T.; Suganuma, H.; Maruyama, T.; Inoue, T.; Muramatsu, Y.; Arai, M.; Komarudin, D.; Ooba, N.; Tomaru, S.; Sasaki, S.; Kubota, K. *Chem. Mater.* **1997**, *9*, 1217-1225.

(19) Clot, O., personal communication.

(20) Hudson, R. D. A.; Manning, A. R.; Gallagher, J. F.; Garcia, M. H.; Lopes, N.; Asselberghs, I.; Van Boxel, R.; Persoons, A.; Lough, A. J. *J. Organomet. Chem.* **2002**, *655*, 70-88.

(21) Wadsworth, H. J.; Wyman, P. A.; Dabbs, S.; Jenkins, S. M. In *European Patent*: 90308500, 1991.

(22) Dondoni, A.; Fantin, G.; Fogagnolo, M.; Medici, A.; Pedrini, P. *Synthesis* **1987**, 998-1001.

(23) Bordwell, F. B. *Acc. Chem. Res.* **1988**, *21*, 456-463.

(24) Bordwell, F. B.; Satish, A. V.; Jordan, F.; Rios, C. B.; Chung, A. C. *J. Am. Chem. Soc.* **1990**, *112*, 792-797.

(25) Bordwell, F. B.; Satish, A. V. *J. Am. Chem. Soc.* **1991**, *113*, 985-990.

(26) Dondoni, A.; Fantin, G.; Fogagnolo, M.; Medici, A.; Pedrini, P. *Tetrahedron* **1988**, *44*, 2021-2031.

(27) Ishiyama, T.; Miyamoto, Y. In *Kokai Tokkyo Koho*; JP2002234893: Japan, 2002.

(28) Zhang, J.-X.; Dubois, P.; Jerome, R. *Synth. Commun.* **1996**, *26*, 3091-3095.

Chapter 5

Characterization of novel gradient bridge NLO chromophores

5.1 Introduction

In probing the hyperpolarizability of a chromophore through the HRS technique, there are two common methods for obtaining the data. The Internal Reference Method (IRM) is essentially a plot of the HRS signal versus concentration, in which the hyperpolarizability represents the slope of a Beer's Law plot. The other technique is through the External Reference Method (ERM), calculated through Equation 5.1, in which the HRS signal of the chromophore of interest is compared to the HRS signal of a solvent. The β of the solvent is known and the comparison is performed at a variety of chromophore concentrations.

$$(\beta_1 / \beta_2) = [(I_1 - I_{solvent}) / (I_2 - I_{solvent})]^{1/2} \qquad (5.1)$$

An option recently available with a highly sensitive HRS apparatus that is a fusion of these common methods is to reference the HRS signal of the pure solvent. This is mathematically expressed in Equation 5.2.[1] This method eliminates confusion caused by the dispersive nature of the hyperpolarizability of a reference

chromophore. Instead, the HRS signal of the chromophore of interest is compared directly to that of the HRS signal given by the solvent that is used.

$$(\mathbf{I}_{sample}/\mathbf{I}_{solvent}) = (\mathbf{N}_{sample}\langle\beta^2_{sample}\rangle + \mathbf{N}_{solvent}\langle\beta^2_{solvent}\rangle)/(\mathbf{N}_{solvent}\langle\beta^2_{solvent}\rangle) \quad (5.2)$$

This method also has the added advantage of avoiding confusion about how β was derived or which reference β's were used. Literature solvent values for β are numerous and possess a wide range of values that reside within a factor of three.[2,3] With the solvent reference method, any confusion over which β value for the solvent was used in the calculation is essentially eliminated.

5.2 Gradient Bridge HRS results

In the initial HRS data obtained at 1.3 μm excitation, some interesting findings were revealed (Table 5.1). The β values for the thiazole "backward" and "forward" chromophores are virtually the same, with the "forward" version slightly higher. It is important to note with this data at 1.3 μm that the closer the λ_{max} of a chromophore is to the excitation wavelength resonance frequency of 650 nm, the more likely the β value is experiencing resonant enhancement. Therefore, it is possible that the thiazole "backward" is more resonance enhanced due to its λ_{max} at 645 nm, compared to that of the thiazole "forward," where it could be slightly less

enhanced with its λ_{max} at 683 nm. One could infer from these results that the thiazole "forward" molecule holds a stronger hyperpolarizability than that of its "backward" counterpart. The DTTA chromophore is likely experiencing the least dispersion among the gradient bridge chromophores examined since it has the highest λ_{max} in chloroform. The two highest β values recorded at this excitation wavelength of 1.3 μm were the DTPA and DPTA chromophores. However, given their λ_{max} values are closer to the resonance frequency of 650 nm then the thiazole "forward" chromophore, these two chromophores (DTPA and DPTA) are likely to exhibit greater resonance enhancement then that of the DPTzA chromophore. Although it is difficult from this data to predict their dispersive behavior, it is apparent that all of these chromophores possess enhanced β values at 1.3 μm.

Table 5.1 Hyper-Rayleigh Scattering Data at 1.3μm excitation

Sample	β relative	λ_{max} in $CHCl_3$ (nm)
DPTA	15607 ± 835	674
DPzTA	12244 ± 176	645
DPTzA	12618 ± 420	683
DTPA	15106 ± 555	673
DTTA	10512 ± 188	789

These results must be compared with hyperpolarizability measurements performed at another wavelength (880 nm) to provide better insight into the trends between these chromophores in this system. By measuring β at this particular wavelength, one can acquire β values that are less resonant, where one and two-photon resonance peaks are far removed from the charge transfer bands of the chromophores (Figure 5.1).

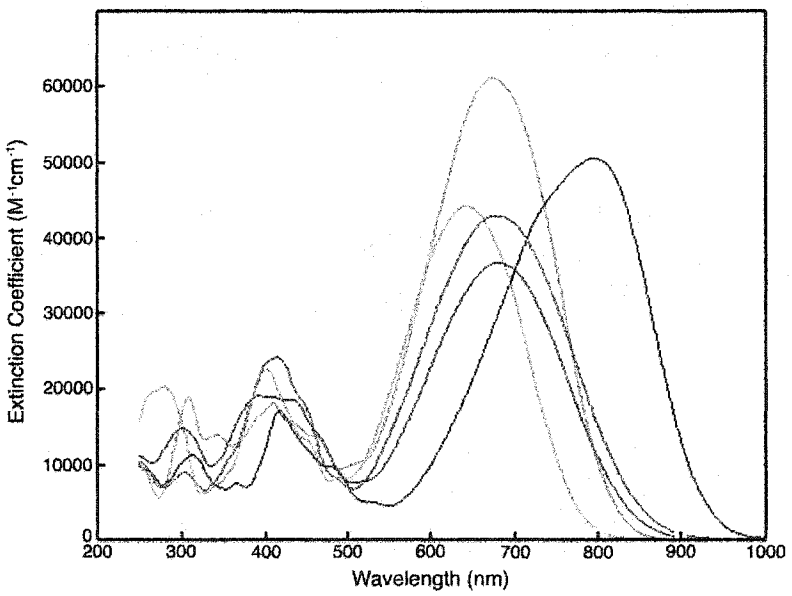

Figure 5.1 UV-vis spectrum of gradient bridge chromophores in $CHCl_3$. The black line is DTTA, red is DPTzA, blue is DTPA, green is DPTA, and cyan is DPzTA.

In order to obtain HRS data that would demonstrate less resonant enhancement than the 1.3 μm excitation provided, the wavelength was adjusted to 880 nm. The results, shown in Table 5.2 and expressed as $\beta_{relative}$ for 880 nm HRS excitation, show two interesting trends. First, the DPTA chromophore still displayed

a particularly stronger hyperpolarizability at this new wavelength over both thiazole "backward" (DPzTA) and "forward" (DPTzA). Second, the DPTzA chromophore has a stronger beta value than that of its isomeric analogue, DPzTA. The 880 nm excitation shows a ~20% improvement in hyperpolarizability with the DPTzA over that of DPzTA. This degree of improvement between these two conformational isomers is greater at 880 nm than at 1.3 μm, likely due to strong reduction in resonant enhancement effects for both chromophores. Due to an unusual fluorescence signature in the DTTA chromophore, the β relative quantity of this chromophore could not be determined.

Table 5.2 Hyper-Raleigh Scattering Data at 880 nm excitation.

Sample	β relative	λ_{max} in $CHCl_3$ (nm)
DPTA	9834 ± 637	674
DPzTA	5446 ± 236	645
DPTzA	6494 ± 522	683
DTPA	9038 +/- 501	673
DTTA	N / A	789

General Information on HRS Apparatus and Data Analysis:

General Comments: All hyper-Raleigh scattering experimental data was performed and obtained by Kimberly Firestone under the guidance of Prof. Philip Reid,

Department of Chemistry, University of Washington. Hyper-Rayleigh scattering (HRS) measurements were performed to quantify the first-hyperpolarizabilities (β) of the chromophores at 880 nm and 1.3 μm excitation wavelengths. At 880 nm, excitation was provided by the output of a mode-locked Ti:sapphire oscillator (Spectra-Physics Tsunami), consisting of 100-fs pulses (full-width at half maximum, or FWHM) at a repetition rate of 80 MHz and 1.5 W incident power. The laser spectrum (FWHM ~20 nm) was monitored during the course of the experiment. The incident light was focused into the middle of a low-volume flow cell. The scattered light was imaged onto the slits of a spectrograph (Acton 300i) equipped with a 700-nm short-pass filter and a piece of blue-green BK7 to reduce background counts. Detection was accomplished with a 1340 by 100 pixel, red-edge enhanced, back-thinned, LN_2-cooled CCD camera (Princeton Instruments). HRS spectra were acquired using exposure times of 120 seconds.

To provide the 1.3-μm excitation wavelength, the Ti:sapphire oscillator was used to pump an optical parametric oscillator (OPO, Spectra Physics OPAL), with an output (FWHM ~20 nm) of 100-fs pulses (FWHM) at an 80 MHz repetition rate at 350 mW incident power. The spectrograph was equipped with either a 650-nm interference filter (40 nm FWHM) or a 700-nm short-pass filter. Camera exposure times ranged from 180-300 seconds.

Solution concentrations ranging from 142 nM to 289 nM in chloroform (Fisher ACS Spectranalyzed) were investigated, with concentrations chosen based on chromophore extinction coefficients to minimize self-absorption of the scattered

light by the chromophores. The sample was flowed continuously through the low-volume flow cell and an in-line 0.1-μm PTFE filter to minimize photodestruction and eliminate particulate matter. Data were analyzed in the MATLAB environment by fitting the HRS emission peaks to a Gaussian functional form to determine the intensity following subtraction of the multi-photon fluorescence background where necessary. HRS intensity was converted to β for each spectrum through Equation 5.2.

HRS was confirmed by quadratic dependence on incident power. Furthermore, the spectral-width of the HRS peak was equal to the incident field and tracked with excitation wavelength. Signal amplitudes were monitored for consistency over the course of successive scans to monitor the onset of bulk photodegradation. No measurable photodegradation was observed during these experiments. Additionally, solution concentrations were carefully chosen to avoid self-absorption of the scattered light by the chromophores. No measurable self-absorption effects were observed at the concentrations employed.

5.3 EO activity measurement

One goal from this study was to obtain preliminary electro-optic activity values of two chromophore samples, the thiazole "forward" chromophore and its thiophene analogue. Amorphous polycarbonate (APC), commercially available from Aldrich [poly(bisphenol A carbonate-*co*-4,4'-(3,3,5-trimethylcyclohexylidene)diphenol], was

chosen as the polymer host due to its good compatibility with virtually all known high-μβ chromophores as well as having a glass temperature (T_g = 205°C) in the appropriate processing range.

General Comments: All sample preparation and film casting was performed by Marnie Haller under the direction of Prof. Alex Jen, Department of Materials Science and Engineering, University of Washingon. The bDTPA formed acceptable films using both cyclopentanone and 1,2,3-trichloropropane. However, the bDPTzA chromophore experienced decomposition in cyclopentanone. This degradation was shown through a simple spectrophotometric experiment. As shown in Figure 5.2, the absorbance values at the λ_{max} of the chromophore decreased with static exposure to the spin casting solvent. In this work, static exposure is defined as a solution of the solute (chromophore) dissolved in the solvent of interest and stored in an inert nitrogen atmosphere, at room temperature, and in the dark.

The action of sonication appeared to accelerate the decomposition process, as shown through preliminary UV-vis measurements (Figure 5.2). This phenomenon is shown by the dramatic decrease in absorbance at its λ_{max}, occurring even over just 2 hours of sonication.

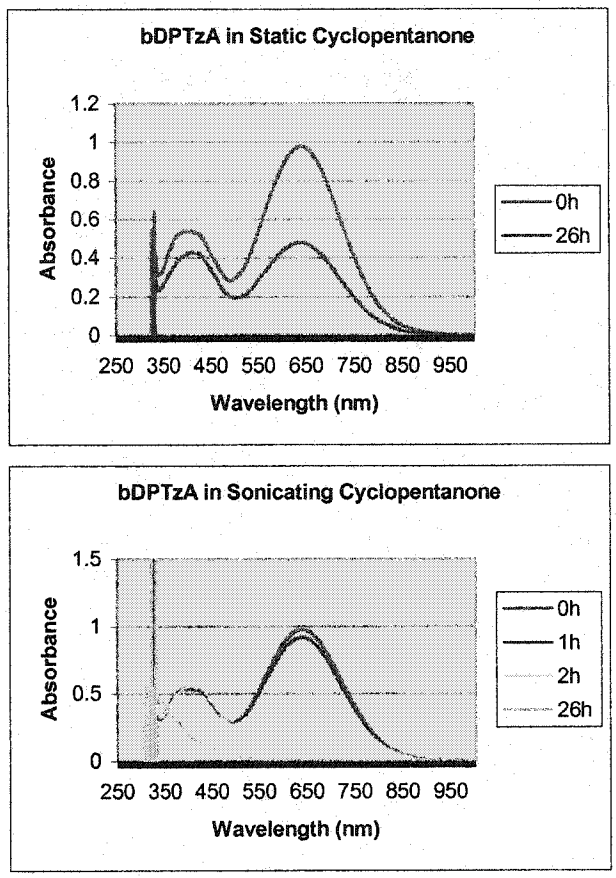

Figure 5.2 UV-Vis spectra of bDPTzA exposed to static cyclopentanone (top) and under sonication (bottom).

The electronics (and degree of reactivity) of the thiazole "forward" chromophore is significantly different from its thiophene analogue. The altered electronics are due to the incorporation of the thiazole "forward" component. The alteration is probably due to the replacement of a carbon atom by a more electronegative nitrogen atom.

It appeared as though the decomposition of the bDPTzA chromophore could be due to interactions with the carbonyl functionality in cyclopentanone. A

chlorinated solvent, 1,2,3-trichloropropane was then chosen as an alterative solvent. However, this solvent also led to decomposition in the bDPTzA chromophore. The UV-Vis spectrum of the resulting bDPTzA films in both cyclopentanone and 1,2,3-trichloropropane is shown in Figure 5.3. In both cyclopentanone and 1,2,3-trichloropropane, the bDPTA chromophore produced good films without any apparent decomposition. The bDPTzA films turned from a blue color to a light pink, following spin-cast baking under vacuum. This color change corresponded to a dramatic drop in the chromophore absorbance band.

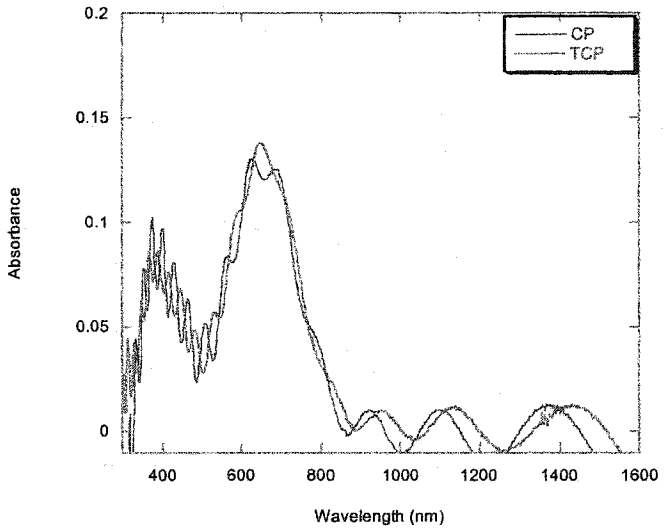

Figure 5.3 UV-Vis spectrum of bDPTzA films using cyclopentanone (CP) and 1,2,3-trichloropropane (TCP). Note the low absorbance of the pink colored films obtained (<0.15) after baking.

This evidence suggested that the nitrogen on the thiazole of bDPTzA might be the contributing factor to the decomposition of the chromophore. It is possible that the lone electron pair on the nitrogen was interacting with acidic functionality of

the solvent, leading to inherent instability in the chromophore and its subsequent decomposition.

In order to determine whether the hyperpolarizability of the bDPTzA chromophore decreases due its interaction with the acidic solvent, a study was devised in which the traditional solvent used for HRS measurements, ACS Fisher Spectanalyzed® chloroform, was doped with an extremely small amount of triethylamine (TEA). This non-nucleophilic base was used to counteract the minute degree of acidity that is associated with spectranalyzed chloroform. A solution of the DPTzA chromophore was prepared where one drop of TEA was added for every 10:1 dilution needed to obtain similar concentrations as neat chloroform.

The resulting HRS measurements of β relative at 880nm revealed that there was no appreciable change in the hyperpolarizability of DPTzA in neat chloroform compared with chloroform with TEA compared to bDPTzA in neat chloroform. The difference in value between the two measurements, 6494 ± 522 in neat chloroform, and 6402 ± 456 in chloroform/TEA, was insignificant and within experimental error. Results from this experiment indicated that a slightly acidic environment in spectranalyzed chloroform does not result in the decomposition of the thiazole "forward" chromophore.

Results similar to those obtained in CP and TCP in an attempt to spin cast films of bDPTzA with DMF (both reagent grade and anhydrous). The chromophore film rapidly decomposed during film preparation. It is likely that decomposition occurs slowly during solvent exposure and is accelerated during film casting with

baking steps (65 °C at ambient pressure and then 85 °C under vacuum). The apparent instability of the thiazole "forward" chromophore in a handful of common organic solvents prompted an examination the mechanism behind the decomposition.

Samples were prepared in which the bDPTzA chromophore (~0.5 mg) was dissolved into each of the following solvents: chloroform, dioxane, propylene carbonate, and DMSO. These samples were then transferred into UV-vis cuvettes. Each solvent represented a range of functional groups that would be examined under static solvent exposure. The samples were prepared in dark conditions to minimize any photochemically induced decomposition. The samples were stored under nitrogen and their UV-vis spectrum examined at 12 h intervals.

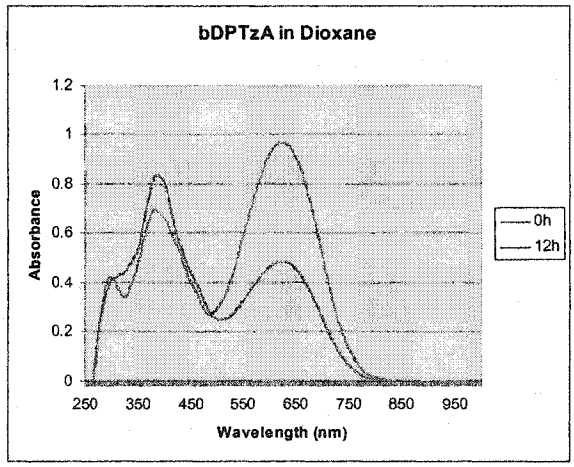

Figure 5.4 UV-vis spectrum of bDPTzA under static dioxane.

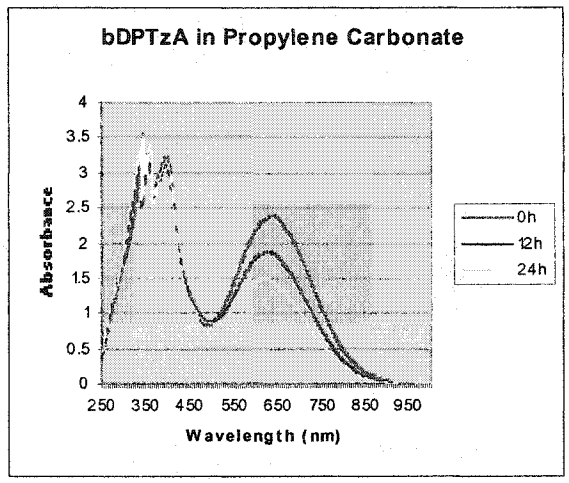

Figure 5.5 UV-vis spectrum of bDPTzA under static propylene carbonate.

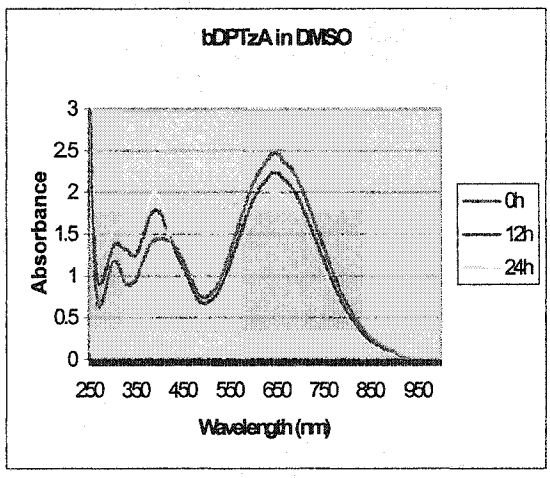

Figure 5.6 UV-vis spectrum of dDPTzA under static DMSO.

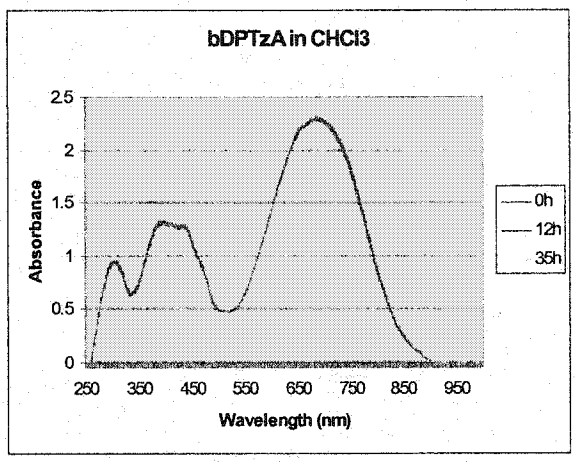

Figure 5.7 UV-vis spectrum of bDPTzA under static chloroform.

The λ_{max} absorbance values of the dDPTzA showed a significant decrease in dioxane, propylene carbonate, and DMSO, as seen in Figures 5.4, 5.5, and 5.6. The chloroform sample showed no appreciable decrease in its λ_{max} absorbance (Figure 5.7). The interesting trend among the solvents that induced decomposition was an apparent increase of a secondary absorbance band in the range of 380-410 nm. While the overall chromophore absorbance decreased over time, this secondary peak increased in a corresponding fashion (Table 5.3). This secondary peak could have two possible origins. First, it could arise from an altered chromophore structure that happens to have a similar absorption band. Second, the absorption band increase could originate from a break in the conjugated structure on one of the ethylene linkages, corresponding to either the absorbance of the donor-bridge or the bridge-acceptor component.

Table 5.3 Summary of bDPTzA static solvent exposure absorbance levels over time on the λ_{max} and its secondary absorbance peak ($\lambda_{2'}$). PC represents propylene carbonate.

		Solvent							
		$CHCl_3$		DMSO		PC		Dioxane	
		λ_{max}	$\lambda_{2'}$	λ_{max}	$\lambda_{2'}$	λ_{max}	$\lambda_{2'}$	λ_{max}	$\lambda_{2'}$
Time (h)	0	2.33	1.30	2.482	1.452	2.395	3.215	0.970	0.695
	12	2.30	1.32	2.241	1.756	1.858	Max	0.485	0.841
	24	2.28	1.38	1.992	1.936	1.467	Max	0.233	1.120

Absorbance spectra of the DPTz (donor-bridge) component revealed a λ_{max} of 389 nm in DMSO. A sample of a thiophene-TCF (bridge-acceptor) component was already available from our laboratory. This component would provide a λ_{max} in close proximity to that of a thiazole "forward" derivative. The λ_{max} of the thiophene-TCF component in DMSO is 463 nm. Previous studies on conjugated EO systems of thiophene and thiazole suggest the largest shift in λ_{max} is on the order of 10-15 nm with a change to a thiazole component.[4,5] Given this information, the absorbance could be ascribed to a break in conjugation between the bridge and acceptor. The increase in the secondary maximum absorbance peak at ~400nm matches with the absorbance maximum peak for the donor bridge intermediate.

In order to confirm that this break in the conjugation was taking place, along with possibly elucidating the resulting product, a ^1H NMR was performed in which

the bDPTzA chromophore was exposed to static d_6-DMSO (99.9%D). The sample was monitored at 0, 24, 48, 72, 144, and 288 h. The 144 h and 288 h samples revealed additional proton peaks. The additional ^{1}H NMR peaks were a set of broad doublets located at 8.01 and 8.03ppm, two overlapping quartets at 4.01 and 3.99 ppm, along with another set of broad doublets at 3.76 and 3.69 ppm. These additional peaks suggest that the both the deuterated and non-deuterated DMSO solvent (0.1% concentration) is undergoing a [4+2] cycloaddition with the second ethylene linkage (between the bridge and acceptor components) of the chromophore (Figure 5.8). The quintets arise from the methyl groups on the DMSO molecules coupling with an allylic stereogenic carbon center.

The integration between the quintets and the allylic hydrogen doublets is in a ratio of 3:1:1. The integration between the allylic hydrogen doublets with the vinyl hydrogen doublets is in a ratio of 1:0.5. These integrations clearly show that both the deuterated and non-deuterated solvent reacted with the diene linkage.

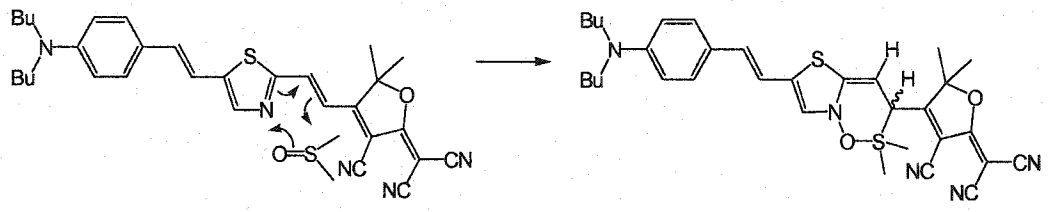

Figure 5.8 The [4+2] cycloaddition reaction between bDPTzA and DMSO.

If just the non-deuterated form of DMSO reacted with the chromophore diene, the ratios between these two groups would be 6:1 and 1:1. However, since the deuterated form also reacted, this ratio is decreased since the ^{1}H protons on the former ethylene linkage are still seen on the resulting NMR spectrum.

To examine the driving force behind the cycloaddition (thermal or photochemical), the NMR sample was exposed for 2.5 h exposure to 256 nm light. The resulting NMR spectrum showed no increase in the cycloaddition signals. The cycloaddition process was therefore determined to be a thermal process. Examining Figure 5.2 again we can see how a static exposure at room temperature provides enough kinetic energy to create the cyclized product over time. Sonication provides additional kinetic energy to the system to accelerate this process, but also results in further decomposition of the chromophore as the cyclized product is instable under these conditions.

Additionally, the cycloaddition is likely regiospecific (Figure 5.8) with the nitrogen bonded to oxygen, with oxygen bonded to a tetragonic sulfur. The overlapping quartet peaks arise from the coupling between the stereogenic allylic hydrogen of the cyclized product with the methyl groups of DMSO. There is no evidence of any additional DMSO methyl peaks arising from a cyclized product with opposing orientation.

The specificity of this reaction is also demonstrated through the evidence that ^{1}H NMR of the DPzTA chromophore when exposed to static DMSO results in no degradation of the chromophore. The regiochemical orientation of the nitrogen atom

on the thiazole alters the electronics of the second ethylene linkage to make it more reactive with DMSO. Electrospray mass spectrometry (positive ion mode) performed by Mass Spectrometry in the Department of Chemistry, University of Washington, showed evidence of the deuterated DMSO cycloaddition product (m/z - 608). The resulting cycloaddition product is likely not very stable since the entire chromophore is decomposing rapidly with the use of sonication (Figure 5.2).

The UV-vis measurements of the other solvents (propylene carbonate, dioxane), which induce degradation of the bDPTzA chromophore, suggest that the second ethylene linkage is altered as well. The mechanism of degradation with these other solvents could be similar to that observed with DMSO. Due to the inherent instability of this thiazole "forward" chromophore, it would be impractical to pursue its macroscopic properties. This was compounded by the fact that the only solvent that displayed a low level of degradation (chloroform) did not show good film processability with APC. The prepared solution was extremely viscous and was similar in consistency to a gel.

5.4 Recommendations and Conclusions

The first demonstrated synthesis and characterization of a thiazole "forward" chromophore has been described. The first order hyperpolarizability of this chromophore displays a 20% improvement over its thiazole "backward" analogue at 880nm excitation. This is the first experimental demonstration that the

regiochemical orientation of a thiazole bridge component does have an influence on the hyperpolarizability. The traditional EZ-FTC type molecule still showed a higher hyperpolarizability than either of the members of the thiazole family.

Theoretical calculations unfortunately cannot predict the degree of reactivity of the proposed chromophore. This limitation was certainly shown through the inherent reactivity in the ethylene linkage between the thiazole "forward" component and the TCF acceptor. The incorporation of the thiazole "forward" component imparts an increased reactivity in the double bond between the thiazole and the acceptor, resulting in decreased stability of the molecule in various common organic solvents. The [4+2] cycloaddition of the thiazole chromophore diene with DMSO has been spectroscopically determined through ^{1}H NMR.

Due to decreased stability in these novel molecules, steps should be taken to address this stability issue with any future thiazole "forward" containing chromophore. Since the reactivity site is placed on the second ethylene linkage between the bridge and the acceptor, a possible approach would be to eliminate this connection altogether, where a direct thiazole "forward" bridge and TCF acceptor bond can be envisioned (Figure 5.9). However, this should be attempted cautiously, as the ethylene functionality in the furan acceptor could potentially undergo a similar [4+2] cycloaddition with DMSO and could potentially exhibit similar inherent instability. It is clear that if thiazole "forward" is to be incorporated into a future generation high-$\mu\beta$ chromophores that the backbone cannot be modeled after traditional "FTC-type" chromophores and the stability (both thermal and

photochemical) of the chromophore should be addressed through novel design and evaluated thoroughly.

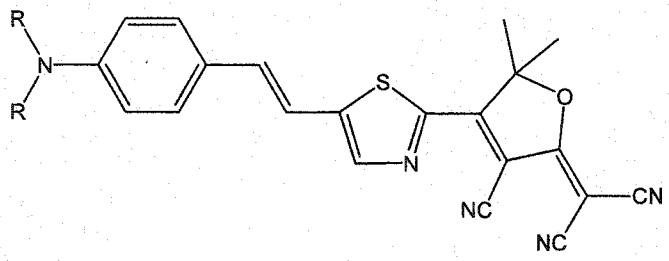

Figure 5.9 Example of a thiazole "forward" chromophore with direct connection between bridge and acceptor.

Notes for Chapter 5

(1) Firestone, K. A.; Reid, P.; Lawson, R.; Jang, S.-H.; Dalton, L. R. *Inorg. Chim. Acta.* **2004**, *in press*.

(2) Kaatz, P.; Shelton, D. P. *Opt. Commun.* **1998**, *157*, 177-181.

(3) Clays, K.; Persoons, A. *Phys. Rev. Lett.* **1991**, *66*, 2980-2983.

(4) Shu, C.-F.; Wang, Y.-K. *J. Mater. Chem.* **1998**, *8*, 833-835.

(5) Wang, Y.-K.; Shu, C.-F.; Breitung, E. M.; McMahon, R. J. *J. Mater. Chem.* **1999**, *9*, 1449-1452.

Bibliography

Ahlheim, M.; Barzoukas, M.; Besworth, P. V.; Blanchard-Desce, F. A.; Hu, Z.-Y.; Marder, S. R.; Perry, J. W.; Runser, C.; Staehelin, M.; Zysset, B. *Science* **1996**, *271*, 335-337.

Akiyama, Y.; Seiji, T.; Hatsusiba, E.; Ohuchi, S.; Okonogi, T. *Bioorg. Med. Chem. Lett.* **1997**, *7*, 533-538.

Bak, B.; Christensen, D.; Hansen-Nygaard, L.; Rastrup-Andersen, J. *J. Mol. Spectrosc.* **1962**, *9*, 222-224.

Banno, M.; Yasui, S.; JP45033887, 1970, p p 4.

Beckmann, S.; Etzbach, K.-H.; Kramer, P.; Lukaszuk, K.; Matschiner, R.; Schmidt, A. J.; Schuhmacher, P.; Sens, R.; Seybold, G.; Wortmann, R.; Wurthner, F. *Adv. Mater.* **1999**, *11*, 536-541.

Bella, S. D.; Fragala, I.; Ratner, M. A.; Marks, T. J. *Chem. Mater.* **1995**, *7*, 400-404.

Blazsek-Bodo, A.; Vernes, M.; Szurkos, A. *Farmacia Bucharest* **1974**, *22*, 345-252.

Bordwell, F. B. *Acc. Chem. Res.* **1988**, *21*, 456-463.

Bordwell, F. B.; Satish, A. V.; Jordan, F.; Rios, C. B.; Chung, A. C. *J. Am. Chem. Soc.* **1990**, *112*, 792-797.

Bordwell, F. B.; Satish, A. V. *J. Am. Chem. Soc.* **1991**, *113*, 985-990.

Bourhill, G.; Bredas, J.-L.; Cheng, L.-T.; Marder, S. R.; Meyers, F.; Perry, J. W.; Tiemann, B. G. *J. Am. Chem. Soc.* **1994**, *116*, 2619-2620.

Brasselet, S.; Cherioux, F.; Audebert, P.; Zyss, J. *Chem. Mater.* **1999**, *11*, 1915-1920.

Bredas, J. L.; Adant, C.; Tackx, P.; Persoons, A.; Pierce, B. M. *Chem. Rev.* **1994**, *94*, 243-276.

Breitung, E. M.; Shu, C.-F.; McMahon, R. J. *J. Am. Chem. Soc.* **2000**, *122*, 1154-1160.

Burland, D. M.; Miller, R. D.; Reiser, O.; Tweig, R. J.; Walsh, C. A. *J. Appl. Phys.* **1992**, *71*, 410-417.

Champagne, B.; Kirtman, B. *Chem. Phys.* **1999**, *245*, 213-226.

Cheng, L.-T.; Tam, W.; Marder, S. R.; Steigman, A. E.; Rikken, G.; Spangler, C. W. *J. Phys. Chem.* **1991**, *95*, 10643-10652.

Cheng, L.-T.; Tam, W.; Stevenson, S. H.; Meredith, G. R.; Rikken, G.; Marder, S. R. *J. Phys. Chem.* **1991**, 10631-10643.

Cho, B. R.; Son, K. N.; Lee, S. J.; Kang, T. I.; Han, M. S.; Jeon, S. J. *Tetrahedron Lett.* **1998**, *39*, 3167-3170.

Chou, S.-S. P.; Hsu, G.-T.; Lin, H.-C. *Tetrahedron Lett.* **1999**, *40*, 2157-2160.

Clays, K.; Persoons, A. *Phys. Rev. Lett.* **1991**, *66*, 2980-2983.

Clot, O., personal communication.

Co, B. W. a.; GB 1246649, 1971, p p 7.

Dalton, L. R. *Nature* **1992**, *359*, 269.

Dalton, L. R.; Sapochak, L. S.; Yu, L. *J. Phys. Chem.* **1993**, *97*, 2871-2883.

Dalton, L. R.; Harper, A. W.; Ghosn, R.; Steier, W. H.; Ziari, M.; Fetterman, H.; Shi, Y.; Mustacich, R. V.; Jen, A. K.-Y.; Shea, K. J. *Chem. Mater.* **1995**, *7*, 1060-1081.

Dalton, L. R.; Harper, A. W.; Wu, B.; Ghosn, R.; Laquindanum, J.; Liang, Z.; Hubbel, A.; Xu, C. *Adv. Mater.* **1995**, *7*, 519-540.

Dalton, L. R.; Harper, A. W.; Robinson, B. H. *Proc. Natl. Acad. Sci.* **1997**, *94*, 4842-4847.

Dalton, L. R.; Harper, A. W. *Polym. News* **1998**, *23*, 114-120.

Dalton, L. R. In *Electrical and optical polymer systems*; Wise, D. L., Wnek, G., Transtolo, D. J., Cooper, T. M., Gresser, J. D., Eds.; Marcel Dekkar: New York, 1998.

Dalton, L. R.; Steier, W. H.; Robinson, B. H.; Zhang, C.; Ren, A.; Garner, S.; Chen, A.; Londergan, T.; Irwin, L.; Carlson, B.; Fifield, L.; Phelan, G.; Kincaid, C.; Amend, J.; Jen, A. *J. Mater. Chem.* **1999**, *9*, 1905-1920.

Dalton, L. R. In *Advances in Polymer Sciences*; Springer-Verlag: Berlin Heidelberg, 2002; Vol. 158.

Dalton, L. R., personal communication.

Di Bella, S.; Fragala, I.; Ratner, M. A.; Marks, T. J. *Chem. Mater.* **1995**, *7*, 400-404.

Dirk, C. W.; Katz, H. E.; Schilling, M. L. *Chem. Mater.* **1990**, *2*, 700-705.

Dirk, C. W.; Caballerro, N.; Kuzyk, M. G. *Chem. Mater.* **1993**, *5*, 733-737.

Dondoni, A.; Fantin, G.; Fogagnolo, M.; Medici, A.; Pedrini, P. *Synthesis* **1987**, 998-1001.

Dondoni, A.; Fantin, G.; Fogagnolo, M.; Medici, A.; Pedrini, P. *Tetrahedron* **1988**, *44*, 2021-2031.

Dondoni, A.; Fantin, G.; Fogagnolo, M.; Medici, A.; Pedrini, P. *J. Org. Chem.* **1988**, *53*, 1748-1761.

El-Mossalomy, E. H.; Ibahim, A. A. *Pigment & Resin Technology* **2002**, *31*, 375-380.

Elkholy, Y. M.; wahba Erian, A.; Helal, M. H. *Pigment & Resin Technology* **2001**, *30*, 168-170.

Ermer, S.; Valley, L., R.; Lipscomb, G. F.; Van Eck, T. E.; Girton, D. G. *Appl. Phys. Lett.* **1992**, *61*, 2272-2274.

Ermer, S.; Valley, L., R.; Lipscomb, G. F.; Van Eck, T. E.; Girton, D. G.; Leung, D. S.; Lovejoy, S. M. *Proc. SPIE* **1993**, *1853*, 183-192.

Ermer, S.; Lovejoy, S. M.; Leung, D. S.; Warren, H.; Moylan, C. R.; Tweig, R. J. *Chem. Mater.* **1997**, *9*, 1437-1442.

Ermer, S.; Lovejoy, S. M.; Bedworth, P. V.; Leung, D. S.; Warren, H. B.; Epstein, J. A.; Girton, D. G.; Dries, L. S.; Taylor, R. E.; Barto, R. R. J.; Eades, W.; Van Eck, T. E.; Moss, A. S.; Anderson, W. M. *Adv. Funct. Mater.* **2002**, *12*, 605-610.

Firestone, K. A.; Reid, P.; Lawson, R.; Jang, S.-H.; Dalton, L. R. *Inorg. Chim. Acta.* **2004**, *in press*.

Franken, P. A.; Hill, A. E.; Peters, C. W.; Weinreich, G. *Phys. Rev. Lett.* **1961**, *7*, 118-120.

Gilchrist, T. L. *Heterocyclic Chemistry*; John Wiley & Sons: New York, 1985.

Gorman, C. B.; Marder, S. R. *Proc. Nat. Acad. Sci.* **1993**, *90*, 11297-11301.

Goswami, A. K.; Cross, L. E.; Buessem, W. R. *J. Phys. Soc. Jap.* **1968**, *24*, 279-281.

Griffins, J.; Riepl, C. J. *Chem. Commun.* **1998**, 1349-1350.

Haller, M.; Luo, J.; Li, H.; Kim, T.-D.; Liao, Y.; Robinson, B. H.; Dalton, L. R.; Jen, A. K.-Y. *Macromolecules* **2004**, *37*, 688-690.

Hantzsch, A.; Arapides, L. *Berichte*, 1888; Vol. 21.

Harper, A. W.; Sun, S.; Dalton, L. R.; Garner, S. M.; Chen, A.; Kalluri, S.; Steier, W. H.; Robinson, B. H. *J. Opt. Soc. Am. B: Opt. Phys.* **1998**, *15*, 329-337.

Hudson, R. D. A.; Manning, A. R.; Gallagher, J. F.; Garcia, M. H.; Lopes, N.; Asselberghs, I.; Van Boxel, R.; Persoons, A.; Lough, A. J. *J. Organomet. Chem.* **2002**, *655*, 70-88.

Hum, G.; Grzyb, J.; Taylor, S. D. *J. Comb. Chem.* **2000**, *2*, 234-242.

Illien, B.; Jehan, P.; Botrel, A.; Darchen, A.; Ledoux, I.; Zyss, J.; L., M. P.; Lahcene, O. *New J. Chem.* **1998**, *22*, 633-641.

Ishiyama, T.; Miyamoto, Y. In *Kokai Tokkyo Koho*; JP2002234893: Japan, 2002.

Jen, A. K.-Y.; Rao, V. P.; Wong, K. Y.; Drost, K. J. *J. Chem. Soc., Chem. Commun.* **1993**, 90-92.

Jen, A. K.-Y.; Rao, V. P.; Drost, K. J.; Wong, K. Y.; Cava, M. P. *J. Chem. Soc., Chem. Commun.* **1994**, 2057-2059.

Jen, A. K.-Y.; Wong, K. Y.; Rao, V. P.; Drost, K. J.; Cai, Y. M. *J. Electron. Mater.* **1994**, *23*, 653-657.

Jug, K.; Chiodo, S.; Janetzko, F. *Chem. Phys.* **2003**, *287*, 161-168.

Kaatz, P.; Shelton, D. P. *Opt. Commun.* **1998**, *157*, 177-181.

Kajzar, F.; Horn, K.; Nahata, A.; Yardley, J. T. *MCLC S&T, Sec. B., Nonlin. Opt.* **1994**, *8*, 205-217.

Karna, S. P.; Prasad, P. N.; Dupuis, M. *J. Chem. Phys.* **1991**, *94*, 1171-1181.

Karna, S. P.; Zhang, Y.; Samoc, M.; Prasad, P. N.; Reinhardt, B. A.; Dillard, A. G. *J. Chem. Phys.* **1993**, *99*, 9984-9993.

Karna, S. P.; Keshari, V.; Prasad, P. N. *Chem. Phys. Lett.* **1995**, *234*, 390-394.

Katz, H. E.; Singer, K. D.; Sohn, J. E.; Dirk, C. W.; King, L. A.; Gordon, H. M. *J. Am. Chem. Soc.* **1987**, *109*, 6561-6563.

Kerr, J. *Philos. Mag.* **1875**, *4*, 337.

Kleinman, D. A. *Phys. Rev.* **1962**, *126*, 1977-1979.

Knott, E. B. *J. Chem. Soc.* **1952**, 4099-4106.

Lalama, S. J.; Garito, A. F. *Phys. Rev. A: At. Mol. Opt. Phys.* **1979**, *20*, 1179-1194.

Lee, S.-H.; Otomo, A.; Nakahama, T.; Yamanda, T.; Kamikado, T.; Yokoyama, S.; Mashiko, S. *J. Mater. Chem.* **2002**, *12*, 2187-2188.

Leng, W.; Zhou, Y.; Xu, Q.; Liu, J. *Macromolecules* **2001**, *34*, 4774-4779.

Levine, B. F.; Bethea, C. G. *J. Chem. Phys.* **1977**, *66*, 1070-1074.

Lipinski, J.; Bartkowiak, W. *Chem. Phys.* **1999**, *245*, 263-276.

Liu, Y.-J.; Liu, Y.; Zhao, X.; Hu, H.-Q.; Zhang, D.-J. L., C.-B. *Chin. J. Chem.* **2001**, *19*, 332-339.

Londergan, T. M.; Zhang, C.; Ren, A.; Dalton, L. *Polym. Prepr. (Am. Chem. Soc., Div. Polym. Chem.)* **2000**, *41*, 783-784.

Luo, J.; Ma, H.; Haller, M.; Jen, A. K.-Y.; Barto, R. R. *Chem. Commun.* **2002**, 888-889.

Luo, J.; Liu, S.; Haller, M.; Liu, L.; Ma, H.; Jen, A. K.-Y. *Adv. Mater.* **2002**, *14*, 1763-1768.

Maradiya, H. R.; Patel, V. S. *Chem. Heterocycl. Compd.* **2003**, *39*, 357-363.

Marder, S. R.; Beratan, D. N.; Cheng, L.-T. *Science* **1991**, *245*, 103-106.

Marder, S. R.; Perry, J. W.; Bourhill, G.; Gorman, C. B.; Tiemann, B. G.; Mansour, K. *Science* **1993**, *261*, 186-189.

Marder, S. R.; Perry, J. W. *Science* **1994**, *263*, 1706-1707.

Marder, S. R.; Gorman, C. B.; Meyers, F.; Perry, J. W.; Bourhill, G.; Bredas, J.-L.; Pierce, B. M. *Science* **1994**, *265*, 632-635.

Marder, S. R.; Cheng, L.-P.; Tiemann, B. G.; Friedli, A. C.; Blanchard-Desce, M.; Perry, J. W.; Skindhøj, J. *Science* **1994**, *263*, 511-514.

Metzger, J. V. *Thiazole and Its Derivatives*; John Wiley and Sons: New York, 1979; Vol. 34.

Meyers, F.; Marder, S. R.; Pierce, B. M.; Bredas, J. L. *J. Am. Chem. Soc.* **1994**, *116*, 10703-10714.

Miller, R. D.; Lee, V. Y.; Moylan, C. R. *Chem. Mater.* **1994**, *6*, 1023-1032.

Moylan, C. R.; Tweig, R. J.; Lee, V. Y.; Swanson, S. A.; Betterton, K. M.; Miller, R. D. *J. Am. Chem. Soc.* **1993**, *115*, 12599-12600.

Moylan, C. R.; Miller, R. D.; Twieg, R. J.; Betterton, K. M.; Lee, V. Y.; Matray, T. J.; Nguyen, C. *Chem. Mater.* **1993**, *5*, 1499-1508.

Nakayama, H.; Sugihara, O.; Fujimura, H.; Matsushima, R.; Okamoto, N. *Opt. Rev.* **1995**, *2*, 236-238.

Nie, W. *Adv. Mater.* **1993**, *5*, 520-545.

Norman, P.; Jonsson, D.; Vahtras, O.; Agren, H. *Chem. Phys.* **1996**, *203*, 23-42.

Oudar, J. L.; Chemla, D. S. *J. Chem. Phys.* **1977**, *66*, 2664-2668.

P., S.-S.; Hsu, G.-T.; Lin, H.-C. *Tetrahedron Lett.* **1999**, *40*, 2157-2160.

Painelli, A. *Chem. Phys.* **1999**, *245*, 185-197.

Patterson, A. M.; Campbell, L. T.; Walker, D. F. *The Ring Index*; 2nd ed.; American Chemical Society, 1960.

Phillips, A. P.; Burrows, R. B.; ZA6805975, 1969, p p22.

Pockels, F. *Lehrbuch der Kristalloptik* Teubner, Leipzig, 1906.

Prasad, P. N.; Williams, D. J. *Introduction to Nonlinear Optical Effects in Molecules and Polymers*; John Wiley and Sons: New York, 1991.

Prim, D.; Kirsch, G.; Nicoud, J. F. *Synlett* **1998**, 383-384.

Quraishi, M. A.; Wajid Khan, M.; Ajmal, M.; Muralidharan, S.; Iyer, S. V. *Anti-Corrosion Methods and Materials* **1996**, *43*, 5-8.

Rangnekar, D. W.; Maladkar, G. J. *Phosphorus, Sulfur, and Silicon and the Related Elements* **2000**, *164*, 199-205.

Rao, V. P.; Jen, A. K.-Y.; Wong, K. Y.; Drost, K. J. *Tetrahedron Lett.* **1993**, *34*, 1747-1750.

Rao, V. P.; Cai, Y. M.; Jen, A. K.-Y. *J. Chem. Soc., Chem. Commun.* **1994**, 1689-1690.

Rao, V. P.; Wong, K. Y.; Jen, A. K.-Y.; Drost, K. J. *Chem. Mater.* **1994**, *6*, 2210-2212.

Rao, V. P.; Jen, A. K.-Y.; Chandrasekhar, J.; Namboothiri, I. N. N.; Rathna, A. *J. Am. Chem. Soc.* **1996**, *118*, 12443-12448.

Reifschneider, W.; US 3511850, 1970, p p5.

Reifschneider, W.; US 3682879, 1972, p p5.

Rojo, G.; de la Torre, G.; Garcia-Ruiz, J.; Ledoux, I.; Torres, T.; Zyss, J.; Agullo-Lopez, F. *Chem. Phys.* **1999**, *245*, 27-34.

Shen, Y. R. *The Principles of Nonlinear Optics*; John Wiley and Sons: New York, 1984.

Shu, C.-F.; Tsai, W. J.; Chen, J.-Y.; Jen, A. K.-Y.; Zhang, Y.; Chen, T.-A. *J. Chem. Soc., Chem. Commun.* **1996**, 2279-2280.

Shu, C.-F.; Wang, Y.-K. *J. Mater. Chem.* **1998**, *8*, 833-835.

Singer, K. D.; Sohn, J. E.; King, L. A.; Gordon, H. M.; Katz, H. E.; Dirk, C. W. *J. Opt. Soc. Am. B: Opt. Phys.* **1989**, *6*, 1339-1350.

Singer, K. D.; Kowalczk, T. C.; Nguyen, H. D.; Beuhler, A. J.; Wargowski, D. A. *Proc. SPIE* **1997**, *3006*, 326-337.

Singer, K. D.; Hubbard, S. F.; Schober, A.; Hayden, L. M.; Johnson, K. In *Characterization Techniques and Tabulations for Organic Nonlinear Optical Materials*; Kuzyk, M. G. D., C. W., Ed.; Marcel Dekker: New York, 1998, pp 311-513.

Song, S.; Lee, S. J.; Cho, B. R. *Chem. Mater.* **1999**, *11*, 1406-1408.

Song, S.; Lee, S. J.; Cho, B. R. *Chem. Mater.* **1999**, *11*, 1406-1408.

Steier, W. H.; Chen, A.; Lee, S. S.; Garner, S.; Zhang, H.; Chuyanov, V.; Dalton, L. R.; Wang, F.; Ren, A. S.; Zhang, C.; Todorova, G.; Harper, A.; Fetterman, H. R.; Chen, D.; Udupa, A.; Bhattacharya, D.; Tsap, B. *Chem. Phys.* **1999**, *245*, 487-506.

Takahashi, T.; Satake, K. *Yakugaku Zasshi* **1951**, *71*, 905-911.

Takahashi, T.; Hayami, M. *Jpn. J. Pharmacol.* **1961**, *81*, 1419-1426.

Tanaka, H.; Kuroboshi, M.; Kameyama, Y. In *Kokai Tokkyo Koho*: Japan, 2003.

Tretiak, S.; Chemnyak, V.; Mukamel, S. *Chem. Phys.* **1999**, *245*, 145-163.

van der Boom, M. E.; Zhu, P.; Evmenenko, G.; Malinsky, J. E.; Lin, W. D., P.; Marks, T. J. *Langmuir* **2002**, *18*, 3704-3707.

van der Boom, M. E.; Evmenenko, G.; Dutta, P.; Marks, T. J. *Polym. Mater. Sci. Eng.* **2002**, *87*, 375-376.

Varanasi, P. R.; Jen, A. K.-Y.; Chandrasekhar, J.; Namboothiri, I. N. N.; Rathna, A. *J. Am. Chem. Soc.* **1996**, *118*, 12443-12448.

Vastag, G.; Szocas, E.; Shaban, A.; E., K. *Pure Appl. Chem.* **2001**, *73*, 1861-1869.

Wadsworth, H. J.; Wyman, P. A.; Dabbs, S.; Jenkins, S. M. In *European Patent*: 90308500, 1991.

Wang, X.; Yang, K.; Kumar, J.; Tripathy, S. K.; Chittibabu, K. G.; Li, L.; Lindsay, G. *Macromolecules* **1998**, *31*, 4126-4134.

Wang, Y.-K.; Shu, C.-F.; Breitung, E. M.; McMahon, R. J. *J. Mater. Chem.* **1999**, *9*, 1449-1452.

Ward, J. F. *Rev. Mod. Phys.* **1965**, *37*, 1-18.

Watanabe, T.; Amano, M.; Tomaru, S. *Jpn. J. Appl. Phys.* **1994**, *33*, 1683-1685.

Willetts, A.; Rice, J. E.; Burland, D.; Shelton, D. P. *J. Chem. Phys.* **1992**, *97*, 7590-7599.

William, D. J. *Angew. Chem. Int. Ed.* **1984**, *23*, 690-703.

Wong, K. Y.; Jen, A. K.-Y.; Rao, V. P.; Drost, K. J. *J. Chem. Phys.* **1994**, *100*, 6818-6825.

Wurthner, F.; Thalacker, C.; Matschiner, R.; Lukaszuk, K.; Wortsmann, R. *Chem. Commun.* **1998**, 1739-1740.

Xu, C.; Wu, B.; Todorova, O.; Dalton, L. R.; Shi, Y.; Ranon, P. M.; Steier, W. H. *Macromolecules* **1993**, *26*, 5303-5309.

Yamamoto, T.; Suganuma, H.; Maruyama, T.; Inoue, T.; Muramatsu, Y.; Arai, M.; Komarudin, D.; Ooba, N.; Tomaru, S.; Sasaki, S.; Kubota, K. *Chem. Mater.* **1997**, *9*, 1217-1225.

Yang, X.-L.; Anemian, R.; Zabulon, T.; Andraud, C.; Brasselet, S.; Ledoux-Rak, I. N.; Zyss, J. *Proc. SPIE* **2000**, *4106*, 222-229.

Zhang, J.-X.; Dubois, P.; Jerome, R. *Synth. Commun.* **1996**, *26*, 3091-3095.

Zhang, C.; Ph.D. thesis, University of California: Los Angeles, CA, 1999.

Zhang, C.; Ren, A. S.; Dalton, L. R. *Polym. Prepr. (Am. Chem. Soc., Div. Polym. Chem.)* **1999**, *40*, 156-157.

VITA

Daniel Michael Casmier is originally from Puyallup, Washington and calls the great Northwest his home. During an internship at the IBM Research Center in San Jose, CA in the summer of 1998, he developed an intense interest in materials chemistry. At Pacific Lutheran University he earned his bachelor of science with an emphasis in biochemistry in 1999. At the University of Washington he earned his doctor of philosophy in Chemistry in 2004.